



THE HONG KONG
POLYTECHNIC UNIVERSITY

香港理工大學

Pao Yue-kong Library

包玉剛圖書館

Copyright Undertaking

This thesis is protected by copyright, with all rights reserved.

By reading and using the thesis, the reader understands and agrees to the following terms:

1. The reader will abide by the rules and legal ordinances governing copyright regarding the use of the thesis.
2. The reader will use the thesis for the purpose of research or private study only and not for distribution or further reproduction or any other purpose.
3. The reader agrees to indemnify and hold the University harmless from and against any loss, damage, cost, liability or expenses arising from copyright infringement or unauthorized usage.

If you have reasons to believe that any materials in this thesis are deemed not suitable to be distributed in this form, or a copyright owner having difficulty with the material being included in our database, please contact lbsys@polyu.edu.hk providing details. The Library will look into your claim and consider taking remedial action upon receipt of the written requests.

The Hong Kong Polytechnic University
Department of Applied Biology and Chemical Technology

Gene Delivery using Core-Shell Nanoparticles

Siu Yuen Shan

A thesis submitted in partial fulfillment of the requirements for the
Degree of Master of Philosophy

August 2006

CERTIFICATE OF ORIGINALITY

I hereby declare that this thesis is my own work and that, to the best of my knowledge and belief, it reproduces no material previously published or written, nor material that has been accepted for the award of any other degree or diploma , except where due acknowledgement has been made in the text.

_____ (Signed)

SIU YUEN SHAN (Name of student)

Abstract

Recently, with the patented technology, we have developed a cationic amphiphilic core-shell nanoparticle composed of well defined poly(methyl methacrylate) hydrophobic cores and poly(ethyleneimine) hydrophilic shell. This particle has the combined properties of cationic polymers, nanoparticles and surface functional groups, making it excellent candidate as gene carrier in gene delivery systems. In our previous studies, we have demonstrated that this novel nanoparticle has comparative advantages over the PEI system for *in vitro* gene delivery.

During the gene transfer process, there are a number of barriers that restrict the success of gene delivery. However, cytoplasmic microinjection studies have demonstrated that inefficient gene transfer from the cytosol to the nucleus is the major limiting step. In order to further enhance the transfection efficiency and to provide the nuclear targeting capability, we have tried the inclusion of a nuclear protein HMGB1 in our system. It has been reported that the high mobility group protein HMGB1 can enhance the transfection efficiency in both naked DNA and liposome-mediated transfections. When DNA is packed with the HMGB1 protein, condensed molecules can form and the transfection efficiency is approximately similar to the calcium phosphate method. In the HVJ-liposome system, HMGB1

serves as a DNA binding protein. Within the nuclear envelop, it assists nuclear access and promotes gene stabilization.

In our present study, HMGB1 protein was added together with DNA and the PMMA-PEI nanoparticles to form the gene delivery complexes. Formation of complexes was demonstrated using agarose gel retardation assay and the DNA with HMGB1 still bound can be released from the complexes with the use of poly(aspartic acids). Therefore, with the incorporation of HMGB1 in our existing PMMA-PEI core-shell nanoparticle system, the resultant HMGB1-DNA-nanoparticle complexes still maintain their DNA condensing capacity, DNA release ability and DNA protection ability. Furthermore, in *in vitro* transfection, complexes formed by first condensing the plasmid DNA with nanoparticles and then binding with the HMGB1 protein gave a transfection efficiency significantly higher than that of the PMMA-PEI nanoparticle system without the presence of HMGB1. We believe that this system with the inclusion of HMGB1 has the potential to be developed into a viable and efficient non-viral gene carrier for use *in vivo*.

Acknowledgements

I would like to take this chance to express my heartfelt gratitude to all the people who assisted and contributed to my M.Phil project.

In here, I would like to extend my sincere thanks to my chief supervisor, Dr Daniel Lee, Assistant Professor, Department of Applied Biology and Chemical Technology, The Hong Kong Polytechnic University, for his patient guidance and encouragement. Throughout the project, he gave numerous invaluable advices, and always be available when I need his help and discussion. I would also like to give my thanks to my co-supervisor Dr. Pei Li, Associate Professor, Department of Applied Biology and Chemical Technology, The Hong Kong Polytechnic University, for her kind support of the project.

Apart from that, I would like to thank Dr. Lijun Li and Ms Xiao Peng for their incessant support and useful discussion throughout the whole project. I would also like to give my special thanks to Dr. Pei Li's research team, Mr. Man Fai Leung and Mr. Edmond Ho for synthesis of the nanoparticles, for technical support in the chemistry area, for their continuous encouragement and friendship.

I would like to show my appreciation to all the technicians of our Department, especially Ms Sarah Yeung, who gave lots of technical support for the confocal laser scanning microscopy.

I would also like to thank all my lovely lab-mates, Miss Hoi Wah Au, Miss Kit Ying Choy, Miss Phibe Li, Miss Wing Ka Tang, Mr. Chi Ming Lau, Mr. Ho Man Ho, Mr. Wai Ying Li and Dr. Xian Hua Zhang for their support and friendship. Finally, I would like to thank my family for their encouragement throughout my study.

Table of Contents

Item	Page
Abstract	i
Acknowledgements	iii
Table of Contents	iv
List of Figures	viii
List of Tables	x
List of Abbreviations	xi
Chapter 1: Background information	1
1.1 Gene therapy	1
1.2 Gene delivery systems	3
1.2.1 The viral systems (biological gene delivery systems)	5
1.2.2 The non-viral systems (non-biological gene delivery systems)	7
1.2.2.1 The physical methods	7
1.2.2.2 The chemical methods/ vectors	8
1.3 Mechanism of gene delivery	11
1.3.1 Condensation with nucleic acids	11
1.3.2 Cellular uptake	12
1.3.3 Release from the endosome	13
1.3.4 Nuclear transport	13
1.4 Barriers of gene transfer in mammalian cells	15
1.4.1 Extracellular level	16
1.4.2 Intracellular level	18

1.4.3	Nuclear level	19
1.5	Cationic polymer based gene delivery systems	20
1.5.1	Poly(ethylenimine), PEI	23
1.6	Development of non-viral gene delivery systems	25
1.7	Our amphiphilic cationic core-shell nanoparticle	27
1.7.1	Characterization of the PMMA-PEI amphiphilic core-shell nanoparticle	28
1.7.2	Previous experimental results in using PMMA-PEI as a gene carrier	29
1.8	High mobility group proteins (HMG)	30
1.8.1	Classification of HMG	30
1.8.2	Structure of high mobility group box 1 protein (HMGB1)	31
1.8.3	Intracellular functions of HMGB1	33
1.8.4	HMGB1 as a novel gene delivery system	36
1.8.5	Nuclear localization signal	37
1.8.6	Interaction between the HMGB1 protein, DNA and the nanoparticle	38
Chapter 2: Materials and methods		39
2.1	Extraction and purification of HMGB1 protein from pig thymus	39
2.1.1	Collection of nuclear pellet from pig thymus	39
2.1.2	Extraction of HMG proteins	40
2.1.3	Fractionation of HMG proteins by CM-Sephadex C25 chromatography	41
2.1.4	Confirmation of HMGB1 protein by SDS-PAGE and western blotting	41

2.1.5	Concentration of HMG proteins and buffer exchange	42
2.1.6	Determination of protein concentration	43
2.2	Mini-preparation of plasmid	43
2.3	Determination of plasmid concentration and purity	45
2.4	Plasmid size confirmation	45
2.4.1	Double restriction digestion	46
2.4.2	Agarose gel electrophoresis	46
2.5	Formation of HMGB1-DNA complexes	46
2.6	Formation of HMGB1-DNA-nanoparticle complexes	47
2.7	Release of DNA from the HMGB1-DNA-nanoparticle complex	48
2.8	Protection against DNase I digestion	48
2.9	Cell culture	49
2.10	<i>In vitro</i> cell transfection studies	49
2.11	Determination of transfection efficiency by Luciferase Assay and Bradford Assay	50
2.12	Cell viability assays	51
2.13	Nanoparticle trafficking studies by confocal laser scanning microscopy (LSM)	52
2.13.1	Labeling of PMMA-PEI core shell nanoparticle and PEI with fluorescein isothiocyanate (FITC)	53
2.13.2	Labeling of pGL-3-Control plasmid with tetramethyl-rhodamine (TM-rhodamine)	53
2.13.3	Trafficking of nanoparticles	54
2.13.4	Confocal laser scanning microscopy	55

Chapter 3: Results and analysis	56
3.1 HMGB1 protein extraction and purification from pig thymus	56
3.2 Formation of HMGB1-DNA complexes	59
3.3 Formation of HMGB1-DNA-nanoparticle complexes	61
3.4 Release of DNA from the HMGB1-DNA-nanoparticle complex	64
3.5 Protection against DNase I digestion	66
3.6 Transfection studies	69
3.7 Cell viability assays	72
3.8 Nanoparticle trafficking studies by confocal laser scanning microscopy (LSM)	73
 Chapter 4: Discussion	 83
4.1 Incorporation of HMGB1 into the gene delivery complex	84
4.2 Transfection efficiency of the HMGB1-DNA-nanoparticle system	87
4.2.1 Nitrogen to phosphate ratio of 2	88
4.2.2 Nitrogen to phosphate ratio of 5	89
4.3 Roles of HMGB1 in the gene delivery complex	93
4.3.1 Nuclear localization signal	93
4.3.2 Transcriptional activator	94
4.3.3 Ligand binding to cell surface	94
4.4 Perspectives	95
4.5 Conclusion	98
 Chapter 5: Appendix	 99
 Chapter 6: References	 106

List of Figures

Figure	Title	Page
Figure 1.1	The desirable properties of an ideal gene delivery system.	4
Figure 1.2	Mechanism of cellular transfection by cationic lipids or polymers.	15
Figure 1.3	Schematic representation of the three levels of barriers along the <i>in vivo</i> gene delivery pathway.	15
Figure 1.4	Barriers at the extracellular level for systemic gene delivery.	16
Figure 1.5	Barriers at intracellular and nuclear levels.	20
Figure 1.6	Graft copolymerization of MAA and 25 kDa branched PEI to form an amphiphilic core-shell nanoparticle.	28
Figure 1.7	Transmission electron micrograph (TEM) of a PMMA-PEI core-shell nanoparticle at high magnification.	29
Figure 1.8	Domain organization of HMGB1.	32
Figure 1.9	Solution structure of the HMG box A and B of the HMGB1 protein.	33
Figure 3.1	Elution Profile of HMG proteins from the CM-Sephadex C25 column.	57
Figure 3.2	(a) Coomassie blue stained SDS-PAGE of the fractionated proteins from CM-Sephadex C25 chromatography. (b) Western blot analysis of the fractionated proteins.	57
Figure 3.3	Agarose gel retardation assay (AGRA) study of complexing between HMGB1 and the pGL-3-Control plasmid.	59

Figure 3.4	AGRA study of the HMGB1-DNA-nanoparticle complex formation.	63
Figure 3.5	Release of DNA from the HMGB1-DNA-nanoparticle complex by poly(aspartic acid).	65
Figure 3.6	Protection of DNA against DNase I digestion.	68
Figure 3.7	<i>In vitro</i> transfection efficiency of PMMA-PEI nanoparticles at various weight ratios in MCF-7 cells.	70
Figure 3.8	<i>In vitro</i> transfection efficiency of different HMGB1-DNA-nanoparticle systems in MCF-7 cells.	71
Figure 3.9	Relative viability of MCF-7 cells at different nitrogen to phosphate ratios for different gene delivery systems.	72
Figure 3.10	Confocal laser scanning microscopic images of HeLa cells after 3 hours and 7 hours of transfection incubation with FITC labeled PEI polymers and PMMA-PEI nanoparticles.	75
Figure 3.11	Confocal laser scanning microscopic images of HeLa cells after 7 hours of transfection incubation with FITC labeled PEI polymers.	76
Figure 3.12	Confocal laser scanning microscopic images of HeLa cell after 3 hours of transfection incubation with double labeled PEI-DNA complexes.	77
Figure 3.13	Confocal laser scanning microscopic images of HeLa cells after 3 hours and 7 hours of transfection incubation with double labeled PEI-DNA complexes and nanoparticle-DNA complexes.	79
Figure 3.14	Confocal laser scanning microscopic images of MCF-7 cells and HeLa cells after 7 hours of transfection incubation with FITC labeled PEI polymers and PMMA-PEI nanoparticles.	81

Figure 3.15	Confocal laser scanning microscopic images of MCF-7 cells after 7 hours of transfection incubation with HMGB1-DNA-nanoparticle complexes.	82
-------------	---	----

List of Tables

Table	Title	Page
Table 1.1	Physical methods for gene delivery.	8
Table 1.2	Comparison of DNA Delivery Systems.	10
Table 1.3	Chemical structures of some commonly studied cationic polymers.	22
Table 1.4	Summary of PMMA-PEI properties as a gene carrier.	29
Table 3.1	The main component of Peaks I to V obtained by CM-Sephadex C25 chromatography of high mobility group proteins performed by Goodwin <i>et al.</i> (1975).	58
Table 3.2	Conversion of N/P ratios to weight ratios for the PEI polymers and PMMA-PEI nanoparticles.	72

List of Abbreviations

AAV	adeno-associated viruses
Abs	absorbance
AGRA	agarose gel retardation assay
BSA	bovine serum albumin
cDNA	complementary DNA
CM	carboxymethyl
cm	centimeter
CO ₂	carbon dioxide
C-terminal	carboxyl-terminal
dd H ₂ O	deionized distilled water
DEAE	diethylaminoethylene
DIC	differential interference contrast
DMEM	Dulbecco's modified Eagle's medium
DNA	deoxyribonucleic acid
DNase I	deoxyribonuclease I
<i>E. coli</i>	<i>Escherichia coli</i>
EDTA	ethylene diaminetetraacetic acid
EtBr	ethidium bromide
FBS	fetal bovine serum
FITC	fluorescein isothiocyanate
g	gram
HCl	hydrochloric acid
HeLa	human cervix adenocarcinoma cells
HGP	Human Genome Project
HMG	high mobility group proteins
HSV	herpes simplex viruses
IgG	immunoglobulin G
kDa	kilodalton
L	liter
LB	Luria Bertani
LSM	confocal laser scanning microscopy
M	molar
MCF-7	human breast adenocarcinoma cells
mg	milligram
MgCl ₂	magnesium chloride
min	minute

mL	milliliter
MTS	3-(4,5-dimethylthiazol-2-yl)-5-(3-carboxy-methoxy phenyl)-2-(4-sulfophenyl)-2H-tetraolium-inner salt
NaCl	sodium chloride
mM	millimolar
NLS	nuclear localization signal
nm	nanometer
N/P	PEI nitrogen to DNA phosphate
NPC	nuclear pore complex
N-terminal	amino-terminal
PAMAM	poly(amidoamine)
pAsp	poly(aspartic acid)
PBS	phosphate buffered saline
PEI	poly(ethylenimine)
PLB	passive lysis buffer
PLL	poly-(L)-lysine
PMMA-PEI	poly(methyl methacrylate)-poly(ethylenimine) amphiphilic core-shell nanoparticles
P/S	penicillin /streptomycin
PVDF	poly(vinylidene fluoride)
RAGE	receptor for advanced glycation end products
RLU	relative luminescence unit
RNase A	ribonuclease A
rpm	rotation per minute
RSS	recombination signal sequences
s	second
SDS-PAGE	sodium dodecylsulfate polyacrymjide gel
SRY	sex-determining region Y
TBE	Tris borate EDTA
TBS-T	Tris-buffered saline containing 0.1% Tween-20
TCA	trichloroacetic acid
TE	Tris-EDTA
TEM	transmission electron microscop
TLR	Toll like receptor
TM-rhodamine	tetramethyl-rhodamine
Tris	Tris (hydroxymethyl) aminomethane
V	voltage
v/v	volume to volume ratio

w/v	weight to volume ratio
w/w	weight to weight ratio
μg	microgram
μL	microliter

Chapter 1: Background information

1.1 Gene therapy

The introduction of foreign DNA or exogenous genes into cells for the purpose of gene expression is called transfection [Heiser 2004]. It is a routine technique commonly used by scientists to study the functions and structures of a particular gene as well as the mechanisms of gene regulation and expression [Bottger *et al.* 1990]. It has also been considered as an advanced and important technique in biomedical science, clinical medicine, biochemistry and pharmacy [El-Aneed *et al.* 2004].

In modern molecular medicine [Isaka *et al.* 1998 and Lundstrom *et al.* 2003], gene therapy is a therapeutic approach with great promise for the treatment of a variety of inherited or acquired disorders [Lundstrom *et al.* 2003, Segura *et al.* 2001 and Liu *et al.* 2002]. This approach is based on the principle of altering the expression level of genes involved in cellular processes and disease progression, by introducing functional genes, e.g. gene segments, oligonucleotides, DNA, RNA or antisense sequences into the target cells of patients [Segura *et al.* 2001, Liu *et al.* 2002 and Thomas *et al.* 2003]. With the introduction of functional genes, normal metabolisms, cellular or physiological responses of the patients

will be restored. In the past 15 years, clinical trials employing gene therapy protocols have included those for cancers, infectious diseases, cardiovascular diseases and rheumatoid arthritis [Ahn *et al.* 2002, Thomas *et al.* 2003, El-Aneed *et al.* 2004 and Mahato *et al.* 2004]. Among these trials, 70% of them are for cancer gene therapies [El-Aneed *et al.* 2004]. In general, the success of gene therapy is mainly dependent on three criteria: the availability of target gene, the efficiency of gene delivery and also the expression of exogenous genes.

With the recent advances in molecular biotechnology (e.g. cDNA microarrays, differential display) and the completion of the Human Genome Project (HGP), better understanding of the pathogenesis of diseases as well as correlations between specific genetic mutations and disorders are available [Isaka *et al.* 1998, Garnett 1999, Lundstrom *et al.* 2003 and Parker *et al.* 2003]. These form the basis for more efficient ways to screen and identify the potential therapeutic genes for treatment. As a result, the development of novel therapeutic strategy for gene therapy, nucleic acid vaccination or other DNA-based medicine is not limited by the step of candidate genes identification. However, this development mainly depends on the ability to deliver the genes of interest into the target cells or tissues, as well as to express it at the correct time with therapeutic efficacy. In other words, one of the important prerequisites for the success of any gene

therapy strategies is the transfection efficiency, which is dependent on effective and specific gene delivery [Zaitsev *et al.* 1997, Cristiano 1998, Luo *et al.* 2000, Heiser 2004 and Mahato *et al.* 2004]. For this reason, in the past decade, more progresses and focuses have been placed on the development of new delivery systems and the improvement of functional gene delivery for *in vitro* and *in vivo* applications.

1.2 Gene delivery systems

A gene delivery system is defined as a gene carrier, a vehicle to carry the genes of interest into a target cell. This concept of a gene delivery system is developed mainly because scientists have realized that direct introduction of naked DNA into a cellular system is inefficient. When delivering the naked DNA intravenously, it is quickly cleared from the circulation, degraded by endogenous nucleases and exhibits poor cellular uptake [Segura *et al.* 2001]. As a result, different ways and agents have been explored in order to increase the transfection efficiency.

A perfect model of gene delivery system or gene carrier should be efficient and effective in transfection with specific targeting and should be safe for human use [Bivas-Benita *et al.* 2004]. Therefore, ideally, the gene carriers should be able to

protect the DNA from enzymatic degradation, bind to target cells, facilitate effective cellular uptake by crossing the cell membrane, and allow for efficient gene expression. Besides, the carriers should be non-toxic, biocompatible, biodegradable and should induce minimal immune response at the effective dosage [Mahato *et al.* 2004]. In general, there are two main groups of gene delivery systems, the viral systems (biological vectors) and the non-viral systems (physical methods and chemical vectors). Each of these systems has its own advantages and limitations but an ideal gene delivery system basically should have a combination of all the above properties.

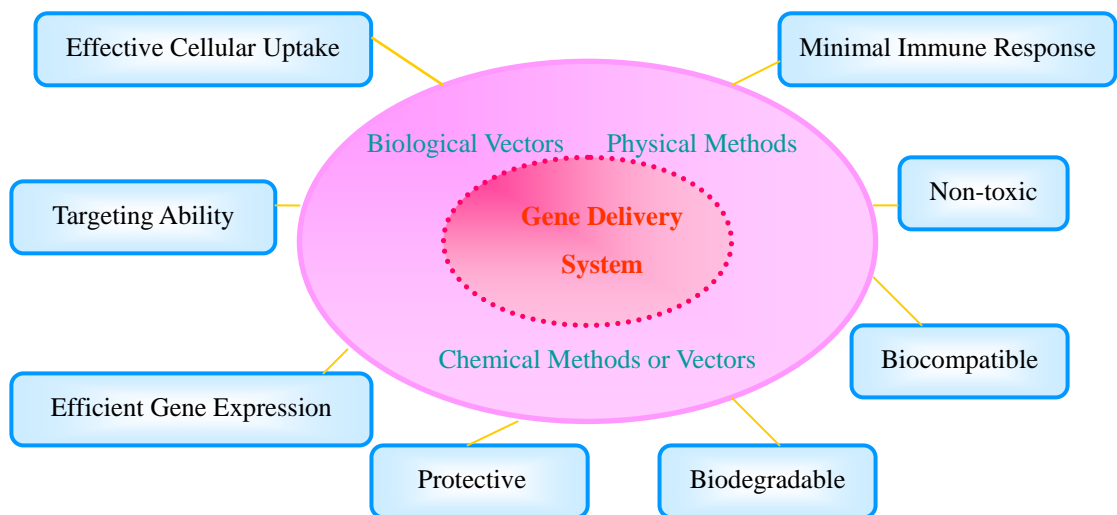


Figure 1.1: The desirable properties of an ideal gene delivery system.

1.2.1 The viral systems (biological gene delivery systems)

Viral systems are also termed as biological gene delivery systems. Under this category, the gene carriers are the viral vectors. By natural mechanisms, viruses have the ability to infect and take over the control of the cellular machinery of their hosts. This provides a path for the viruses to transfer and consequently to express their genetic materials for viral replication in the host cells during infection. Based on this natural phenomenon, viral vectors become one of the promising candidates for gene delivery. Examples of viral vectors include the retroviruses, the adenoviruses, the adeno-associated viruses (AAV), the herpes simplex viruses (HSV) and the vaccinia viruses [Stone *et al.* 2000 and Heiser 2004]

Viruses, due to their infectious nature, must have their genomes modified before being used as gene delivery agents. Based on the available knowledge in virology, engineered or recombinant viral vectors have been developed. These engineered viral vectors are modified to eliminate the pathogenicity while retaining their high efficiency in gene transfer [Bottger *et al.* 1990]. Therefore, viral vectors are generally considered as powerful tools and are the most frequently used vehicles for clinical studies. Nowadays, around 85% of clinical protocols for gene therapy utilize viral vectors [Garnett 1999].

Although they have been used in many clinical trials, the safety of viral vectors is the major concern. Some viruses may provoke mutagenesis and carcinogenesis [Liu *et al.* 2002] (e.g. retroviruses), others may induce host immune responses (e.g. adenoviruses), and thus repeated administration may be difficult. Apart from the safety concerns, viral systems have other limitations too, including the small size limit on transgenes, the difficulty in scale-up production and the lack of specific targeting. All these limitations have resulted in a renewal of interest in non-viral systems. Viral gene delivery systems were dealt a severe blow near the end of 2002 when two children with severe combined immunodeficiencies (SCID) developed leukemia-like conditions after being treated with gene therapy in France [Thomas *et al.* 2003, Cavazzana-Calvo *et al.* 2004]. This incidence exemplified the potential risk posed by viral vectors and thus the urgent need to develop new, safe and stable alternatives. The non-viral gene carriers thus became attractive systems.

1.2.2 The non-viral systems (non-biological gene delivery systems)

Non-viral systems are also called non-biological gene delivery systems. Under this category, they can be further subdivided into the physical and chemical methods.

1.2.2.1 The physical methods

For the physical methods, mechanisms different from those of the biological systems are utilized. In order to overcome the physical barriers presented by the cells or tissues, usually some sort of mechanical forces are applied to disrupt the integrity of the cell membrane, and the transgene is picked up by the cell or tissue proactively [Heiser 2004]. Currently, several physical methods are available, these include microinjection, conventional or high-pressure needle injections, particle bombardment, electroporation and ultrasound irradiation [Li *et al.* 2001, Gresch *et al.* 2001, Niidome *et al.* 2002 and Heiser 2004]. Since their development, these physical methods have been used mainly for *in vitro* gene transfer processes. However, new improvements on these physical methods that allow them to be used for *in vivo* applications have been achieved very recently [Li *et al.* 2001 and Heiser 2004].

As most of the physical methods require the use of physical instruments, this allows for the development of more quantitative and standardized gene delivery systems that can be used in large-scale clinical applications [Heiser 2004]. Furthermore, having the ability to transfect different cell types with high transfection efficiency at localized spots, physical methods are viable alternative means for *in vivo* gene delivery. Yet, there are still hurdles to overcome including the low transfection efficiency in primary cells, the high cell mortality, or even the very low number of transfected cells with microinjections [Gresch *et al.* 2001].

Table 1.1: Physical methods for gene delivery.

Physical method	Principles
Microinjection	Injecting DNA intracellularly
Conventional needle injection	Physical force
High pressure needle injection	Hydrodynamic force
Particle bombardment	Micro-carrier accelerated by high pressure gas
Electroporation	Electric pulse
Ultrasound	Irradiation with ultrasound

* Information is adopted from Heiser 2004.

1.2.2.2 The chemical methods/ vectors

The chemical methods include those transfection protocols involving synthetic agents or chemicals. These synthetic substances are generally called transfection reagents or synthetic vectors [Heiser 2004]. In general, chemical methods are the

most commonly used and well-established technique for mammalian cells transfection *in vitro*. Recently, with the development of chemical technology and chemical engineering, a vast diversity of synthetic substances with desirable properties can be synthesized. This has resulted in the rapid development in the use of synthetic compounds for *in vivo* gene delivery. Some examples of these chemical reagents are calcium phosphate, DEAE (diethylaminoethylene)-dextran, cationic lipids and cationic polymers [Heiser 2004].

Among these many different types of non-viral gene delivery systems, cationic lipids and polymers are the most investigated. However, in general, due to their toxicity and the lack of abilities for receptor recognition, endosome escape or nuclear targeting, they have relatively low transfection efficiency when compared with that of the viral vectors. But on the other hands, they are relatively easy to produce in large-scales. They also have superior safety profiles with low or no immunogenicity, and high flexibility for chemical modifications (e.g attachment of targeting ligands). Furthermore, the non-viral vectors can protect the DNA from degradation by nucleases both inside and outside the cell. With these significant advantages, there is a continuous interest in them despite their comparatively lower transfection efficiency.

Table 1.2: Comparison of DNA Delivery Systems.

Gene delivery system	Advantages	Disadvantages
Biological vectors	<ul style="list-style-type: none"> ✓ High transfection efficacy ✓ Suitable for systemic delivery ✓ Potential for targeting selected cell types 	<ul style="list-style-type: none"> ✗ Complicated manufacturing processes ✗ High quality control requirement ✗ High cost ✗ Interference with preexisting immunity against the biological vectors ✗ Safety concerns: may be carcinogenic ✗ Limitations on the gene sizes
Physical methods	<ul style="list-style-type: none"> ✓ High local transfection efficiency ✓ Not cell type dependent ✓ Easy to standardize the process ✓ Less limit on gene size ✓ Useful for <i>ex vivo</i> application ✓ Reduced natural clearance or low dose needed to achieve a desirable biological response 	<ul style="list-style-type: none"> ✗ Usually require specific instruments ✗ High cell mortality ✗ Low transfection efficiency in primary cells ✗ Very low number of transfected cells in the case of microinjection.
Chemical methods	<ul style="list-style-type: none"> ✓ Highly effective with cultured cells ✓ Relatively simple manufacturing for gene-based products ✓ Less limit on gene size ✓ Easy for storage and quality control ✓ Low immunogenicity ✓ Easy to modify (for synthetic carriers) 	<ul style="list-style-type: none"> ✗ Limited clinical application so far ✗ Challenging to prepare consistent formulations ✗ High cytotoxicity ✗ Low transfection efficiency for the non-dividing cells ✗ Not suitable for systemic administration (in the case of synthetic carriers)

* Reference: Pollard *et al.* 1998, Godbey *et al.* 1999b, Liu *et al.* 2002, Parker *et al.* 2003, Schatzlein *et al.* 2003 Gresch *et al.* 2004, and Heiser 2004.

1.3 Mechanism of gene delivery

With the ultimate goal of developing a most effective *in vivo* gene delivery system, together with the fact that the efficiencies of gene delivery achieved *in vitro* are never reproducible *in vivo*, scientists have recently started to study the mechanisms involved in gene delivery. These studies will identify the barriers for gene delivery systems and therefore will provide the important and useful fundamental information for further development of gene delivery systems.

Gene delivery is a multi-step process [Liu *et al.* 2002]. Currently, with the help of fluorescence imaging systems and microscopy, many studies have been performed to track the intracellular path of the gene delivered. In general, the gene delivery pathway of synthetic vectors can be divided into four parts. They are condensation with nucleic acids, cellular uptake, release from the endosome and nuclear transport.

1.3.1 Condensation with nucleic acids

For synthetic vectors mediated transfection (e.g. “polyfection” for the polymers mediated transfection and lipofection for the lipids mediated transfection), the genetic materials are first condensed with the carriers. Theoretically, the polycations (the positive charges of the synthetic vectors) interact with the

polyanionic genetic materials through the negatively charged phosphate groups by electrostatic interaction [Dufes *et al.* 2005]. With the appropriate cation and anion charge ratio, they form condensed, compact and ordered particles, which are called “polyplexes” or “lipoplexes” [Bieber *et al.* 2002 and Parker *et al.* 2003]. Generally speaking, the cationic polymers condense the nucleic acids into nanoparticles with different morphologies e.g. rods, toroids and spheroids [Garnett 1999]. While for the cationic lipids, liposome is formed by first self-assembly and the nucleic acids are condensed in the interior of the liposome [Templeton *et al.* 1997].

1.3.2 Cellular uptake

After forming the complexes, polyplexes and lipoplexes are positively charged at the surfaces. This allows them to electrostatically interact with the negatively charged cell membrane non-specifically. Thus the complexes initially form aggregates on the cell membrane surface [Godbey *et al.*, 1999b]. After the interaction, the complexes are immediately internalized into the cells by the endocytosis process [Kircheis *et al.*, 2001 and Thomas *et al.*, 2003].

1.3.3 Release from the endosome

After the internalization process of the complexes, the endocytosed particles (endosome) are normally directed to lysosomes for degradation [Godbey *et al.* 1999b, Thomas *et al.* 2003 and Heiser 2004]. During this cellular trafficking stage, the endosome matures from the “early” stage to the “late” stage. When the internal pH of the endosome drops from 6 to 5, the “late” stage endosome is then fused with the lysosomes which contain lots of hydrolytic enzymes and nucleases [Thomas *et al.* 2003]. Therefore, the nucleic acids or the complexes must escape from the endosome before the fusion takes place. Although the mechanism for the endosome release is yet unknown, it is believed that depending on the chemical properties of the synthetic vectors, the complexes can be released from endosomes by destabilizing the endosomal membrane.

1.3.4 Nuclear transport

After endolysosomal disruption, the complexes are released to the cytoplasm, and eventually, they are translocated to the nucleus where they will be transcribed and expressed. Nucleases are also present in the cytoplasm but studies showed that cationic polymers/ lipids can protect the transgenes effectively [Thomas *et al.* 2003]. Although the principle for transporting the

complexes or the nucleic acids to nucleus is poorly understood, two hypotheses have been suggested. Complexes or nucleic acids with a diameter smaller than the peripheral channels of the nuclear pore (10nm in diameter) are believed to be transported in a way similar to the transportation of nucleoproteins (up to 50 kDa). These complexes are transported across the nuclear envelop through the nuclear pores by passive diffusion. While for the larger complexes, the nuclear transport depends on an active transport process involving the nuclear pore complex (NPC) [Ludtke *et al.* 1999, Li *et al.* 2001 and van der Aa *et al.* 2006].

In addition, in order to have gene expression, the nucleic acids should dissociate from the synthetic vector. In most cases, dissociation occurs in the cytoplasm prior entry into the nucleus. But there are some exceptions too. For example separation between poly(ethylenimine) (PEI) and the nucleic acid is not necessary, as the expression levels are comparable when the polyplexes and nucleic acids were directly injected into the nucleus separately [Pollard *et al.* 1998, Godbey *et al.* 1999b and Heiser 2004]. The general intracellular pathway of polyfection and lipofection is summarized in Figure 2.

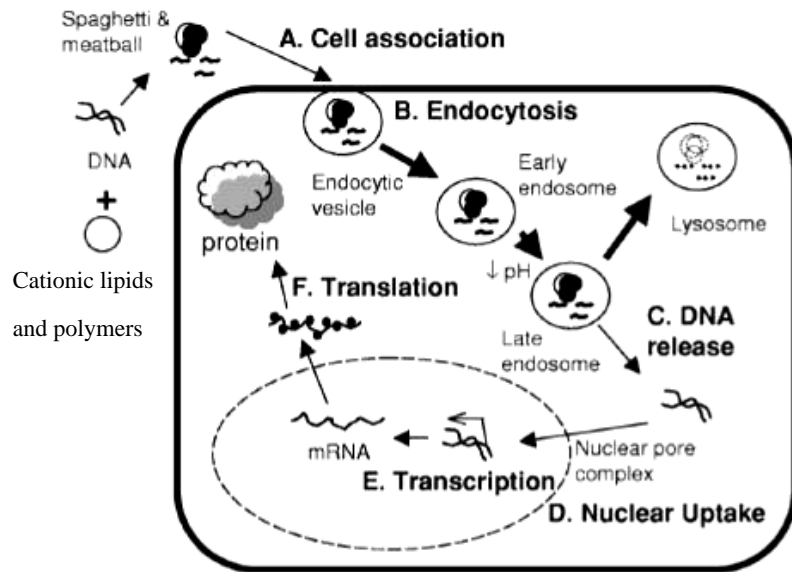


Figure 1.2: Mechanism of cellular transfection by cationic lipids or polymers. (Figure is adopted from Liu *et al.* 2002 and modified.)

1.4 Barriers of gene transfer in mammalian cells

In general, the barriers along the *in vivo* gene delivery pathway can be classified in three levels: extracellular level, intracellular level and nuclear level. While for *in vitro* pathway, only the latter two levels are involved.

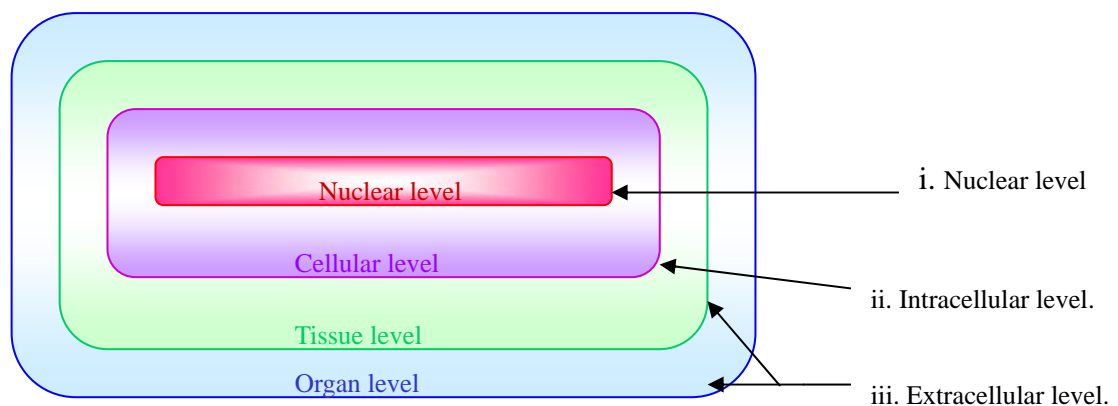


Figure 1.3: Schematic representation of the three levels of barriers along the *in vivo* gene delivery pathway. (Figure is adopted from Shoji *et al.* 2004 and modified.)

1.4.1 Extracellular level

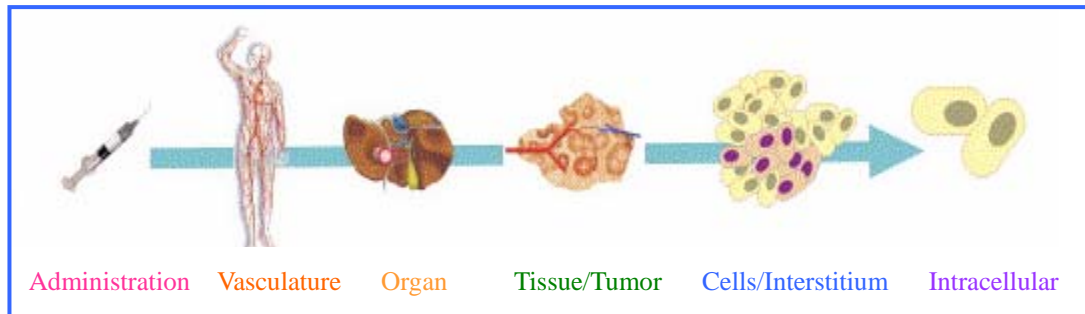


Figure 1.4: Barriers at the extracellular level for systemic gene delivery. (Figure is adopted from Dufes *et al.* 2005.)

The barriers in the extracellular level are those related to the chemical stability of the nucleic acids being transferred and the physical stability of the carriers [Wiethoff *et al.* 2003]. For *in vivo* studies, several routes of administration have been examined. Among them, systemic gene delivery represents one of the major hurdles of gene therapy [Liu *et al.* 2002 and Parker *et al.* 2003].

In the extracellular environment, many enzymes (e.g. nucleases, lipases) are present. Once the nucleic acids have been administered into the body, they may be degraded rapidly and thus chances for the transgenes to reach the target sites are reduced [Segura *et al.* 2001, Liu *et al.* 2002 and Wiethoff *et al.* 2003]. Apart from the enzymes, the mononuclear phagocytic system, which is one of our bodies' immune systems, can remove or inactivate any foreign material present in the body fluid [Kirchies *et al.* 2001]. Therefore, if the transgenes are

introduced intravenously, they might be rapidly cleared from the circulation [Segura *et al.* 2001, Liu *et al.* 2002 and Parker *et al.* 2003].

In addition, the positively charged surface of polyplexes and lipoplexes are very important for cellular uptake. However, in the extracellular matrix, many endogenous negatively charged molecules such as serum albumin, glycosaminoglycans are present. The interactions between these endogenous molecules and the polyplexes or lipoplexes might result in the neutralization of the charges of the complexes and therefore prevent cellular association [Wiethoff *et al.* 2003]. Apart from the obstacles contributed by our body mechanisms or the internal environment, the size of the complexes is another key factor. In systemic gene delivery, in order to reach the target cells, the synthetic vectors and DNA complexes needs to travel in the blood circulation system to the target organs, then to the tissues, the interstitium and finally the target cells [Dufes *et al.* 2005]. If the complexes are too large, they may encounter resistance in penetrating these barriers and finally cannot reach the target sites.

1.4.2 Intracellular level

At the intracellular level, the endocytosis process, which involves binding of complexes onto the cell surface, internalization, formation of endosomes, lysosome fusion, and lysis of endosomes, is the major obstacle for gene delivery.

And this process also affects the integrity of the transgenes [Luo *et al.* 2003].

Endocytosis is a process in which the cells uptake external materials by engulfing them with the cell surface membrane. Once endocytosis is triggered, the cell membrane is infolded or extended to form a vesicular compartment [Soper *et al.*

1997], and the complexes are internalized. The internalized complexes are then targeted to the endo-lysosomal compartments, involving the direction of early endosomes to the late endosomes and subsequently to the lysosomes. If the

complexes cannot escape from the endosomes before the lysosome fusion takes place, the plasmid DNA will be degraded by the hydrolytic enzymes and the

nucleases carried by the lysosomes. Therefore, the successfulness of endosomal escape is one of the key factors for effective gene delivery [Luo *et al.* 2003 and Wiethoff *et al.* 2003].

Apart from the endo-lysosomal entrapment, the internalized complexes will also encounter the diffusional barrier of the cytoplasm [Lechardeur *et al.* 2002].

Inside the cytoplasm, other than the cytosol and the organelles, network of

cytoskeletons (e.g. actin filaments, microtubules and intermediate filaments) are also present. All these contribute to an intensive molecular crowding of the cytoplasm, which limits the diffusion of large sizes complexes [Lechardeur *et al.* 2002]. As a result, this will further decrease the number of complexes or intact plasmids that reach the nucleus.

1.4.3 Nuclear level

After the complexes have escaped from the endolysosomal compartment, the transgenes must be transported to the nucleus. However, transportation of genetic materials across the nuclear membrane is one of the major limiting steps for efficient non-viral gene delivery [van der Aa *et al.* 2006]. In order to translocate the transgenes to the nucleus of the non-proliferating cells, and allow an efficient localization of the transgenes into the nucleus for gene expression, the complexes of transgenes and carriers should either be smaller than the nuclear pore (~ 10 nm) for passive diffusion or has a nuclear localization signal (NLS) for active transport through the central channel of the NPC [Ludtke *et al.* 1999, Wiethoff *et al.* 2003 and Heiser 2004]. Figure 5 summarizes the barriers at the intracellular and nuclear levels.

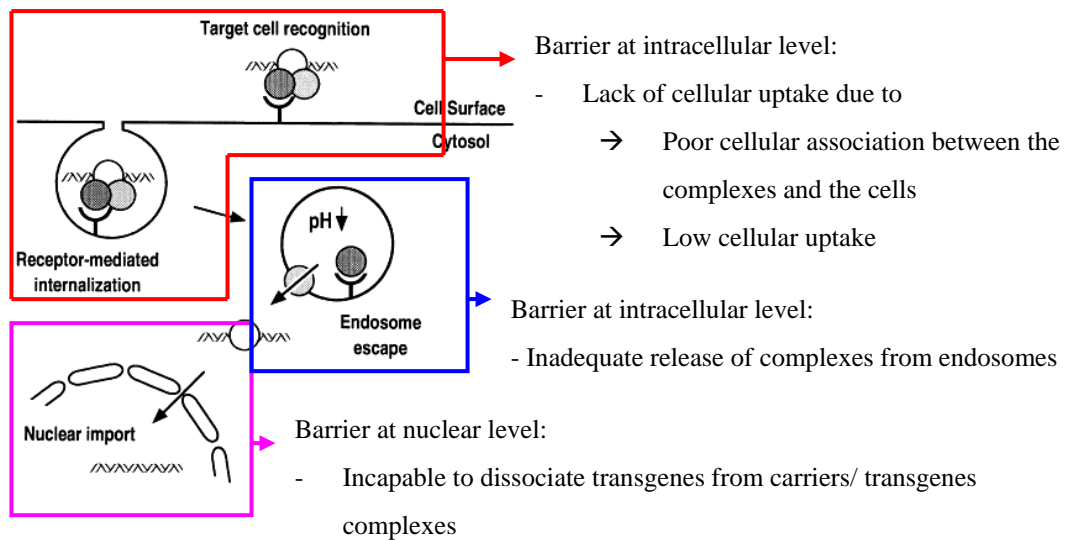


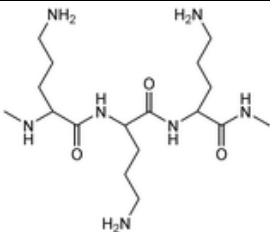
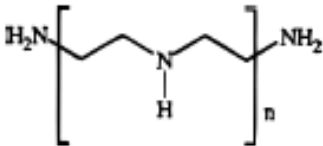
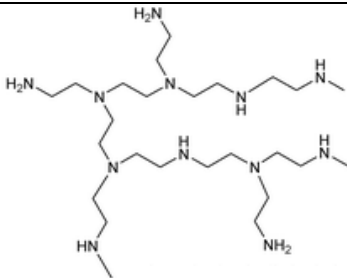
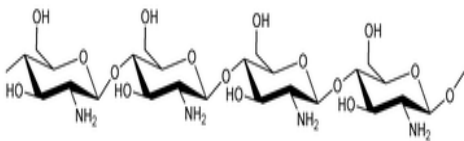
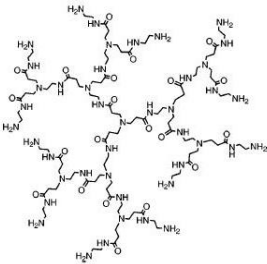
Figure 1.5: Barriers at intracellular and nuclear levels. (Figure is adopted from Uherek *et al.* 2000 and modified.)

1.5 Cationic polymer based gene delivery system

Among the different types of non-viral gene delivery system, polymeric gene delivery systems have received particular attention [Park *et al.* 2006]. Under this polymer-based category, polymers can be classified into three groups, neutral polymers [e.g. poly(ethylene) glycol, poly(vinyl) pyrrolidone], anionic polymers [e.g. poly(acrylate)] and cationic polymers [poly(ethylenimine), poly(vinylamine)] [Garnett 1999]. Cationic polymers are considered as the most promising and valuable candidates for use as gene carriers [Garnett 1999]. Table 1.3 illustrates the chemical structures of some commonly studied cationic polymers and summarizes some of the studies.

The use of cationic polymers as gene carriers was first reported in 1988 by Wu *et al.*, in which an asialooroso-mucoid-poly-(L)-lysine conjugate was used for hepatoma cell line transfection [Wu *et al.* 1988]. Unlike the cationic lipids, cationic polymers are highly water soluble molecules [Heiser 2004]. In general, all the cationic polymers contain very high charge density attributable to the presence of primary amines. Under physiological pH, these amine groups will be protonated, and provide positive charges to form stable complexes with nucleic acids (polyplexes). As a result, it is believed that the cationic polymers can protect the DNA from degradation, and the positive charges on the surface will enhance the cellular uptake process. Furthermore, these primary amine groups also provide useful functional sites for chemical modification, allowing different ligands and peptides to be easily conjugated to the polymers and improve the transfection efficiency [Segura *et al.* 2001].

Table 1.3: Chemical structures of some commonly studied cationic polymers. (De Smedt *et al.* 2000, Segura *et al.* 2001, Thomas *et al.* 2003 and Park *et al.* 2006)

Chemical Structure	Studies
 <p>Poly-L-lysine (PLL)</p>	<ul style="list-style-type: none"> - Pluronic-grafted poly-(L)-lysine [Jeon <i>et al.</i> 2003] - Galactosylated poly(L)-lysine with PLL MW 1.8, 13, 29 kDa [Nishikawa <i>et al.</i> 1998] - Folate-poly(ethylene glycol)-poly(L)-lysine conjugate with PLL MW 1kDa [Cho <i>et al.</i> 2005]
 <p>Linear Poly(ethylenimine) (Linear PEI)</p>	<ul style="list-style-type: none"> - 22 kDa PEI, <i>in vitro</i> and <i>in vivo</i> delivery to lung epithelial cells [Ferraris <i>et al.</i> 1997] - 22 kDa PEI, <i>in vivo</i> delivery to solid tumor [Coll <i>et al.</i> 1999]
 <p>Branched Poly(ethylenimine) (Branched PEI)</p>	<ul style="list-style-type: none"> - 25 kDa PEI, aerosol delivery in mouse lung [Gautam <i>et al.</i> 2000] - Acid- labile PEI [Kim <i>et al.</i> 2005] - PEG-PEI graft copolymers [Nguyen <i>et al.</i> 2000]
 <p>Chitosan</p>	<ul style="list-style-type: none"> - 150 kDa chitosan, <i>in vitro</i> study [Li <i>et al.</i> 2003] - Trimethylated chitosans, <i>in vitro</i> study [Kean <i>et al.</i> 2005] - 390 kDa chitosan, <i>in vitro</i> study [Mao <i>et al.</i> 2001]
 <p>Poly(amidoamine) Dendrimer (PAMAM)</p>	<ul style="list-style-type: none"> - Arginine-grafted PAMAM dendrimer [Kim <i>et al.</i> 2006 and Choi <i>et al.</i> 2004] - PAMAM dendrimers with a trimesyl core [Zhang <i>et al.</i> 2005] - Fractured PAMAM dendrimers, <i>in vitro</i> study [Tang 1996]

1.5.1 Poly(ethylenimine), PEI

So far, three different forms of cationic polymers have been used for transfection studies. They are the linear [e.g. spermine, poly-(L)-lysine], the branched [e.g. branched poly(ethylenimine)] and the spherical [e.g. dendrimers] forms. Among the several studied polymers, poly(ethylenimine) with various molecular weights has been revealed to be the most promising one.

PEI is a cationic polymer that has been widely used in industries with a broad range of molecular weights and different degrees of branching [Godbey *et al.* 1999b, Kircheis *et al.* 2001 and Bieber *et al.* 2002]. It is an organic polymer produced by the acid catalyzed polymerization of aziridine monomers (branched PEI) or 2-oxazoline monomers (linear PEI). In 1995, Boussif *et al.* demonstrated that PEI had a great potential as a gene carrier, and PEI has then been described as a “versatile vector”. Since then, PEI has an increasing popularity as a potential candidate for gene delivery [Godbey *et al.* 1999a and 2000]. Currently, PEI has been successfully used to transfect a variety of cells (e.g. 3T3, HepG2, COS-7, HeLa, EA.hy 926, B16), and *in vivo* studies in mice and rat have been carried out (e.g. adult mice’s brain, rat kidney, Newborn mice’s liver) [Boussif *et al.* 1995, Abdallah *et al.* 1996, Boletta *et al.* 1997, Kircheis *et al.* 1997, Godbey *et al.* 1999a, Godbey *et al.* 1999c and Kircheis *et al.* 2001].

Apart from having a vast diversity of structures, i.e. with different molecular weights and branching, PEI also has the highest cationic charge density, making it the most promising cationic polymer for non-viral gene delivery system [Kircheis *et al.* 2001, Ahn *et al.* 2002 and Heiser 2004]. This high positive charge density provides a strong DNA binding and a strong proton buffering capacity, contributing to its excellent transfection efficiency.

Branched PEI consists of 25%, 50% and 25% of primary, secondary and tertiary amines, respectively. Its primary amines are reported to form complexes with nucleic acids via electrostatic interactions [Ahn *et al.* 2002]. While for the secondary and tertiary amines, since only two thirds of amines are protonated at the physiological pH [Kircheis *et al.* 2001], they are reported to provide a buffering capacity over a wide range of pH [Godbey *et al.* 1999b, Ahn *et al.* 2002, Heiser 2004 and Cook *et al.* 2005]. Therefore, PEI is able to protect the nucleic acid from enzymatic degradation by buffering the acidic pH of the lysosome and inhibiting the activities of the lysosomal nucleases [Kuo 2003 and Zhu *et al.* 2005]. In addition, once the PEI is in the endosome, it will be protonated and intramolecular charge repulsion will occur. As a result, an influx of chloride ions is triggered, osmotic swelling occurs and subsequently the endosome ruptures. Finally, the polyplexes are released into the cytoplasm. This

phenomenon is called the “proton sponge effect” [Pollard *et al.* 1998 and Breunig *et al.* 2004], and is hypothesized to facilitate “endosomal escape” of the polyplexes. Consequently, this allows sufficient gene transfer without the need of endosome disruptive reagents (e.g. chloroquine) [Cook *et al.* 2005].

Although PEI has a high complex stability and high transfection efficiency, like other cationic polyplexes, it tends to aggregate in aqueous solution, and becomes poorly soluble in water. As a result, large particle complexes with a broad size distribution are formed and this leads to poor diffusion in the vascular periphery [Zhu *et al.* 2005]. Furthermore, cytotoxicity and non-specific interaction with biological components are the two hurdles that still await overcoming [Agarwal *et al.* 2005 and Cook *et al.* 2005].

1.6 Development of non-viral gene delivery systems

Today, there is still no single system that can provide the efficiency, safety and stability required for clinical use. According to Yang *et al.* (2006) human gene therapy is still in its experimental stage, and “has not proven very successful in clinical trials”. So, many exploratory studies are still being carried out.

In developing the gene transfer systems, scientists usually use two main strategies. The first strategy is the continuous exploring of new materials for use

as gene carriers. Recently, with the advanced development of nanotechnology, nanomaterials, with their unique sub-cellular and sub-micron size properties that make them superior in many human activities, have attracted increased attention as potential therapeutic carriers [Panyam *et al.* 2003, Salata 2004 and Yang *et al.* 2006].

The second strategy is the modification of existing carriers in order to overcome obstacles at different levels. For nanoparticles, surface modification is the most commonly used method. Desirable agents (e.g. cells specific targeting ligands, endosomal lysis agents, nuclear targeting agents) are linked to the particle surface to form different types of conjugates. For example, PEI-poly(ethylene glycol) copolymer can minimize the non-specific interaction with the fibrinogen, and allows longer circulation time for the polyplex to reach its target [Godbey *et al.* 1999b and Curiel *et al.* 2005]. Surface-shielded transferrin-poly(ethylenimine) has also been shown to has target gene (e.g. tumor necrosis factor-alpha) expression in distant tumors and inhibit tumor growth after systemic application [Kircheis *et al.*, 2002 and Curiel *et al.*, 2005].

1.7 Our amphiphilic cationic core-shell nanoparticle

Although nanoparticles can be tailor-made and synthesized easily, the encapsulation of large hydrophilic DNA molecules into very small hydrophobic nanoparticles has proven to be very difficult. Recently, our research team has developed a novel systemic method, which has already been patented, to prepare well-defined amphiphilic core-shell nanoparticles with different sizes, compositions, structures and functions. This is done by the process of graft copolymerisation in which a vinyl monomer is grafted onto an amine-containing water-soluble polymer. And finally, latex of monodispersed core-shell nanoparticles is generated. These core-shell particles have the combined properties of cationic polymers, nanoparticles and surface functional groups, thus making them excellent candidates as gene carriers in gene delivery systems.

In this project, poly(methyl methacrylate)-poly(ethylenimine) [PMMA-PEI] amphiphilic core-shell nanoparticles synthesized by our novel patented method were used for study. MAA was copolymerised with the cationic branched 25 kDa PEI in a 1 to 2 ratio (w/w). Each of the nanoparticles resulted has a PMMA hydrophobic core and a PEI hydrophilic shell. In our previous study, the ratio of 1:2 was found to be the best ratio. By using this ratio, we can obtain a stable core-shell complex that can maintain a narrow size distribution after complexing

with plasmid DNA [Zhu *et al.* 2005].

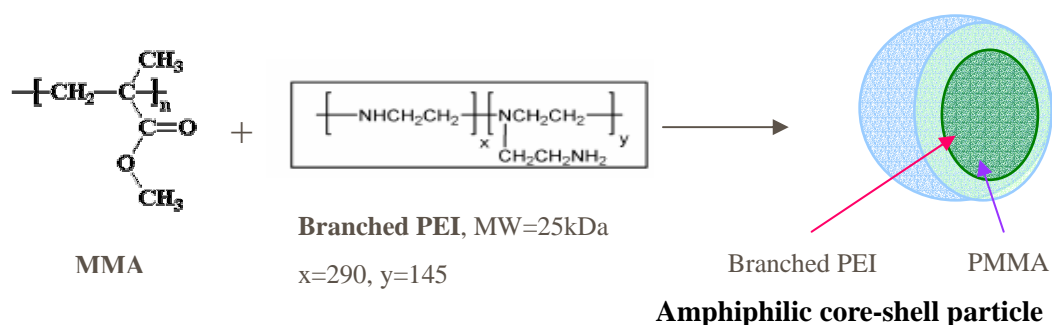


Figure 1.6: Graft copolymerization of MAA and 25 kDa branched PEI to form an amphiphilic core-shell nanoparticle.

1.7.1 Characterization of the PMMA-PEI amphiphilic core-shell nanoparticles

Under the transmission electron microscope (TEM), our PMMA-PEI nanoparticles are spherical in shape with a well defined core-shell nanostructure and hairy PEI shells. Zeta potential and particle size measurements showed that our nanoparticles have a positive surface charge of around +40 mV and with a mean size of 146 nm in diameter. The high positive zeta potential indicates that the PMMA-PEI core-shell nanoparticles are very stable in the aqueous environment and can complex with the negatively charged DNA.

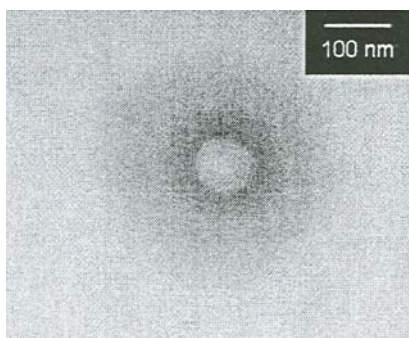


Figure 1.7: Transmission electron micrograph (TEM) of a PMMA-PEI core-shell nanoparticle at high magnification. (The micrograph is adopted from Zhu *et al.* 2005.)

1.7.2 Previous experimental results in using PMMA-PEI as a gene carrier

Previously, we have studied the possibility to use PMMA-PEI core-shell nanoparticles as a new gene delivery system. The properties of this new system are summarized in Table 1.4 and the data has been published in *Bioconjugate Chemistry* [Zhu *et al.* 2005].

Table 1.4: Summary of PMMA-PEI properties as a gene carrier [Zhu *et al.* 2005].

Studies	Properties
Plasmid complexation	PMMA-PEI can form stable complexes with plasmids. The size of the polyplexes is approximately 120 nm in diameter and is highly monodispersed.
Disassembly Assay	The condensed plasmids in the polyplexes remain intact and can be disassembled from the nanoparticles by poly(aspartic acid).
DNase I Protection Assay	The condensed plasmids in the polyplexes are protected from DNase I enzymatic degradation.
Cytotoxicity Assay	Less toxic than the 25 kDa branched PEI
Transfection Study	More efficient as gene carriers in transfecting cells than the 25 kDa branched PEI.

All the above properties indicate that the PMMA-PEI core-shell nanoparticle has a great potential as a carrier for gene delivery. Thus in this project, we are going to further improve the transfection efficiency of this system. One of our ideas is the addition of a nuclear targeting component to the nanoparticle-DNA complex to see whether it can enhance the nuclear translocation process. The nuclear protein, HMGB1, being the most abundant and ubiquitous non-histone protein in the nucleus, was chosen as the nuclear targeting ligand in this study.

1.8 High mobility group proteins

1.8.1 Classification of HMG

The high mobility group proteins belong to a family of non-histone chromosomal proteins, which are expressed ubiquitously in the nucleus of higher eukaryotic cells. They were first discovered by Goodwin, a British scientist in the 1970s and were identified and named according to their high mobility property in polyacrylamide gel electrophoresis [Bianchi *et al.* 2000]. Traditionally, the HMG family consists of six proteins and is subdivided into three subfamilies: the HMG-1/-2 subfamily, the HMG-I/Y subfamily and the HMG-14/-17 subfamily [Bustin 1999]. However, with the discovery of more HMG-like nuclear proteins, HMG proteins are now being referred to the canonical HMG proteins (the

traditional HMG proteins) as well as the HMG-motif proteins (HMG like nuclear proteins). The HMG-motif proteins are different in sequence but with functional domains of similar tertiary structure to that of the canonical HMG proteins. Recently, the HMG subfamilies were renamed according to their characteristic functional sequence motif (the DNA or chromatin binding motif). They are now called the HMGA subfamily, the HMGB subfamily and the HMGN subfamily [Bustin 2001 and Catez *et al.* 2004]. The HMGA proteins are the subfamily of HMG proteins that contain the “AT-hook” as the functional motif. While for the HMGB and the HMGN proteins, their functional motifs are the “HMG-box” and the “nucleosomal binding domain” respectively.

1.8.2 Structure of high mobility group box 1 protein (HMGB1)

The high mobility group box proteins consist of three members: HMGB1, HMGB2 and HMGB3. Among these three proteins, HMGB1 is the most abundant one and is a 25 kDa, highly conserved, 215 amino acids protein which has been investigated for approximately 30 years [Pullerits *et al.* 2003, Andersson *et al.* 2004]. It has 99% identity among all mammals and only two residues out of its 215 amino acids are substituted in rodent and human versions [Erlandsson Harris *et al.* 2004]. Furthermore, it is a non-histone chromosomal

protein and is characterized by its distinct three domains structure.

HMGB1 contains two HMG box domains, the HMG box A (amino acids 1-79) and the HMG box B (amino acids 89-163), at the N-terminal. These two HMG boxes are homologous folded with 80 amino acid residues, in which 29% of them are identical and 65% are similar [Degryse *et al.* 2001]. Furthermore, they are formed by two short and one long three alpha helical segments, twisted into a L-shaped structure [Sutrias-Grau *et al.* 1999]. The HMG boxes are basic in nature and bind to the negatively charged DNA in the nucleus [Imamura *et al.* 2000]. At the C-terminal of the HMGB1 protein, there is a polyacidic tail (amino acids 186-215). This acidic domain contains a run of 30 aspartate and glutamate residues and is linked to the HMG box B by about 20 amino acid residues [Baxevanis *et al.* 1995 and Thomas *et al.* 2001]. This polyacidic tail is negatively charged and interacts with the histone proteins [Imamura *et al.* 2000].

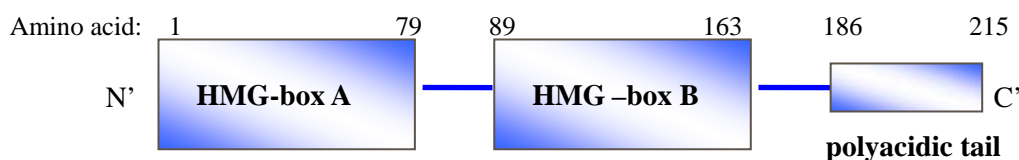


Figure 1.8: Domain organization of HMGB1. (Figure is adopted from Yang *et al.* 2005 and modified.)

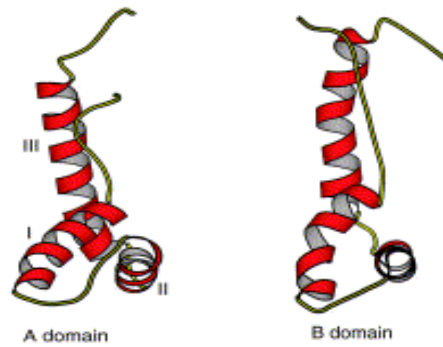


Figure 1.9: Solution structure of the HMG box A and B of the HMGB1 protein. (Figures are adopted from Thomas *et al.* 2001.)

1.8.3 Intracellular functions of HMGB1

HMGB1 protein is relatively abundant in all tissues and species. It is present in more than 1 million copies per single nucleus [Degryse *et al.* 2001], around one tenth that of the histones [Bustin 1999]. It was found that HMGB1 protein participates in many DNA-related activities that involve changes in the structure of the DNA and organization of the chromatin fibers [Bustin 1999]. These activities include transcription regulation, chromosomal replication, recombination, chromatin assembly or disassembly and DNA repair [Stros *et al.* 1994, Wunderlich *et al.* 1997 and Lee *et al.* 2000].

HMGB1 binds DNA through the minor groove. This expands the groove, facilitates the unwinding of DNA and induces considerable bending of the double helix [Bustin 1999, Ina *et al.* 2000 and Li *et al.* 2003]. In general, HMGB1

protein binds DNA without sequence specificity but with structural preferences, i.e. they have high affinity for the distorted DNA and linear DNA [Thomas 2001], e.g. cruciform DNA, single strand DNA, *cis*-platin induced kinks, stem loops, four-way junctions and bent DNA [Stros *et al.* 1994, Lee *et al.* 2000 and Lum *et al.* 2001]. In addition, HMGB1 also binds to the negatively supercoiled DNA preferentially, and protects relaxation in the negatively supercoiled DNA in the presence of topoisomerase I [Sheflin *et al.* 1993 and Stro *et al.* 1994]. In general, HMGB1 protein is described as an architectural element and also acts as molecular chaperon.

Being a nuclear protein, HMGB1 protein facilitates the formation of nucleoprotein complexes, determines the nucleosomal structure and stability. It also binds the chromatin with bends and kinks structures at exit and entry points to the nucleosome [Thomas 2001].

Furthermore, several *in vitro* studies suggested that HMGB1 protein plays a role in gene regulation as a *trans* activator or quasi-transcription factor [Aizawa *et al.* 1994]. It was found that HMGB1 protein has interactions with several transcriptional activators and which in turn interacts with transcription factors (TF) IID, (TF) IIA and (TF) IIA [Sutrias-Grau *et al.* 1999]. As a result, this facilitates the binding of the transcription factors to the template strand and forms

the transcription initiation complex. Furthermore, HMGB1 was found to have an opposite action with those of H1 histone. Some scientists proposed that HMGB1 competes with H1 histone for four way junctions [Varga-Weisz *et al.* 1994] and to relax the chromatin structure [Chau *et al.* 1998]. In other words, HMGB1 may help to unwind or fluidize the chromatin [Agresti *et al.* 2003]. Apart from this, the HMGB1 protein also helps certain steroid hormone responsive elements to bind their appropriate receptors (e.g. binding of estrogen receptors to the estrogen responsive elements), and as a result it enhances the transcriptional activity [Verrier *et al.* 1997]. Besides transcription, the HMGB1 protein has also been found to participate in the V(D)J recombination process of the immunoglobulin gene. During this process, the lymphocyte-specific proteins recombination activating gene (RAG) 1 and 2 recruit HMGB1 protein to the cognate binding sites. Through the protein-protein interaction, DNA is bent, and now, an appropriate length between two recombination signals (12-RSS or 23-RSS) are produced and so the V(D)J recombination process occurs [van Gent *et al.* 1997, Swanson 2002 and Bergerons *et al.* 2006].

1.8.4 HMGB1 as a novel gene delivery system

The HMGB1 protein has two features that make it an interesting candidate for use as a gene delivery system. The HMGB1 protein has nucleophilic sequences, which are the HMG boxes. This enables HMGB1 to bind and condense DNA. This HMGB1-packaged DNA has a diameter of 40 nm only and is in a compact spherical shape [Wunderlich *et al.* 1997]. Therefore it may be favored in transfecting cells. In fact, it has been reported that the HMGB1 protein can enhance the transfection efficiency in both naked DNA and liposome-mediated transfection. When DNA is packed with HMGB1, condensed molecules can be formed and the transfection efficiency is approximately similar to the calcium phosphate method [Bottger *et al.* 1988 and Bottger *et al.* 1998].

Apart from its DNA binding ability, the nuclei-trafficking property of the HMGB1 protein is also considered as an important feature. In the HVJ-liposome system, HMGB1 protein is served as a DNA binding protein. Within the nuclear envelop, it assists nuclear access and promotes gene stabilization [Hangai *et al.* 1996 and Isaka *et al.* 1998].

1.8.5 Nuclear localization signal

There are a number of barriers that restrict the success of gene delivery, but the inefficient gene transfer from the cytosol to the nucleus has recently been considered as the major limiting step, especially in postmitotic and quiescent cells [Bremner *et al.* 2004]. By learning from the viruses which have evolved to have nuclear trafficking property, some studies suggest that the use of nuclear localization signal (NLS), which have the ability to interact with nuclear receptors (such as importin beta and transportin), might improve the cyto-nucleoplasmic transport through the nuclear pores [Escricous *et al.* 2003, Bremner *et al.* 2004 and van der Aa *et al.* 2006].

Nuclear localization signals are often basic, positively charged and containing several lysine and arginine residues. They may be either mono or bipartite [Hebert 2003]. Although the nuclear localization signal of HMGB1 is not yet found, the nuclear localization signals of some transcription factor-type HMG proteins have been identified in the HMG domain. Furthermore, some of them may have similar amino acid sequences with HMGB1 [Hebert 2003 and Harris *et al.* 2006]. Besides, cytosolic microinjection experiments have demonstrated that HMGB1 protein can reach the nuclei of HeLa cells and bovine fibroblasts in a few minutes [Rechsteiner *et al.*, 1979]. Since the gene transfected into eukaryotic

cells needs to be targeted to the nucleus before gene expression can take place, the HMGB1 protein is a very attractive nuclear targeting agent for gene delivery.

1.8.6 Interaction between the HMGB1 protein, DNA and the nanoparticle

In this project, we investigated the effect of the HMGB1 protein as a component in our core-shell nanoparticle gene delivery. When the HMGB1 protein is added to the PMMA-PEI nanoparticle and plasmid DNA, the HMG boxes may bind with the negatively charged DNA and the C-terminal acidic tail may interact with our cationic PMMA-PEI core shell nanoparticle to reinforce the stability of the complex. The effects of different complexing orders were studied, as these will affect the topology of the complexes and thus will affect the efficiency of the new system. In addition, the HMGB1 protein may offer additional protection to the plasmid DNA from nuclease degradation and may enhance the transfection efficiency by acting as a nuclear targeting ligand.

Chapter 2: Materials and methods

2.1 Extraction and purification of HMGB1 protein from pig thymus

(according to the methodology of Goodwin *et al.* (1975), with some modifications as below.

2.1.1 Collection of nuclear pellet from pig thymus

316 mg of pig thymus was collected from the Tsuen Wan Slaughterhouse. The minced thymus tissue was homogenized with 2.8 folds (w/v) of 0.075 M NaCl, 0.025 M EDTA (pH8.0) at 11,000 rpm by Ultraturra. The tissue was further homogenized at 11,000 rpm in a domestic blender (Janson SG260-C). After that, the homogenate was filtered through double cheesecloth to remove connective tissue and then centrifuged at 4 °C, 2000 X g for 30 min (by using Centrifuge with Beckman AJ10 rotator). The pellet was then saved and washed thrice more with 2.8 folds (w/v) of 0.075 M NaCl, 0.025 M EDTA, by blending 2 min (stop every 30 s) and centrifuging at 4 °C for 20 min, 15 min and 15 min respectively.

2.1.2 Extraction of HMG proteins

The saved pellet (chromatin) was then extracted three times with 0.35 M NaCl, 10 mM Tris-HCl (pH 7.5) by blending at half speed for 2 min (stop every 30 s), followed by centrifugation at 4 °C, 4000 X g for 15 min. The volume of extraction buffer was roughly equal to the weight of the tissue. The total extract (the supernatant) was made 2% (w/v) with respect to trichloroacetic acid (TCA) by the addition of 100% (w/v) TCA solution. The homogenate was held on ice for 90 min for protein extraction. The precipitate was removed by centrifugation at 4 °C, 4000 X g for 15 min, and the supernatant was filtrated through GA55 glass filter paper (Advance Tech, Toyo) by using a vacuum pumping system.

The total HMG protein was isolated from the clear filtrated supernatant by acetone precipitation. The supernatant was first made up to 0.3 M hydrochloric acid (HCl) by the addition of 10.17 M HCl. Then six times volumes of cold acetone was added. The mixture was kept on ice for 60 min, and the precipitate was collected by centrifugation at 4 °C, 4000 X g for 15 min. The pellet was then washed twice with cold acetone/ 0.1 M HCl (6:1 v/v) and thrice with pure acetone. The washed pellet was then freeze dried for 3 days.

2.1.3 Fractionation of HMG proteins by CM-Sephadex C25 chromatography

The total HMG proteins were re-dissolved in 7.5 mM sodium borate buffer (pH 8.8), and dialyzed overnight against 1 L of 0.15 M NaCl, 7.5 mM sodium borate buffer (pH8.8). The dialyzed sample was then clarified by centrifugation at 4 °C, 9000 X g for 30 min, and was applied to a 3.5 X 25 cm Carboxymethyl (CM)-Sephadex C25 ion exchange column (Sigma).The column was equilibrated with 7.5 mM sodium borate buffer (pH 8.8) previously and the HMGB1 proteins were then eluted by a liner salt gradient with a flow rate of 1 mL/min. The liner salt gradient was generated by using two chambers of gradient forming device, each containing 600 mL 0.15 M NaCl and 2 M NaCl in 7.5 mM borate buffer (pH 8.8). 3 mL fractions were collected and the absorbances at 280, 230 nm of eluate were measured by spectrometer.

2.1.4 Confirmation of HMGB1 protein by SDS-PAGE and western blotting

Different fractions were pooled according to the peaks in the chromatogram. The pooled fractions were then analyzed on a SDS-12% polyacrylamide gel. The samples were mixed with appropriate amounts of loading buffer (contained β -mercaptoethanol and bromophenol blue). Together with the SDS-PAGE standard low range marker (Bio-Rad), they were boiled for 10 min and loaded

into the wells of the gel respectively. The electrophoresis was performed at 100 V for 15 min and changed to 200 V for another 50 min.

After finished the gel electrophoresis, proteins on the gel were transferred to a PVDF membrane (Milipore) by semi-dry blotting (Bio-Rad) at 15 V for 30 min. The membrane was then blocked in Tris-buffered saline containing 0.1% Tween-20 (TBS-T) and 5% w/v non-fat milk for 2 hours and was probed with a monoclonal mouse IgG anti-HMGB1 antibody (1:1000 dilution; Stressgen Bioreagents Corporation) for another 1 hour. Horseradish peroxidase goat anti-mouse IgG conjugate (1:2500 dilution; Zymed Laboratories Inc.) was incubated with the blot for 1 hour and the HMGB1 protein was visualized by SuperSignal West Pico substrate (Pierce). The image was photographed by Lumi-ImagerTM (Roche Molecular Biochemical).

2.1.5 Concentration of HMG proteins and buffer exchange

The fractions with the pure HMGB1 were concentrated by Amicon[®] Ultra-15, with 10,000 Nominal Molecular Weight Limit (Millipore). 15 mL sample was loaded into the Amicon and was centrifuged at 4 °C, 3500 rpm for 15 min by a swinging bucket rotator. Steps were repeated until the protein sample was concentrated to 1 – 2 mL. 15 mL of 0.15 M NaCl, 10 mM Tris-HCl (pH 8.0) was

loaded into the Amicon and was centrifuged at 4 °C, 3500 rpm for 15 min. Buffer exchange was performed two times more. The retentate was aliquot and store at -80 °C.

2.1.6 Determination of protein concentration

The concentration of the purified HMGB1 protein was determined by Bradford Assay. The Bradford dye was prepared by diluting 1 part dye reagent concentrate (Bio-Rad) with 4 parts of deionized distilled water (ddH₂O). 10 µL of sample solution was mixed with 190 µL of diluted dye reagent, and incubated at room temperature for 10 min. Absorbance at 595 nm was measured by 550 Microplate Readers (Bio-Rad). All the measurements were performed in duplicate. A bovine serum albumin (BSA) standard curve ranging from 1 - 6 µg was performed for calibration.

2.2 Mini-preparation of plasmid

In this project, the commercially available pGL-3-Control (Promega) plasmid was used. This plasmid contains a SV40 promoter and enhancer in order to drive the expression of the firefly luciferase reporter gene encoded.

The pGL-3-Control plasmid was amplified in the transformed JM109 *E.coli* cells

by first plating the frozen cells on Luria Bertani (LB) agar plate with 50 µg/mL ampicillin, with streak plate technique, and was incubated at 37°C for overnight (16 hours). A single isolated colony was then picked up from the plate and subcultured in 5 mL LB broth supplemented with 50 µg/mL ampicillin. The broth was then shaken overnight at 37 °C, 250 rpm.

The amplified plasmid was then purified by using the Rapid Plasmid Miniprep Purification System (Marligen Bioscience Incorporated). Bacterial cells were collected from 1 mL overnight culture by centrifugation at 9000 rpm for 1 min. Steps were repeated until 5 mL of overnight culture were harvested. The pelleted bacterial cells were then resuspended in 250 µL Cell Suspension Buffer with RNase A. 250 µL of Cell Lysis Solution was added to the suspension and mixed gently by inverting the tube for 5 times. The whole tube was incubated at room temperature for 5 min. 350 µL of Neutralization Buffer was added and the solution was gently mixed by inverting the tube for another 5 times. The whole tube was then incubated on ice for 5 min and cloudy precipitates were observed. After 5 min incubation, the solution was then centrifuged at 13000 rpm for 10 min. The supernatant was saved, loaded into a spin cartridge and centrifuged at 13000 rpm for 1 min. The spin cartridge was then washed by 500 µL of Optional Wash Buffer followed by 700 µL of Wash Buffer, with centrifugation at 13000

rpm for 1 min respectively. Another 1 min centrifugation was performed. 75 μ L of pre-warmed TE Buffer was added to the center of the spin cartridge and incubated at room temperature for 1 min. The plasmid DNA was then collected by centrifugation at 13000 rpm for 2 min.

2.3 Determination of plasmid concentration and purity

The concentration and the purity of the plasmid were measured by ultraviolet absorbance with a GeneQuant DNA/RNA calculator (Pharmacia Biotech). The diluted plasmid was then added to a quartz cuvette and placed into the DNA calculator. And finally different parameters (Abs_{260nm} , Abs_{280nm} , $Abs_{260nm/280nm}$, double stranded DNA concentration and purity) were recorded.

For the GeneQuant DNA/RNA calculator, the concentration of double stranded DNA was equivalent to 50 μ g/mL, when Abs_{260nm} was equal to 1 in a 10 mm pathlength cell. And the purity of the plasmid was determined by $Abs_{260nm/280nm}$.

Ratios with values lower than 1.8 indicates the presence of contaminants.

2.4 Plasmid size confirmation

In order to confirm the identity of the purified plasmid, the molecular size of the plasmid was checked by double restriction digestion followed by agarose gel

electrophoresis.

2.4.1 Double restriction digestion

0.3 µg of purified plasmid DNA was cut by *BamHI* and *HindIII* in 1 X Buffer K (Amersham Biosciences). The reaction mixture was centrifuged briefly and incubated at 37 °C for 3 hours.

2.4.2 Agarose gel electrophoresis

The agarose gel was prepared by dissolving 0.8% (w/v) agarose in 0.5 X Tris-borate EDTA (TBE) buffer containing 0.5 µg/mL ethidium bromide (EtBr). The samples were mixed with appropriate amounts of 6 X blue/orange loading dye (Promega) and loaded into the wells of gel respectively. A 1 kb DNA Step Ladder Marker (Promega) was also added in a separate well. Electrophoresis was performed at 80 V for 1.5 hours. The plasmid DNA in the gel were visualized by ultraviolet transillumination and photographed by a Lumi-ImagerTM (Roche Molecular Biochemical).

2.5 Formation of HMGB1-DNA complexes

Different amounts of HMGB1 were mixed with 0.3 µg of pGL-3-Control plasmid in 0.15 M NaCl, 10 mM Tris-HCl complexing buffer (pH 8.0) [Bottger

*et al.*1990 and Mistry *et al.* 1997]. The mixtures were then incubated at room temperature for 30 min [Mistry *et al.* 1997]. The formation of HMGB1-DNA complexes were studied by agarose gel retardation assay (AGRA) and the optimal ratio between HMGB1 and DNA was determined for complex formation.

2.6 Formation of HMGB1-DNA-nanoparticle complexes

Different amounts of the nanoparticle (PMMA-PEI core shell nanoparticle) were mixed and incubated with 0.3 µg of pGL-3-Control plasmid and appropriate amounts of HMGB1, according to the complexing ratio determined in Section 2.5. The complexing ratio between the nanoparticle and DNA was expressed as PEI nitrogen to DNA phosphate ratio (N/P), in which 15.05 µg of PMMA-PEI contains 100 nmol of amine nitrogen and 1 µg of DNA contains 3 nmol of phosphate [Boussif O. *et al.* 1995 and Gautam A. *et al.* 2000]. Different complexing orders were studied and the formation of HMGB1-DNA-nanoparticle complexes was analyzed by agarose gel retardation assay (AGRA) with a 0.8% agarose gel.

2.7 Release of DNA from the HMGB1-DNA-nanoparticle complex

The ability to release of the DNA from the HMGB1-DNA-nanoparticle complex and the integrity of the released DNA were investigated by the addition of poly(aspartic acid) [pAsp] (Sigma). pAsp were mixed with nanoparticle-DNA and HMGB1-DNA-nanoparticle complexes in a pAsp to DNA molar ratio of 100. The mixture was then incubated at room temperature for 2 hours. The released DNA was analyzed with 0.8% agarose gel electrophoresis. The molar ratios between the pAsp and 0.3 µg of pGL-3-Control plasmid were calculated using the value that 0.3 µg of the plasmid has 8.648×10^{-14} mol of nucleotides.

[Number of mole of nucleotides for 0.3 µg pGL-3-Control plasmid:

$$(0.3 \times 10^{-6}) \text{ g} / (5256 \times 660 \text{ g/mol}) = 8.648 \times 10^{-14} \text{ mol}]$$

2.8 Protection against DNase I digestion

HMGB1-DNA-nanoparticle complexes were mixed with different amounts of DNase I (Amersham Pharmacia Biotech Inc.) in 1 X Digestion Buffer (6 mM MgCl₂, 40 mM Tris-HCl pH 7.5) and incubated at 37 °C for 10 min. The DNase I was then inactivated by adding 0.5 X EDTA (to a final concentration of 50 mM) followed by heating at 80 °C for 5 min. The DNA was then released from the complexes by incubating with pAsp as described in Section 2.7. Their integrities

were examined by 0.8% agarose gel electrophoresis.

2.9 Cell culture

The MCF-7 cells (human breast adenocarcinoma) and HeLa cells (human cervix adenocarcinoma) were cultured in Dulbecco's modified Eagle's medium (DMEM) with high glucose (Hyclone) for MCF-7 and low glucose (Hyclone) for HeLa cells, respectively, and supplemented with 10% (v/v) heat-inactivated fetal bovine serum (FBS, Hyclone), 1% penicillin /streptomycin (P/S, Hyclone) at 37 °C, 5% CO₂. The cells were subcultured when they reached 70-80% confluency, and passaged at 3-5 days intervals in a 1:3-1:4 dilution.

2.10 In vitro cell transfection studies

MCF-7 cells were seeded in 24 well plates (Iwaki) at an initial density of 1.2×10^5 cells per well and the plates were incubated at 37 °C, 5% CO₂ for 24 hours. After incubation, the medium was removed and the cells were washed with 500 µL 1 X phosphate buffered saline (PBS) twice. LipofectamineTM 2000 (Invitrogen) was prepared according to the manufacturer's manual. The nanoparticle-DNA and HMGB1-DNA-nanoparticle complexes were prepared according to Zhu *et al.* (2005) and the conditions determined in Section 2.5. Before complexing, plasmid DNA, HMGB1 protein and nanoparticle were

diluted in 50 μL of serum and antibiotic free high glucose DMEM medium, respectively. After complex formation, 150 μL of each complex suspension with 0.4 μg of pGL-3-Control plasmid was added to each well containing serum and antibiotics free medium. After 4 hours incubation at 37 $^{\circ}\text{C}$, 5% CO_2 , the medium was replaced with high glucose DMEM supplemented with 10% FBS, 1% P/S and incubated for another 20 hours.

2.11 Determination of transfection efficiency by Luciferase Assay and

Bradford Assay

After an additional 20 hours of incubation, the expression level of the firefly luciferase reporter gene was analyzed by Luciferase Assay System (Promega) and the results were normalized with the total protein content determined by Bradford Assay (Bio-Rad).

Medium in the wells was first removed and the cells in each well were washed with 500 μL 1 X PBS twice. The cells were then removed and lysed by the addition of 100 μL 1 X passive lysis buffer (PLB). The plates were then incubated at room temperature with gently shaking for 30 min. After 30 min, 20 μL of the cell lysate was transferred into an Eppendorf tube containing 35 μL of firefly luciferase substrate. The relative luminescence unit (RLU) was measured

with a Turner Designs TD-20/20 Luminometer (Promega), programmed with 2 s delay followed by 10 s reading.

After the Luciferase Assay, the remaining cell lysate were collected and centrifuged at 13000 rpm 4°C for 5 min. The supernatant from each samples were saved for Bradford Assay. 10 µL of supernatant of each sample was transferred to a 96 well plate for Bradford assay (refer to Section 2.1.7). The total protein content for each sample was determined by the BSA standard curve. And the transfection efficiency was expressed as RLU/mg of total protein. For preparation of the BSA standard curve, 1 X PLB was used for BSA dilution.

2.12 Cell viability assays

MCF-7 cells were seeded in 96 well plates (Iwaki) at an initial density of 5×10^3 cells per well and the plates were incubated at 37 °C, 5% CO₂ for 24 hours. After incubation, the medium was removed and the cells were washed with 100 µL 1 X phosphate buffered saline (PBS) twice. LipofectamineTM 2000 (Invitrogen), nanoparticle-DNA complexes and HMGB1-DNA-Nanoparticle complexes were prepared at room temperature. 50 µL of each complex suspension with 0.1 µg of pGL-3-Control plasmid were added to each well. After 4 hours of incubation at 37 °C, 5% CO₂, the medium was replaced with high glucose DMEM

supplemented with 10% FBS, 1% P/S and incubated for another 20 hours.

20 μ L of Cell Titer96[®] AQ_{ueous} One Solution (Promega) was added to each well of the 96 well plates containing the samples in 100 μ L culture medium. After 3 hours of incubation at 37 °C, 5 % CO₂, the amount of soluble formazan produced by cellular reduction of the MTS [3-(4,5-dimethylthiazol-2-yl)-5-(3-carboxymethoxy phenyl)-2-(4-sulfophenyl)-2H-tetraolium-inner salt] was quantified by measuring the absorbance at 490 nm (550 Microplate Readers, Bio-Rad). The relative cell viability was calculated as following equation:

$$\text{Relative cell viability (\%)} = (\text{Abs}_{490\text{nm}} \text{ of sample} / \text{Abs}_{490\text{nm}} \text{ of control}) \times 100$$

2.13 Nanoparticle trafficking studies by confocal laser scanning microscopy

(LSM)

In order to study the intracellular pathway and cellular uptake of our new non-viral gene delivery system (HMGB1-DNA-Nanoparticle complex), fluorescent labeling technique and confocal microscopy were used.

2.13.1 Labeling of PMMA-PEI core shell nanoparticle and PEI with fluorescein isothiocyanate (FITC)

0.7 mg of PEI of PMMA-PEI nanoparticle (5 mg/mL) and 0.2 mg of PEI polymer (2 mg/mL) were mixed with FITC (Sigma) in borate buffer (0.1 M, pH 8.5), respectively. These reaction mixtures were then incubated at 37 °C on a shaker for 4 hours. The unbound FITC were removed by dialysis against 1 L of deionized distilled water (ddH₂O) overnight. The labeled nanoparticles and PEI polymers were stored at 4 °C before used.

2.13.2 Labeling of pGL-3-Control plasmid with tetramethyl-rhodamine (TM-rhodamine)

pGL-3-Control plasmid was labeled with TM-rhodamine by using the *Label IT*[®] TM-Rhodamine Nucleic Acid Labeling Kit (Mirus). 5 µg of plasmid was mixed with 5 µL of *Label IT* Reagent in 1 X Labeling Buffer A. The reaction volume was loaded up to 50 µL by molecular biology-grade H₂O. The reaction mixture was centrifuged and the tube was sealed with parafilm, incubated at 37 °C for 2 hours. The microspin column was prepared by first resuspending the resin by vortexing. Then the excess buffer in the column was removed by centrifugation at 735 X g for 1 min. After 2 hours of incubation, the reaction mixture was

applied slowly to the top center of the resin and the purified TM-rhodamine labeled plasmid was collected by centrifugation at 735 X g for 2 min. The labeled plasmid was store at 4 °C before used.

2.13.3 Trafficking of nanoparticles

MCF-7 cells and HeLa cells were cultured in a chamber slide II (Iwaki, 8 chambers per slide) at an initial density of 4×10^4 cells per well at 37 °C, 5% CO₂ for 10 hours in 400 µL of high glucose DMEM medium or low glucose DMEM supplemented with 10% FBS, 1% P/S. After 10 hours of incubation, the medium was removed and the cells were washed with 400 µL 1 X PBS twice. 50 µL of fluorescent labeled complexes were prepared at room temperature. For each well of the chamber, complex with 3 µg of PEI with the N/P ratio of 5 was used for transfection. After the incubation at 37 °C, 5% CO₂ for 1 or 3 hours, the medium was replaced with fresh medium supplemented with 10% FBS, 1% P/S and incubated for another 2 or 3 hours.

Post-transfection, medium was removed and the cells were washed with 400 µL 1 X PBS twice. If HMGB1 was present in the complexes, 1 X PBS with 0.02% (v/v) Tween 20 was used. The cells were fixed with 200 µL of 4% (v/v) paraformaldehyde in PBS for 30 min at room temperature. After 30 min of

fixation, the cells were washed with 400 μ L 1 X PBS twice, and the chambers on the slide were removed carefully. The slide was mounted with 2.5% (w/v) antifade solution (1, 4-Diazabicyclo [2, 2, 2] octane) and a cover slip (Iwaki).

2.13.4 Confocal laser scanning microscopy

The slide was observed with the LSM 510 META confocal microscope (Zeiss).

An argon laser with excitation lines at 458, 477 and 514 nm was used to induce green fluorescence, and a helium/ neon laser with excitation line 543 nm was used to induce red fluorescence. FITC green fluorescence was excited at 488 nm and their emission was collected by a 515-565 nm band pass filter. While for TM-rhodamine, red fluorescence was excited at 543 nm, and their emission was collected by a 575-640 nm band pass filter. The differential interference contrast (DIC) and the fluorescence was captured, digitized and processed with the Zeiss LSM Image Examiner software.

Chapter 3: Results and analysis

3.1 HMGB1 protein extraction and purification from pig thymus

Crude nuclear protein extracts from the pig thymus were purified through the CM-Sephadex C25 column. The elution profile in our HMG protein purification process (Figure 3.1) resembles the chromatogram published in 1975 by Goodwin *et al.*, i.e. with five peaks and Peaks IV-V were eluted after the linear salt gradient was applied. By electrophoretic analysis and amino acid analysis, Goodwin *et al.* (1975) demonstrated that Peak II contained the purified HMGB1 protein. Our SDS-PAGE analysis (Figure 3.2a) and western blotting results (Figure 3.2b) also illustrated that Peak II (Fraction 26-50) contained the purified HMGB1 protein. According to the result from Bradford Assay, the total yield of HMGB1 purified from 316 mg of pig thymus was 10.57 mg/kg.

In the western blotting result, weak positive signals were also observed in Peak III and Peak V (Figure 3.2b). This may be due to the protein being degraded as a result of the 2% trichloroacetic acid treatment [Goodwin *et al.* 1975]. Table 3.1 summarizes the content of each of the five peaks suggested by Goodwin *et al.* (1975).

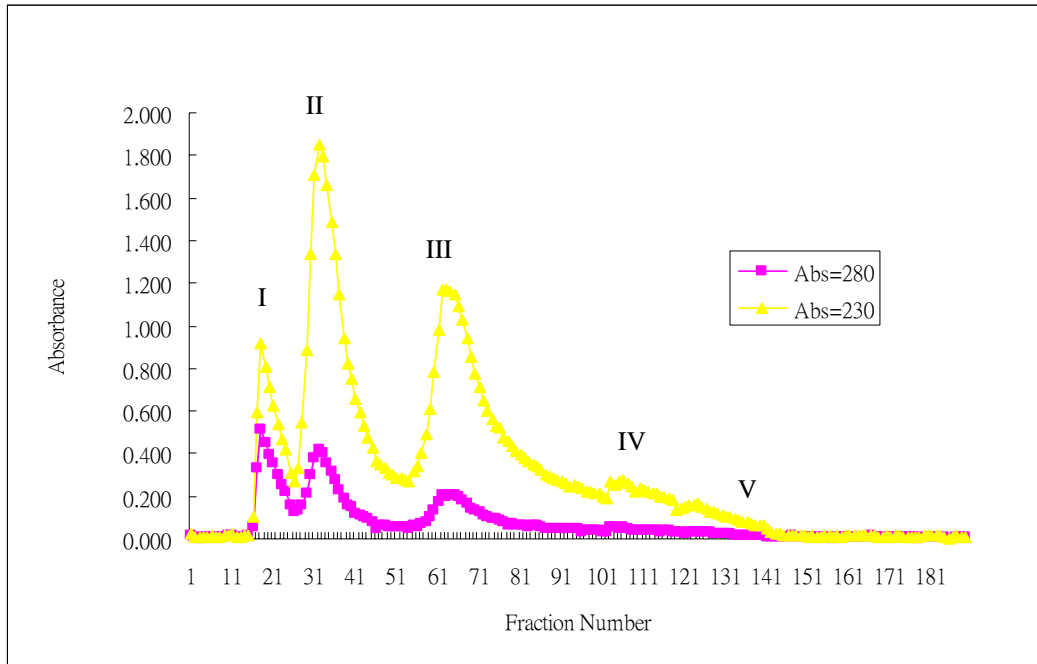


Figure 3.1: Elution Profile of HMG proteins from the CM-Sephadex C25 column. The column was equilibrated with 7.5 mM borate buffer (pH 8.8) and eluted as described in methodology. Gradient started at Fraction 90. 3 mL fractions were collected.

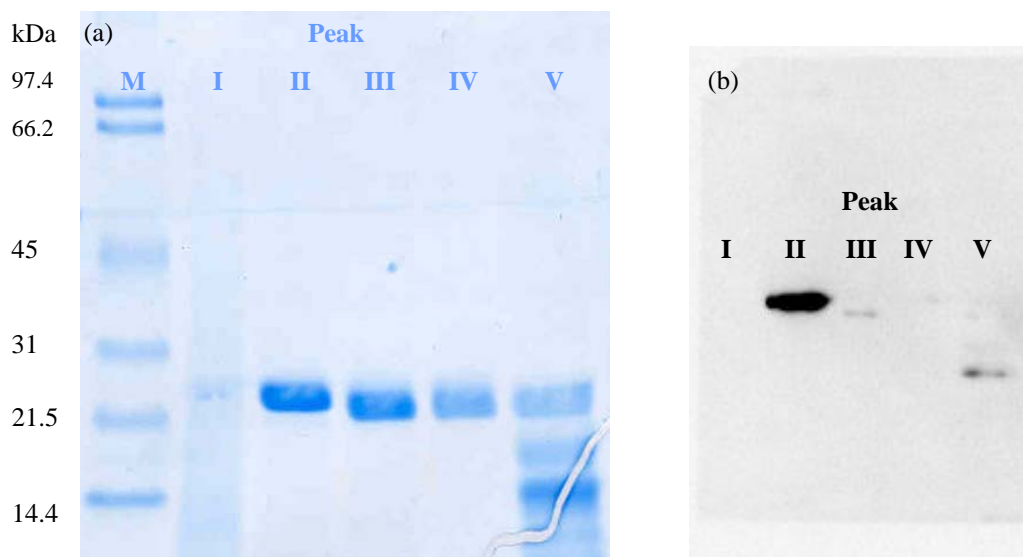


Figure 3.2: (a) Coomassie blue stained SDS-PAGE of the fractionated proteins from CM-Sephadex C25 chromatography. The Lane numbers correspond to the peaks identified from the chromatogram (Figure 3.1). M is the standard low range marker (Bio-Rad). (b) Western blot analysis of the fractionated proteins. Mouse anti-HMG1 monoclonal antibody at 1:1000 dilution (Stressgen bioreagents) was used as the first antibody.

Table 3.1: The main component of Peaks I to V obtained by CM-Sephadex C25 chromatography of high mobility group proteins performed by Goodwin *et al.* (1975).

Peak	Main components
I	A mixture of unbounded proteins
II	HMG 1 protein
III	HMG 2 protein
IV	A mixture of HMG 3 and 17 proteins
V	HMG 8 protein

3.2 Formation of HMGB1-DNA complexes

The optimal ratio for HMGB1-DNA complex formation was determined by agarose gel retardation assay. In Figure 3.3, Lanes 1 and 2 were the negative control lanes which contained DNA only and the mixture of BSA and DNA, respectively. While in Lanes 3-12, different amounts of HMGB1 were used for HMGB1-DNA complex formation to achieve the HMGB1 to DNA ratios shown below the lanes.

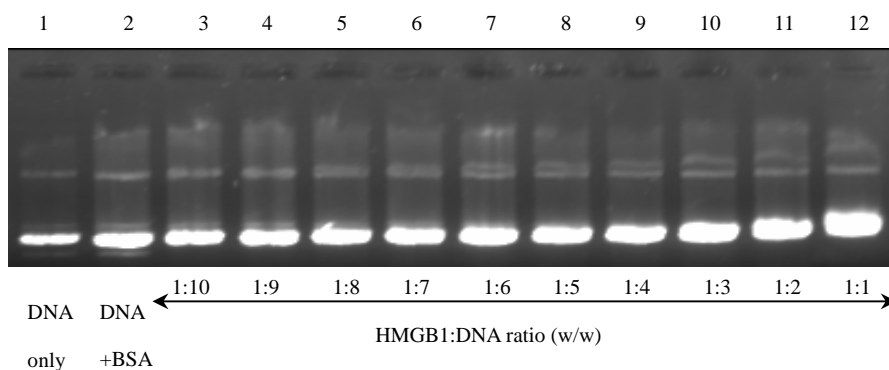


Figure 3.3: Agarose gel retardation assay (AGRA) study of complexing between HMGB1 and the pGL-3-Control plasmid. 0.3 μ g plasmid was incubated with different amounts of the HMGB1 protein at room temperature for 30 min. 0.3 μ g bovine serum albumin (BSA) was used as a negative control. The HMGB1-DNA complexes were analyzed with electrophoresis on a 0.8% agarose gel.

In Lanes 1 and 2, two bands were observed in each lane. The one with a higher mobility was the supercoiled form DNA while the other one with a slower mobility was the nicked form DNA. When 0.3 μ g of plasmid DNA was mixed

with an increasing amount of the HMGB1 protein (Lanes 3-12), a gradual upward shift of the major supercoiled DNA band was observed. The retarded mobility of the supercoiled DNA demonstrated the formation of the HMGB1-DNA complex [Kato *et al.* 1991]. At the HMGB1: DNA ratio (w/w) of 1:3, the retardation became more significant, and this ratio was similar to the resultant ratio determined by Namiki *et al.* (1997) in *in vitro* studies and the ratio used by Kato *et al.* (1991) for *in vitro* and *in vivo* studies. Therefore the ratio (w/w) of 1:3 was used in our subsequent experiments.

3.3 Formation of HMGB1-DNA-nanoparticle complexes

The amount of nanoparticles required for the formation of HMGB1-DNA-nanoparticle complexes was determined and shown in Figure 3.4. In Figures 3.4a and 3.4b, Lanes 1 and 2 were the control lanes which contained only DNA and only the HMGB1-DNA complex respectively. While for Lanes 3-8 different amounts of nanoparticles were employed. An increase in the nanoparticle to DNA ratio (w/w) resulted in the upshifting of the DNA. Bands started to disappear in the gel but at the same time, bands became visible at the bottom of the wells of the respective lanes. This phenomenon demonstrated the formation of the HMGB1-DNA-nanoparticle complex, and the retardation of plasmid DNA indicated charge neutralization and/ or an increase in the size of the complex [Bozkir A. *et al.*, 2004].

At the nanoparticle to DNA (w/w) ratio of 0.91, with the PEI nitrogen to DNA phosphate (N/P) ratio of 2 (Lane 6 in both Figures 3.4a and 3.4b), all the DNA was retained in the well without passing into the agarose gel. This indicated that all the DNA was interacting with the nanoparticles, and the ratio of 0.91 showed the minimum amount of nanoparticles required for complex formation.

However, as shown in our previous study [Zhu *et al.* 2005], the ratio determined by agarose gel retardation assay may not be the best ratio for transfection. Although all of the DNA or the HMGB1-DNA complexes have been taken up by the nanoparticle in the determined ratio, the complexes may not be stable due to the reduction of the positive surface charge. They may tend to aggregate and have an uneven or broad size distribution. Furthermore, in the gene transfer process, cellular uptake is governed by the electrostatic interaction between the positive surface charge of the complex and the negatively charged cell membrane. Therefore, if the positive surface charge of the complex is too low, it may not be able to facilitate the cellular uptake process and hence results in reduced transfection efficiency.

Our previous study has demonstrated that with a further increase in the nanoparticle to DNA ratio, the stability of the nanoparticle-DNA complex was greatly improved. For this reason, in the subsequent studies, apart from the ratio (w/w) of 0.91 (with the N/P ratio 2), the ratio (w/w) of 2.29 (with the N/P ratio 5) was also chosen. In other words, HMGB1-DNA-nanoparticle complexes were formed at the ratio (w/w/w) 1:3:2.73 (N/P ratio of 2) and 1:3:6.87 (N/P ratio of 5), respectively.

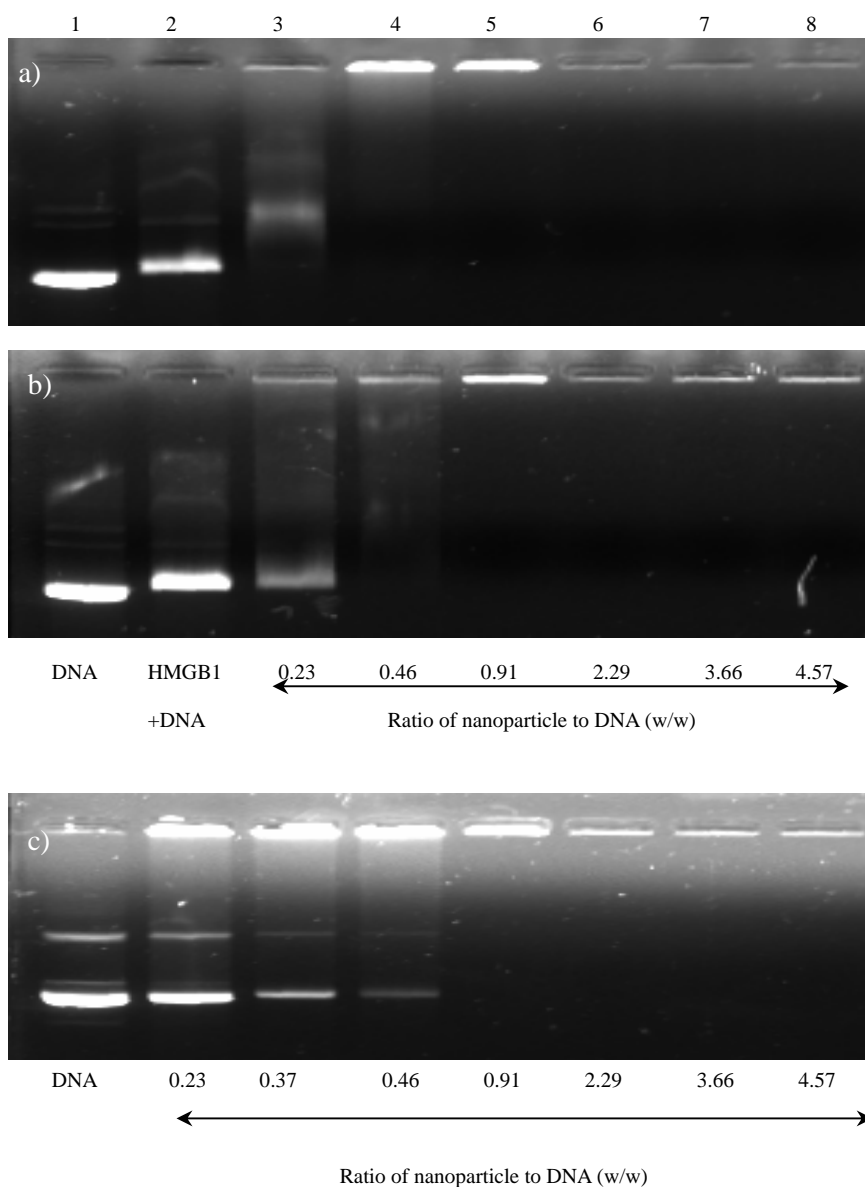


Figure 3.4: AGRA study of the HMGB1-DNA-nanoparticle complex formation. The HMGB1-DNA-nanoparticle complexes were prepared at room temperature, by mixing 0.1 μg HMGB1, 0.3 μg pGL-3 Control plasmid and various amounts of the PMMA-PEI nanoparticle to achieve the nanoparticle to DNA ratios shown below the lanes. Complexes were formed by a) first incubating HMGB1 with plasmid DNA for 30 min followed with incubation with nanoparticles for another 20 min. b) first incubating the nanoparticles with plasmid DNA for 20 min followed with incubation with HMGB1 for another 30 min. c) The formation of nanoparticle-DNA complex was used as a reference. All the complexes were analyzed by 0.8% agarose gel electrophoresis.

3.4 Release of DNA from the HMGB1-DNA-nanoparticle complex

We tested the possibility of releasing the DNA from the complex by treating it with poly(aspartic acid). In Figures 3.5a and 3.5b, the complexed DNA in the nanoparticle-DNA complex and in the HMGB1-DNA-nanoparticle complex was shown to be released from the complexes through an exchange reaction with the polyanion pAsp. It was noticeable that the DNA released from the HMGB1-DNA-nanoparticle complex by poly(aspartic acid) (Lanes 8 and 10) has a slower mobility than the uncomplexed DNA (Lane 1). This shows that the DNA released from the complex was not free DNA. By comparing the mobility of the released DNA from the HMGB1-DNA-nanoparticle complex and the HMGB1-DNA complex (Lane 6), their similar mobility indicated that DNA can be released from the nanoparticle, but still bound with the HMGB1 protein. This observation suggested that regardless of the complexing order, the HMGB1-DNA-nanoparticle complex may retain its nuclear targeting ability after the endocytosis process and may help to direct the therapeutic gene into the nucleus for expression.

In addition, from Figures 3.5a and 3.5b, it can be seen that the plasmid DNA released from all types of complexes (Lanes 4, 6, 8, 10) still maintained its biologically active form. The majority of the DNA was in the supercoiled form

with only a small amount in the open circular form.

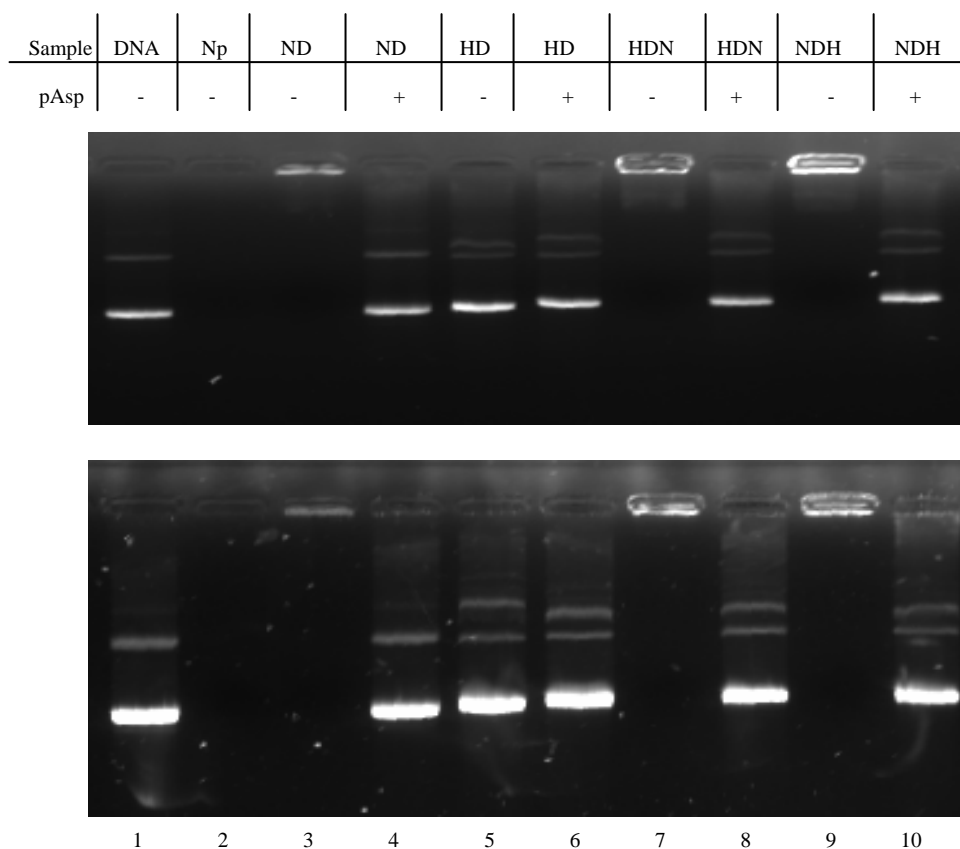


Figure 3.5: Release of DNA from the HMGB1-DNA-nanoparticle complex by poly(aspartic acid) [pAsp]. Complexes were formed in the HMGB1: DNA: nanoparticle (w/w/w) ratio of a) 1:3:2.73 and b) 1:3:6.87. The release study was performed by incubating the complexes with pAsp in a DNA:pAsp molar ratio of 1:100, at room temperature for 2 hours. Lane 1: DNA only (DNA); Lane 2: nanoparticle only (Np); Lane 3: nanoparticle-DNA complexes (ND); Lane 4: nanoparticle-DNA complexes + pAsp; Lane 5: HMGB1-DNA complexes (HD); Lane 6: HMGB1-DNA complexes + pAsp; Lane 7: HMGB1-DNA-nanoparticle complexes (by complexing HMGB1 and DNA first, HDN); Lane 8: HMGB1-DNA-nanoparticle complexes + pAsp; Lane 9: HMGB1-DNA-nanoparticle complexes (by complexing nanoparticle with DNA first, NDH); Lane 10: HMGB1-DNA-nanoparticle complexes + pAsp.

3.5 Protection against DNase I digestion

The extents of protection against nuclease degradation offered by the HMGB1-DNA-nanoparticle systems were investigated by using DNase I as a model enzyme [Bozkir *et al.*, 2004]. In Figure 3.6, naked DNA, nanoparticle-DNA complexes and HMGB1-DNA-nanoparticle complexes, with N/P ratios 2 and 5 were examined. Column 1 was the negative control, in which the samples were treated with no enzymes.

Figure 3.6 shows that when naked DNA was treated with 0.1 unit of DNase I (Column 3), smears appeared in the gel lanes. This indicated that most of the DNA was degraded. Further increase in the DNase I to 0.5 unit (Column 4) completely digested the DNA.

At the nitrogen to phosphate ratio of 2 (the upper row), an increase in DNase I from 0.05 to 0.5 unit (Columns 2-4) yielded an intensity of the plasmid DNA recovered from HMGB1-DNA-nanoparticle complexes that was similar to that of the negative control. This indicated that the plasmid DNA in the complex remained intact. However, at 1 unit DNase I treatment (Column 5), the intensity of the supercoiled DNA were reduced. This implied that the plasmid DNA was unprotected and degradation occurred. This was confirmed by increasing the

DNase I from 2 to 6 units (Columns 6-8) and degraded smears of DNA were observed.

At the nitrogen to phosphate ratio of 5 (the lower row), when the HMGB1-DNA-nanoparticle complex independent of the complexing order were mixed and incubated with an increasing amount of DNase I, there was no significant degradation of the plasmid DNA. Although some smears were observed at higher DNase I amounts (Columns 7 and 8), the majority of the plasmid DNA remained intact.

The results in Figure 3.6 suggested that the HMGB1-DNA-nanoparticle complex formed at higher nitrogen to phosphate ratio (N/P=5) was better protected than the one formed with a lower N/P ratio (N/P=2). At a higher ratio, more nanoparticles were used for complex formation and it thus has a higher DNA binding strength [Cook *et al.* 2005]. Comparing the results of the nanoparticle-DNA system and those of the HMGB1-DNA-nanoparticle systems, it was also found that the incorporation of the HMGB1 protein has no adverse effect on the DNA protection ability of the gene delivery system.

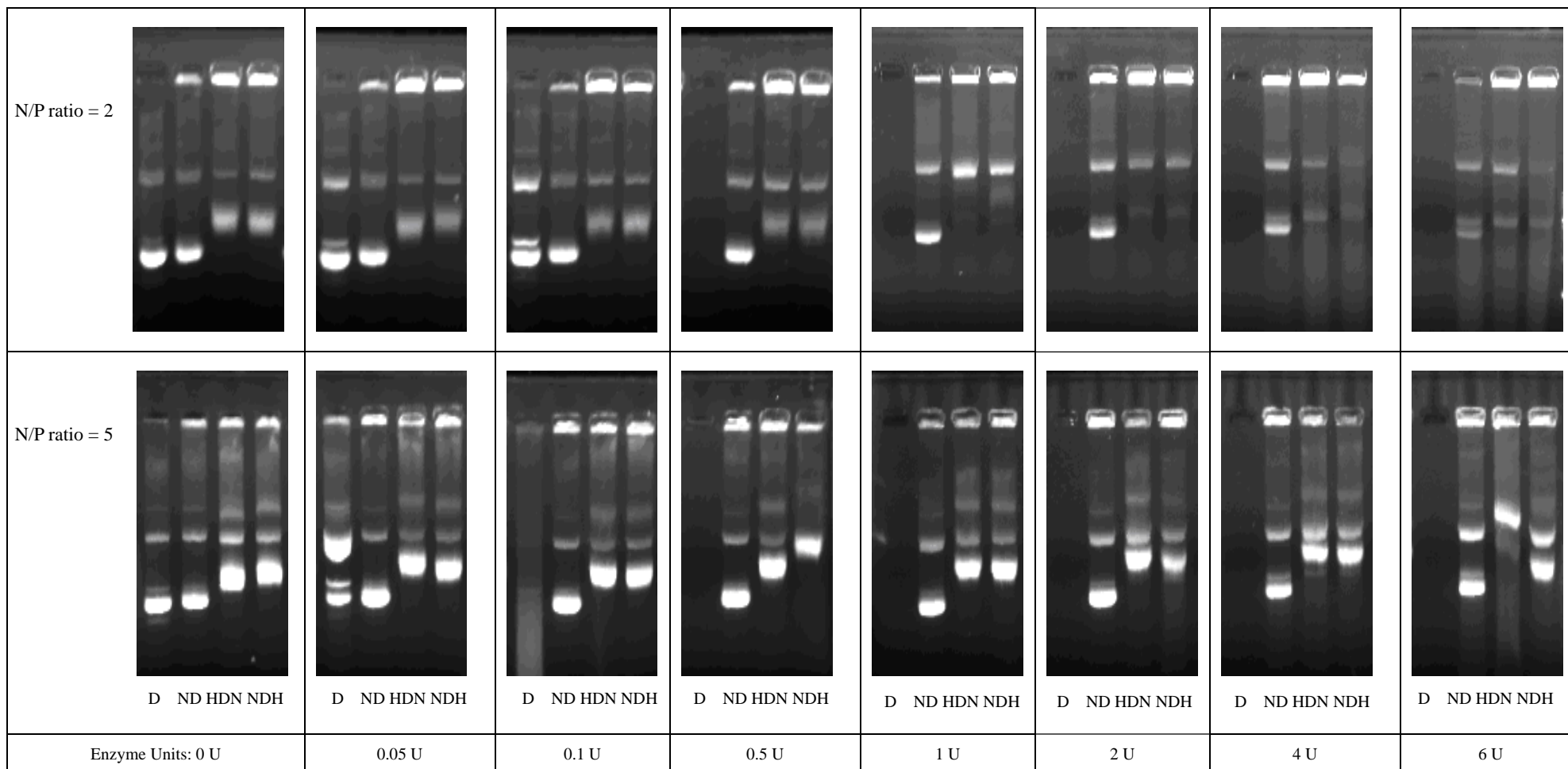


Figure 3.6: Protection of DNA against DNase I digestion. The complexes were formed in N/P ratios 2 (the upper row) and 5 (the lower row), and treated with different units of DNase I at 37 °C, for 15 min. D: Plasmid DNA only. ND: Nanoparticle-DNA complexes. HDN: HMGB1-DNA-nanoparticle complexes formed by complexing the HMGB1 with plasmid DNA first. NDH: HMGB1-DNA-nanoparticle complexes formed by complexing the nanoparticle with plasmid DNA first.

3.6 Transfection studies

The transfection efficiency of the PMMA-PEI nanoparticles at different nanoparticle to DNA (w/w) ratios was tested and the results were shown in Figure 3.7. Lipofectamine™ 2000, representing a well established commercially available transfection agent, was used as a control. In MCF-7 cells, the transfection efficiency of our system was found to increase with an increase in the nanoparticle to DNA mass ratio and showed the highest efficiency at the ratio of 2.29 (N/P=5). This trend may be attributed to the increase in the surface charge of the nanoparticle-DNA complexes. In fixed dose of DNA, increasing the nanoparticle to DNA (w/w) ratio means increasing the amount of nanoparticles for complex formulation. As a result, polyplexes with more positive surface charges were formed. According to our previous study [Zhu *et al.* 2005], at low mass ratios, the polyplexes became unstable and aggregated to form large sized particles. On the other hand, when increasing the nanoparticle composition, the stability of the polyplexes was improved, because there were enough positive surface charges for preventing polyplexes aggregation.

However, in Figure 3.7, at the ratio of 9.14 or above, the further increase in the nanoparticle to DNA (w/w) ratio showed a drop in the transfection efficiency.

This decline may be due to the reason that excess positive surface charges will

distort the cell membrane and lead to cell lysis. In addition, at the ratio of 2.29, its transfection efficiency was comparable to that of Lipofectamine™ 2000, showing that under the experimental conditions used, our gene delivery system of PMMA-PEI nanoparticles was as efficient as the best commercially available transfection system.

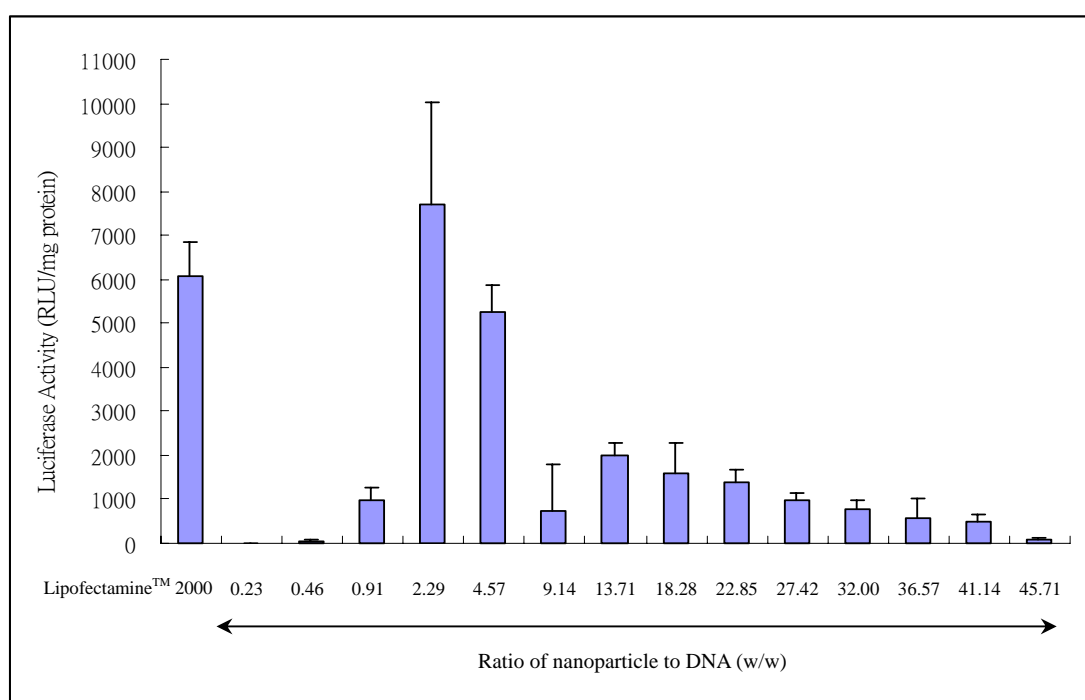


Figure 3.7: *In vitro* transfection efficiency of PMMA-PEI nanoparticles at various weight ratios in MCF-7 cells. The complexes were prepared by incubating 0.4 µg of pGL-Control plasmid with various amounts of PMMA-PEI nanoparticles at room temperature for 20min. Cells were transfected for 4 hours and expression detected after a further 20 hours of incubation. The transfection efficiency was expressed in relative luminescence units (RLU) per mg of protein.

The transfection efficiencies of the HMGB1-DNA-nanoparticle systems were compared with those of the nanoparticle-DNA system, and Lipofectamine™ 2000 and the results were shown in Figure 3.8. When DNA was first bound to HMGB1 protein and then complexed to the PMMA-PEI nanoparticles, the transfection efficiency was found to be similar to those using the PMMA-PEI nanoparticles alone. However, when HMGB1 was added after the formation of nanoparticle-DNA complexes, significantly higher transfection efficiencies were observed, especially at the nanoparticle to DNA (w/w) ratio of 2.29.

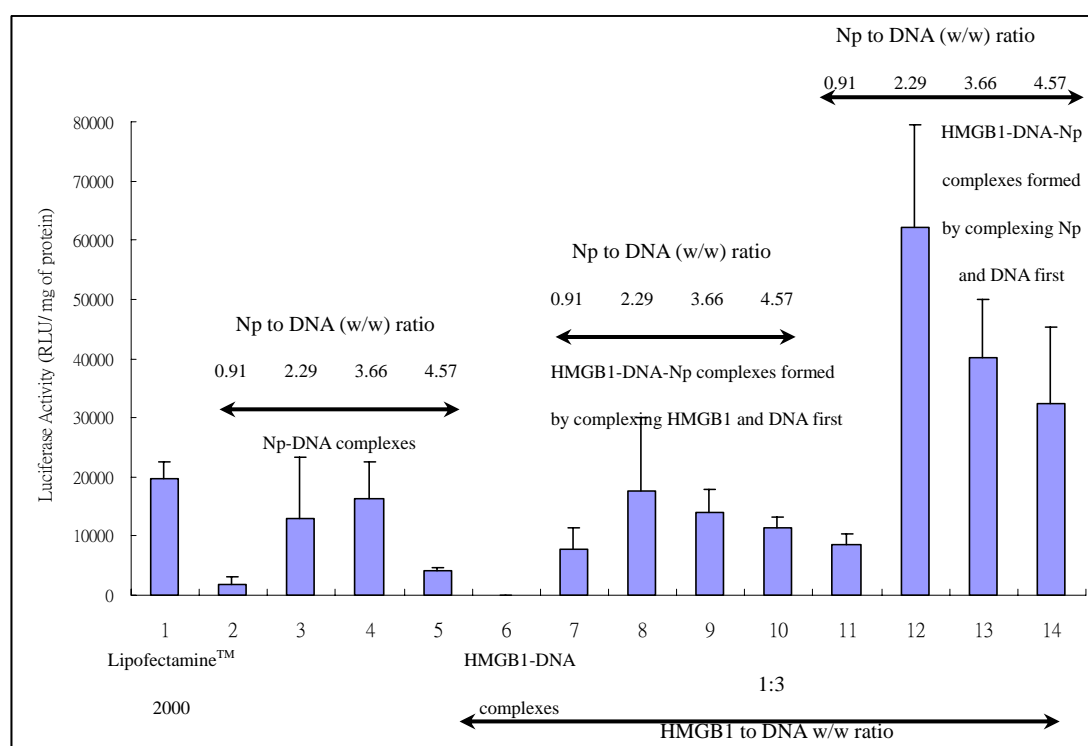


Figure 3.8: *In vitro* transfection efficiency of different HMGB1-DNA-nanoparticle systems in MCF-7 cells. The HMGB1-DNA-nanoparticle complexes were prepared by mixing 0.133 μg of HMGB1 protein, 0.4 μg of pGL-Control plasmid and various amounts of PMMA-PEI nanoparticles in different orders. Cells were transfected for 4 hours and expression detected after a further 20 hours of incubation. In the figure, “Np” stands for “nanoparticle”.

3.7 Cell viability assays

The cytotoxicity of the HMGB1-DNA-nanoparticle complex in the MCF-7 cells was investigated by MTS assay. Figure 3.9 shows that the inclusion of HMGB1 in the DNA-nanoparticle complex was not significantly toxic to the MCF-7 cells as the average relative cell viability was around 80%. This is independent of the order of complexing.

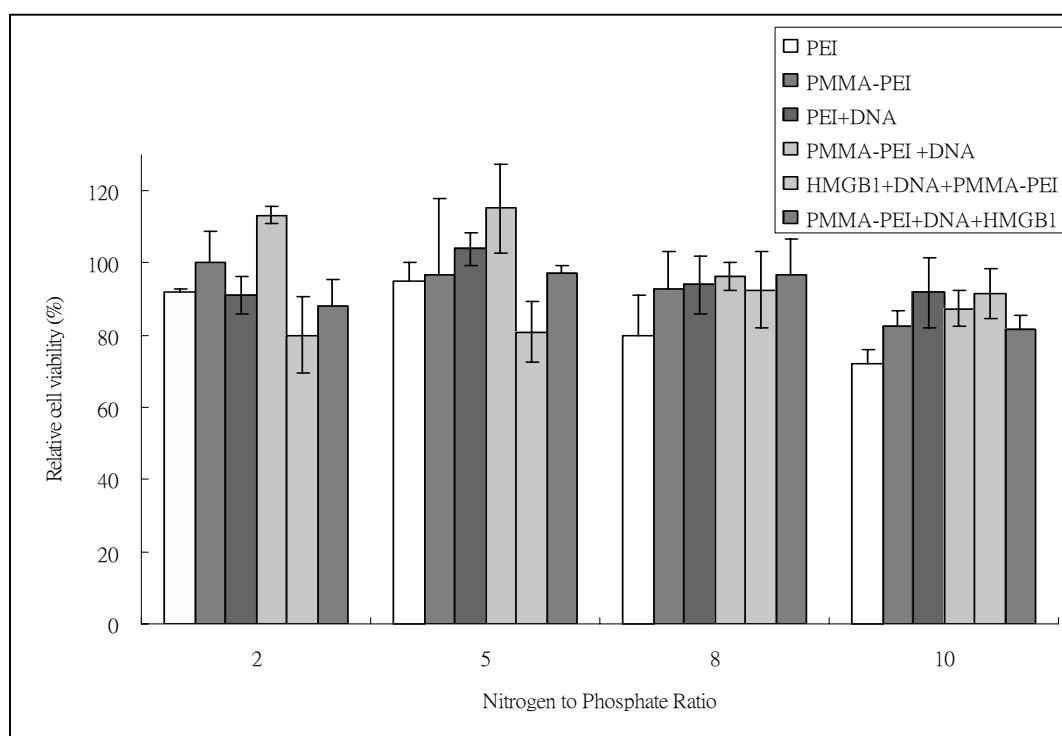


Figure 3.9: Relative viability of MCF-7 cells at different nitrogen to phosphate ratios for different gene delivery systems. The results were expressed as a percentage with respect to the positive control in which only the culture medium was added to the cells.

Table 3.2 Conversion of N/P ratios to weight ratios for the PEI polymers and PMMA-PEI nanoparticles

Nitrogen to Phosphate Ratio	2	5	8	10
PEI to DNA (w/w) Ratio	0.26	0.65	1.04	1.30
PMMA-PEI to DNA (w/w) Ratio	0.91	2.29	3.66	4.57

3.8 Nanoparticle trafficking studies by confocal laser scanning microscopy

(LSM)

Movement of the gene carrier and the DNA was tracked through the confocal laser scanning microscopy. Figures 3.10a and 3.10b show the intracellular distribution of the FITC labeled PEI polymers and PMMA-PEI core-shell nanoparticles in HeLa cells after 1 hour of transfection followed with 2 hours of post-transfection incubation. The results demonstrated that both PEI polymers and PMMA-PEI nanoparticles were efficiently internalized by the HeLa cells. In general, the green fluorescent signals of the PEI polymers were found in the nucleus (Figures 3.10a) showing that unlike other non-viral systems, PEI can effectively enter the cell nucleus. While for the nanoparticles, the majority of the green fluorescent signals appeared in the perinuclear region of the HeLa cells (Figure 3.10b). However, fluorescent signals within nucleus were also observed in a few of the cells (Figure 3.10b).

To test the effect of a longer transfection time, transfection was carried out for 3 hours followed with 4 hours of post-transfection incubation. With the increased transfection and post-transfection incubation time, the nanoparticles were found to show a similar fluorescence pattern as that of the PEI polymers in the HeLa cells. Green fluorescent signals were found in both the cytoplasm and the nucleus

(Figures 3.10c and 3.10d). Some punctured vesicles were also observed (Figure 3.11a), indicating that some of the PEI polymers were probably still in the endo-lysosomal compartment. Furthermore, from the serial optical plane images (Figure 3.11b), the fluorescence signals were found to be located mainly within the focal planes corresponding to the inside of the cell, with decreasing intensities when the focal planes were moved towards the bottom and the top surfaces of the cells. Therefore, we can confirm that the FITC labeled PEI polymers and nanoparticles were internalized into the HeLa cells.

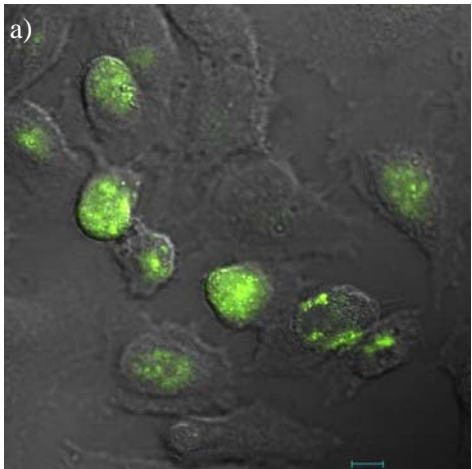
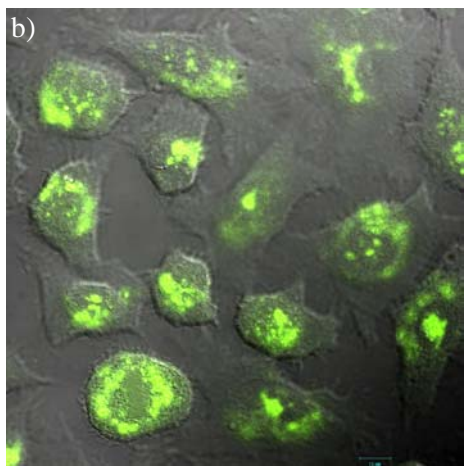
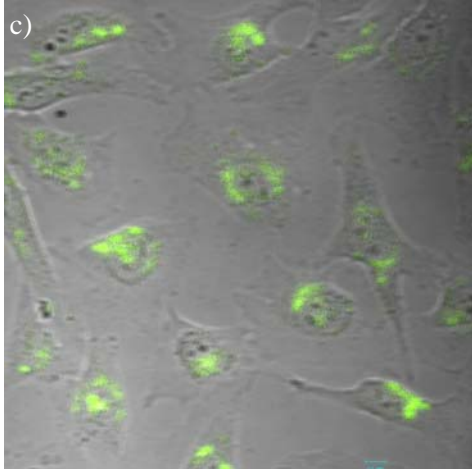
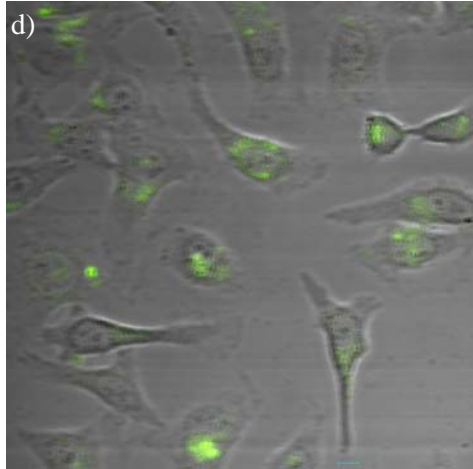
Total transfection time	FITC labeled PEI polymers	FITC labeled PMMA-PEI nanoparticles
3 hours (1 hours transfection with 2 hours post-transfection)		
7 hours (3 hours transfection with 4 hours post-transfection)		

Figure 3.10: Confocal laser scanning microscopic images of HeLa cells after 3 hours and 7 hours of transfection incubation with a) and c) FITC labeled PEI polymers; b) and d) FITC labeled PMMA-PEI nanoparticle. The original magnification of a)-b) was 63X; c)-d) was 40X. Bar=10 μ m.

FITC labeled PEI polymers

Total transfection time: **7 hours**
(3 hours transfection with 4 hours
post-transfection)

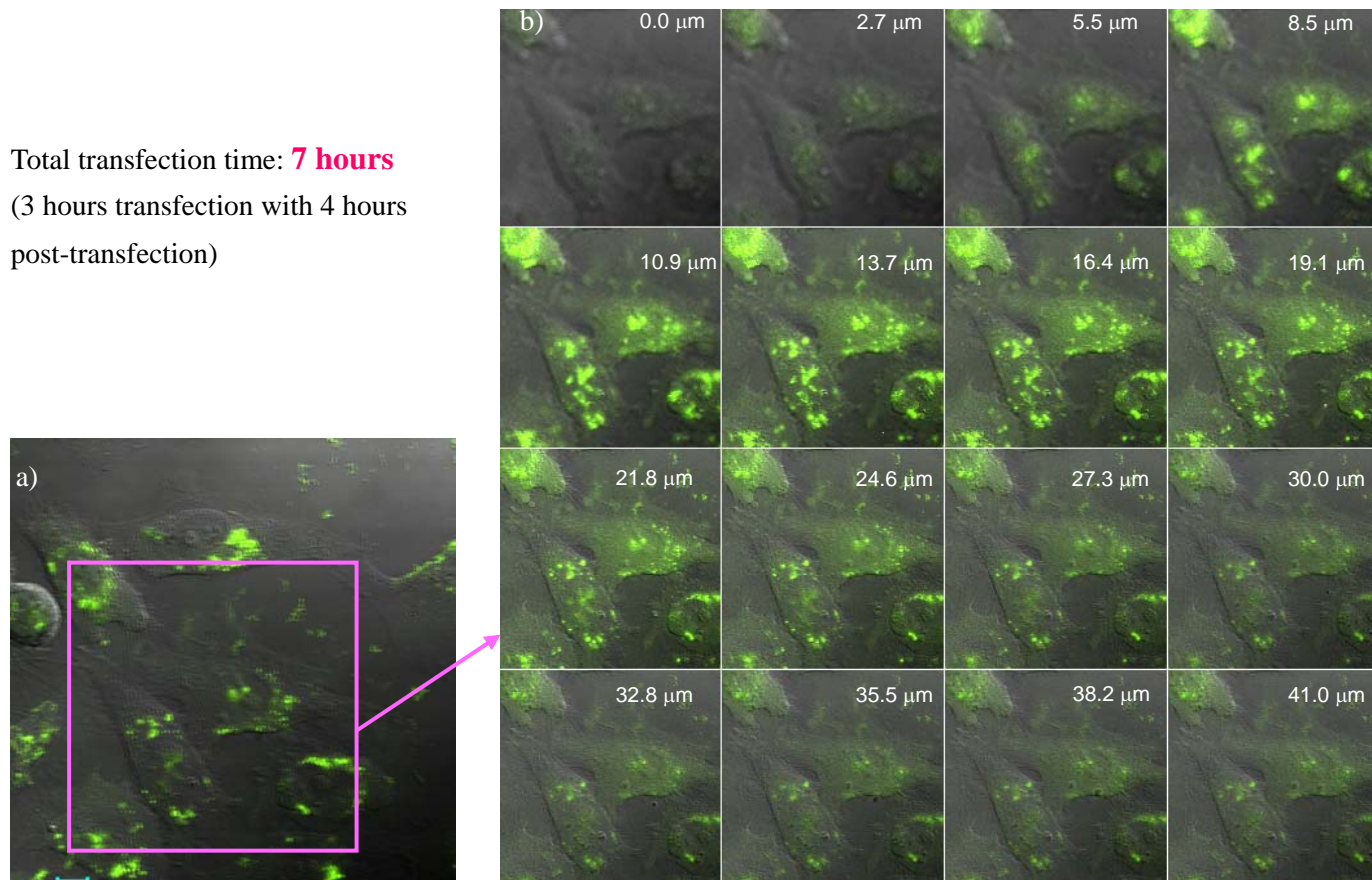


Figure 3.11: Confocal laser scanning microscopic images of HeLa cells after 7 hours of transfection incubation with FITC labeled PEI polymers. Images in b) are a series of optical sections from different optical planes of a) achieved by vertical movement of the objective (along the z-section). The strongest intensities with focal planes at nucleus were observed in the 13.7 μm – 19.1 μm slices. The original magnification was 40 X. Bar=10 μm .

To track the path of the foreign DNA, polyplexes were doubly labeled and transfected into HeLa cells (1 hour of transfection and 2 hours of post-transfection incubation). Figure 3.12 shows the results obtained. Generally, three fluorescent colors were detected in the HeLa cells. These were the green, red and yellow signals. The green fluorescent signal corresponds to the PEI polymers or the nanoparticles and the red fluorescent signal corresponds to the TM-rhodamine labeled pGL-3-Control plasmid. The yellow signal will be obtained when the green fluorescent signal overlaps with the red one, and this will indicate the co-localization of the PEI polymers or the nanoparticles with the plasmid DNA.

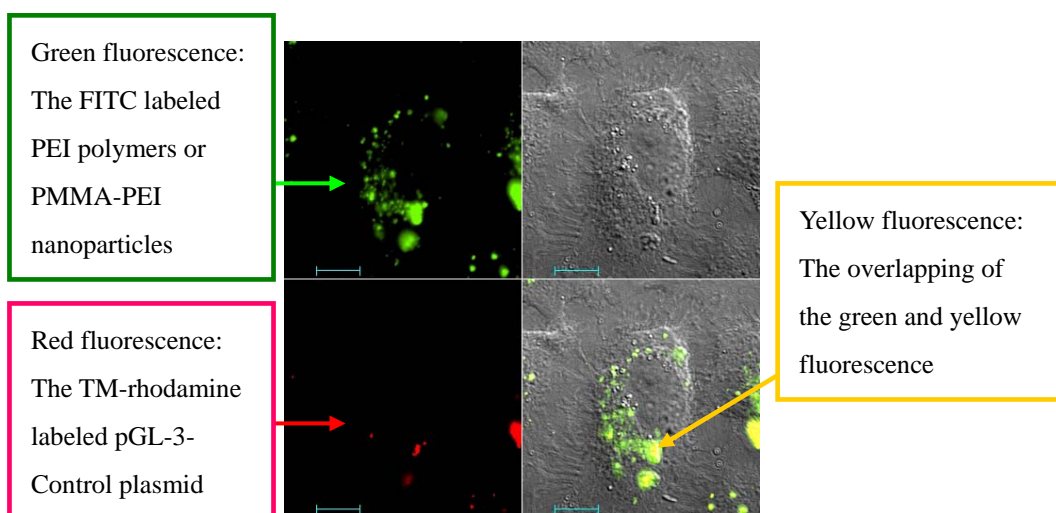


Figure 3.12: Confocal laser scanning microscopic images of HeLa cell after 3 hours of transfection incubation with double labeled PEI-DNA complexes. PEI polymers and PMMA-PEI nanoparticles were labeled with FITC (green) and the pGL-3- Control plasmid was labeled with TM-rhodamine (Red). Upper right: differential inference contrast (DIC) images; upper left: green fluorescence images; lower left: red fluorescence images; lower right: overlapped images. The original magnification was 63 X. Bar=10 μ m.

The overall observation is that both the PEI-DNA (Figure 3.13a) and the nanoparticle-DNA (Figure 3.13b) complexes were internalized by the HeLa cells, and appeared in the cytoplasm as well as in the perinuclear region of the cells. However, no free red fluorescent signals were detected indicating the absence of free DNA and this implies that the plasmid DNA was most probably still complexed to the PEI polymers or the nanoparticles. This observation also suggests that the polyplexes may protect the plasmid DNA against nucleases degradation in the cytoplasm by keeping the DNA in the complexed form.

With a prolonged transfection (3 hours) and post-transfection (4 hours) protocol, apart from being found in the cytoplasm, the yellow fluorescent signal was also detected inside the nucleus of the HeLa cells (Figures 3.13c and 3.13d). Interestingly, no free red fluorescent signals were observed in the cytoplasm nor the nucleus. Therefore, this demonstrates that the plasmid DNA was translocated to the nucleus together with the PEI polymers or the nanoparticles.

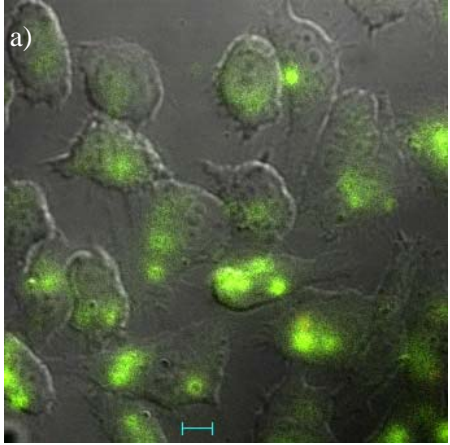
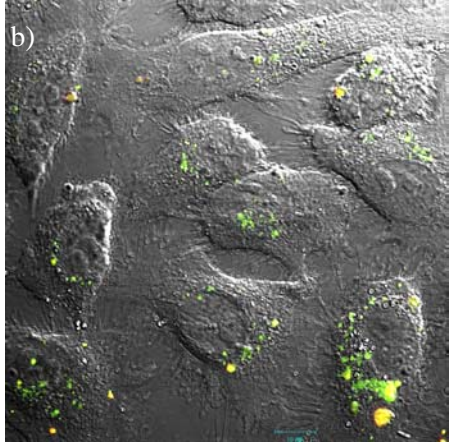
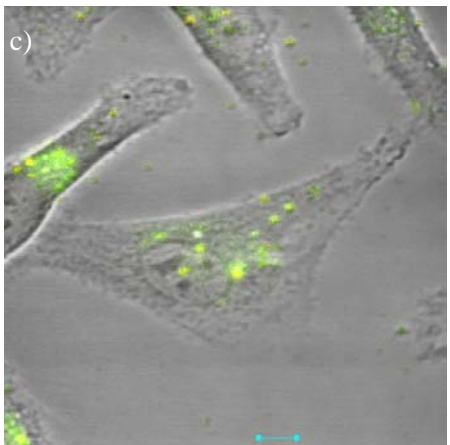
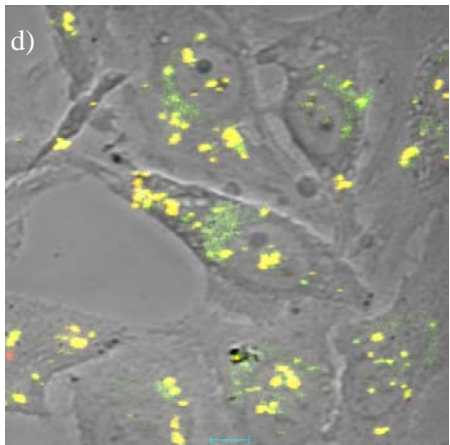
Total transfection time	Double labeled PEI-DNA polyplexes	Double labeled nanoparticle-DNA polyplexes
3 hours (1 hours transfection with 2 hours post-transfection)		
7 hours (3 hours transfection with 4 hours post-transfection)		

Figure 3.13: Confocal laser scanning microscopic images of HeLa cells after 3 hours and 7 hours transfection incubation with a) and c) double labeled PEI-DNA complexes; b) and d) double labeled nanoparticle-DNA complexes. PEI polymers and PMMA-PEI nanoparticles were labeled with FITC (green) and the plasmid DNA was labeled with TM-rhodamine (red). The original magnification of a)-b) was 63X; c)-d) was 40X. Bar=10 μ m.

In MCF-7 cells with the prolonged protocol, i.e. 3 hours of transfection and 4 hours of post-transfection incubation, the green fluorescent signals of the PEI polymers or the nanoparticles were detected in the majority of the cells, indicating that both the PEI polymers and the nanoparticles were efficiently internalized by the MCF-7 cells (Figures 3.14a and 3.14b). However, unlike that in the HeLa cells (Figures 3.14c and 3.14d), the PMMA-PEI nanoparticles displayed more nuclear localization in the MCF-7 cells than that of the PEI polymers. Most of the green fluorescent signals of the PEI polymers were found in the cytoplasm.

With the HMGB1-DNA-nanoparticle complexes, signals could also be detected in both the cytoplasm and the nucleus of the MCF-7 cells after 3 hours of transfection and 4 hours of post-transfection incubation (Figure 3.15). However, the order of complexing appeared to have made some differences in the transfection process. When the plasmid DNA was first complexed with the nanoparticles before binding to the HMGB1 protein (Figure 3.15b), the fluorescent signals were more readily observed in the MCF-7 cells. When the plasmid DNA was bound with the HMGB1 protein before complexing with the nanoparticles, less fluorescent signals were observed (Figure 3.15a).

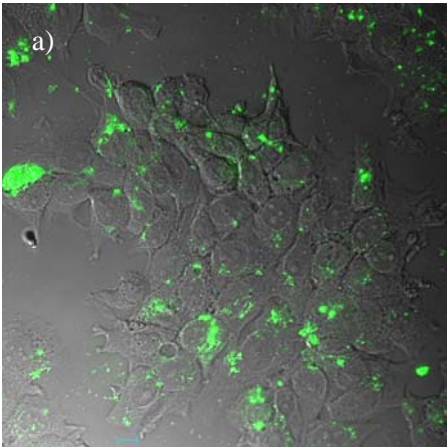
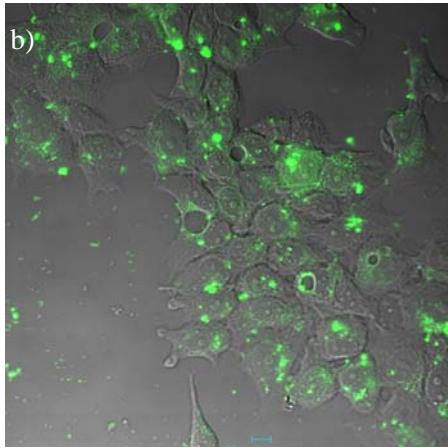
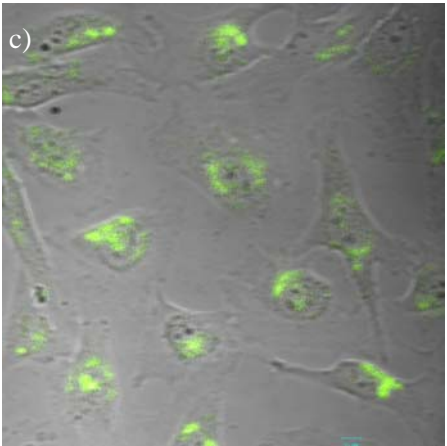
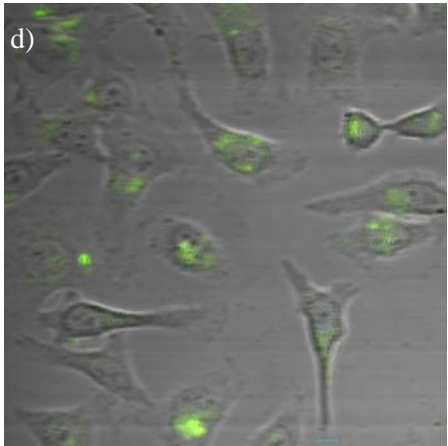
Cell type	FITC labeled PEI polymer	FITC labeled PMMA-PEI nanoparticle
MCF-7 cells		
HeLa cells		

Figure 3.14: Confocal laser scanning microscopic images of MCF-7 cells and HeLa cells after 7 hours transfection incubation with a) and c) FITC labeled PEI polymers; b) and d) FITC labeled PMMA-PEI nanoparticle. The original magnification of a)-b) was 63X; c)-d) was 40X. Bar=10 μ m

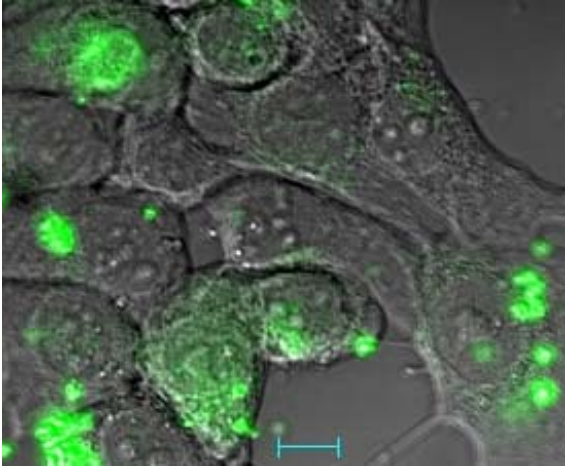
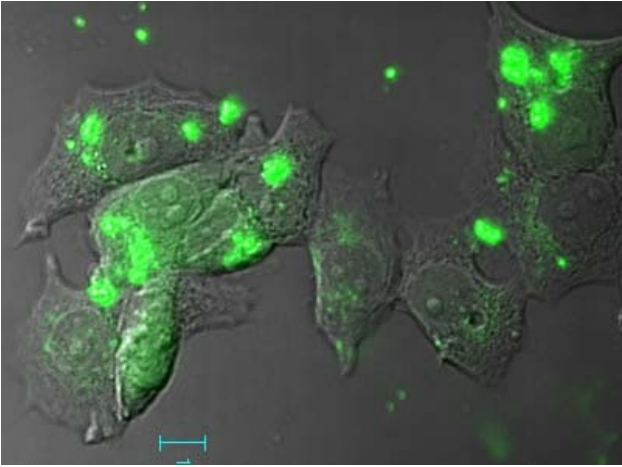
Total transfection time	HDN complexes	NDH complexes
7 hours (3 hours transfection with 4 hours post-transfection)		

Figure 3.15: Confocal laser scanning microscopic images of MCF-7 cells after 7 hours of transfection incubation with HMGB1-DNA-nanoparticle complexes. PMMA-PEI nanoparticles was labeled with FITC. The HDN complexes were formed by incubating HMGB1 with pGL-3-Control plasmid first, while the NDH complexes were formed by incubating pGL-3-Control plasmid with nanoparticle first. The original magnification was 40 X. Bar=10 μ m.

Chapter 4: Discussion

In the past decade, many empirically designed non-viral gene carriers were developed. However, these currently available systems are still comparatively low in transfection efficiency when compared with the viral systems. In addition, due to our bodies' immune system (e.g. the mononuclear phagocytic system) and the presence of many endogenous negatively charged molecules, the availability of these synthetic non-viral systems for effective gene transfer is further hampered *in vivo*. As a result, recently scientists started to study the mechanisms involved in gene transfer [Kircheis *et al.* 1997 and Kichler *et al.* 2001]. Quantitative cytoplasmic microinjection studies have demonstrated that only 0.1% of the naked DNA or 1% of DNA in form of a polyplex injected into cytoplasm can reach the nucleus and expressed [Pollard *et al.* 1998, Zanta *et al.* 1999 and Bremner *et al.* 2004] Therefore, it is generally believed that the transport of transgene from the cytoplasm to the nucleus is the major limitation step for a successful gene delivery process [Zanta *et al.* 1999 and Segura *et al.* 2001].

In this study, the addition of a nuclear HMGB1 protein as a component in our existing PMMA-PEI core-shell nanoparticle gene delivery system was investigated. Being a transfection active nuclear protein [Bottger *et al.* 1988,

Bottger *et al.* 1990, Mistry *et al.* 1997 and Bottger *et al.* 1998], HMGB1 has the nuclei-trafficking property in the HVJ-liposome system [Hangai *et al.*, 1996 and Isaka *et al.* 1998] and has the ability to condense DNA into spherical shapes [Wunderlich *et al.* 1997]. As a result, it may enhance the transfection efficiency through the improvement of nuclear transport.

4.1 Incorporation of HMGB1 into the gene delivery complex

HMGB1 is a ubiquitous protein with high cellular level in the thymus (10^6 molecules per cell) [Yang *et al.* 2005]. The purified HMGB1 protein has been demonstrated to have the ability to condense the plasmid DNA in a dose dependent manner (Figure 3.3). The formation of HMGB1-DNA complexes was indicated by the typical retardation mobility pattern in agarose gel electrophoresis [Kato *et al.* 1991].

In forming the HMGB1-DNA-nanoparticle complexes, HMGB1 did not affect the DNA condensing capacity of the PMMA-PEI. In the absence or presence of the HMGB1 protein, the plasmid DNA was fully bound to the nanoparticle at the N/P ratio of 2 (with mass ratio equal to 0.91, Figures 3.4). Furthermore, with HMGB1-DNA-nanoparticle complexes formed in the two different complexing orders, there are no difference in this DNA complexing capacity of

the nanoparticles (Figures 3.4a and 3.4b). This implies that the addition of HMGB1 does not change significantly the overall charges in the complexes, owing to the small amount used.

In the release study (Figure 3.5), the plasmid DNA released from all types of complexes still maintained its initial structure. The majority of the released plasmid DNA was in the supercoiled form with a small percentage in the open circular form. This indicates that the incorporation of HMGB1 in the gene delivery complex did not affect the biological activity of the plasmid DNA. Therefore, after the gene transfer process, this biological active plasmid can be transcribed and expressed actively. The results of the release study also revealed that the plasmid DNA can be released from the HMGB1-DNA-nanoparticle complex, but still with the HMGB1 protein bound (Figure 3.5). This observation suggests that the HMGB1-DNA-nanoparticle complex may retain its nuclear targeting ability even if the nanoparticle is disassembled from the complex during the gene transfer process. This may help to direct the exogenous gene into the nucleus for expression.

In addition, with the inclusion of HMGB1 in the gene delivery complex, the DNA protection ability was slightly affected at a low N/P ratio. At N/P ratio of 2, the HMGB1-DNA-nanoparticle complex has a slightly decreased protection

ability against DNase I (Upper row of Figure 3.6). However, this kind of consequence was not observed at a higher N/P ratio. At N/P ratio of 5, the DNA protection ability of the HMGB1-DNA-nanoparticle system was not found to be different from that of the nanoparticle-DNA system (Lower row of Figure 3.6). This suggests that when the HMGB1 protein is included, the gene delivery complex could still maintain its DNA protection ability.

Based on the observations above, the incorporation of HMGB1 in the gene delivery complexes has no adverse effects on the DNA condensing capacity, the DNA release ability and the DNA protection ability. More importantly, the released plasmid DNA from the HMGB1-DNA-nanoparticle system was still bound with the HMGB1 protein. This observation may suggest that the new system may have an added advantage in the DNA translocation process.

4.2 Transfection efficiency of the HMGB1-DNA-nanoparticle system

In our *in vitro* transfection studies in MCF-7 cells, the transfection efficiency (based on the Luciferase Assay) of the various systems can be ranked in the following order: NDH (the HMGB1-DNA-nanoparticle complex formed by complexing the nanoparticle with the DNA and then bound with the HMGB1 protein) > HDN (the HMGB1-DNA-nanoparticle complex formed by bounding the HMGB1 with the DNA and followed by complexing with the nanoparticle) \approx ND (nanoparticle-DNA complex) \approx LipofectamineTM 2000.

The above ranking result differs slightly from our original idea. Our initial thought was that the HDN system might probably have a higher transfection efficiency. Since after internalization into the cell, the HMGB1 bound DNA might be released intact from the complexes into the cytoplasm, and the HMGB1 protein might then help the plasmid DNA to enter the nucleus. Although slightly different from what we had initially expected, the transfection results in fact still indicated that the HMGB1 protein can enhance the *in vitro* transfection efficiency. The difference in the expected and the experimental results has also demonstrated that the exact complexing order is one of the critical factors affecting expression of the exogenous gene.

4.2.1 Nitrogen to phosphate ratio of 2

In the *in vitro* transfection studies at the N/P ratio of 2, which is the minimum amount of nanoparticles required for complex formation, the presence of HMGB1 in the gene delivery complex can increase the luciferase gene expression in the MCF-7 cells (HDN = NDH > ND). In the gene delivery process, surface charges and sizes of polyplexes are the two parameters that strongly affect the intracellular uptake rate [Wiewrodt *et al.* 2002 and Zhu *et al.* 2005]. At low N/P ratios, the surface positive charge of the nanoparticle will be neutralized by the negatively charged DNA. With the zeta potential close to zero, this polyplex will become unstable. As a result, polyplex aggregation will occur and large particle will form [Zhu *et al.* 2005]. The large size and the neutral surface charge impede cellular uptake.

The results of transfection studies also suggest that, when the HMGB1 protein is added into the gene delivery complex, the transfection efficiency of the system is slightly enhanced. With the presence of the positively charged HMGB1 protein, it may either reduce the amount of amine functional groups required for full DNA complexation (in the cases of the HDN system) or increase slightly the availability of positively charged functional groups in the complex (in the cases of the NDH system). These two phenomena may result in

an increase in the positive charge on the polyplex surface and thus, may improve cellular uptake.

4.2.2 Nitrogen to phosphate ratio of 5

When the gene delivery complexes were formed at the N/P of 5, the NDH system showed the highest transfection efficiency, with 3 to 4 folds higher than those of the other three systems (the HDN, the ND and the commercially available LipofectamineTM 2000 systems). Interestingly, the NDH and the HDN systems both contained the same components but the NDH system had a much higher transfection efficiency than that of the HDN system. In our cytotoxicity tests, we observed that at the N/P ratio of 5, the NDH system had a lower toxicity than that of the HDN system (Figure 3.9). This may probably be one of the factors contributing to its higher transfection efficiency than that of the HDN system.

For our core-shell nanoparticle, the PEI polymers were grafted onto the PMMA core. These PEI polymers can interact with negatively charged substances via electrostatic interactions. In the NDH system, the PEI polymers can bind with the phosphate groups of the plasmid DNA and the negatively charged amino acids on the acidic tail of the HMGB1 protein. In the NDH system, HMGB1

was added in the last step of complex formation and the addition of HMGB1 may reduce the number of free primary amines present on the surface of the complex. These free primary amines have been suggested to contribute to the toxicity mediated by the particle [Fischer *et al.* 2003]. As a result of HMGB1 binding, decrease in the number of free primary amines might reduce the toxicity of the whole system. Furthermore, Lee *et al.* (2001) have also found from their experiments that coating of positively charged conjugates on the surface of the negatively charged polyplexes can further reduce the cytotoxicity of the PEI-DNA polyplexes. Coating the HMGB1 protein onto the surface of our polyplexes might have the same effect.

While in the HDN system with the nanoparticle coating on the surface of the complex, if the HMGB1 is required to offer their nuclear targeting function, the HMGB1-DNA complex should be first released from the whole complex. However, from the confocal images of the ND system (Figure 3.13d), plasmid DNA was translocated to the nucleus together with the PMMA-PEI nanoparticle. This observation reveals that our nanoparticle system may have a similar intracellular pathway as that of the PEI-DNA polyplex (Figure 3.13c). Prior separation of the DNA and the nanoparticles is not necessary for nuclear entry [Pollard *et al.* 1998 and Godbey *et al.* 1999a]. Furthermore, both of our

nanoparticle and the PEI polymer underwent nuclear localization even when they were not complexed with plasmid DNA (Figures 3.10-3.11 for HeLa cells and Figures 3.14a-3.14b for MCF-7 cells) [Godbey *et al.* 1999a]. Therefore, from these observations, we can predict that after the endocytosis process, the PMMA-PEI nanoparticle in the HDN system may still bind with the HMGB1-DNA complex and enter the nuclear together. As a result, without disassembly from the nanoparticle, the HMGB1 protein may not be exposed to the surface of the complex and this may probably prevent the HMGB1 protein to interact with the transport receptors. Thus, this may hinder cargo recognition for nuclear transportation [Mubkonge *et al.* 2003 and Bremner *et al.* 2004]. This could perhaps explain why the HDN system has a transfection efficiency similar to those of the ND system. It is also supported by the fact that in confocal images of the HDN and NDH systems (Figures 3.15a and 3.15b), the green fluorescent signal of the FITC-labeled nanoparticle was more readily observed in the NDH system than in the HDN system.

Another possible factor affecting the transfection efficiency of a system is the size of the polyplex. At the N/P ratio of 5, the weight/weight ratio of HMGB1 to nanoparticle was 1/6.83. This indicates that nanoparticle was present in a large excess amount when compared with the HMGB1 protein. Therefore, in

the NDH system, when the plasmid DNA was first bound with the PEI polymers of the nanoparticle, the PEI shell has already become less water-soluble and shrunk [Zhu *et al.* 2005]. And this nanoparticle-DNA complex may have a more organized and condensed structure than that of the HMGB1-DNA complex (in the case of HDN system). As a result, the final size of the NDH complex may be smaller than that of the HDN system, and was more favorable for intracellular uptake. Furthermore, for the PMMA-PEI nanoparticle, the PEI polymers on the shell layer may not fit so closely together due to mutual repulsion. Gaps may then be present [Godbey *et al.* 1999c]. Therefore, for the NDH system, HMGB1 may fill into these gaps and may bind to the polyplex without significantly increasing the complex size but with obvious enhancement in the *in vitro* transfection efficiency.

4.3 Roles of HMGB1 in the gene delivery complex

In our present study, we have demonstrated that the NDH system has a higher transfection efficiency than those of the ND system and the commercially available LipofectamineTM 2000 system. Therefore, we firmly believe that in the gene delivery complex, HMGB1 has an important role in enhancing gene expression. In the following sections, we propose three possible roles of HMGB1 in the gene delivery complex.

4.3.1 Nuclear localization signal

One of the possible roles of HMGB1 in the gene delivery complex is to act as a nuclear localization signal. Being a nuclear protein, HMGB1 is required to be imported from the region where it is translated (the cytoplasm) to the region where it functions (the nucleus) [Uherek *et al.* 2000]. Cytoplasmic microinjection of HMGB1 has demonstrated that HMGB1 can rapidly migrate from the cytoplasm into the nucleus [Rechsteiner *et al.* 1979], and Tsuneoka *et al.* (1986) have demonstrated that nuclear accumulation of HMGB1 is an active transport. Although the NLS position for the HMGB1 protein has not been identified yet, the NLS in SRY and other DNA-binding proteins has been identified in the HMG box [Poulat *et al.* 1995 and LaCasse *et al.*, 1995].

Therefore, it is likely that nuclear accumulation of HMGB1 after its translation may rely on a NLS in the HMGB1 molecule. As a result, the enhancement of luciferase gene expression may be due to the nuclear targeting ability of the HMGB1 protein which, like other NLS peptides, facilitates migration of the gene delivery complex towards the nucleus [Mesika *et al.* 2005].

4.3.2 Transcriptional activator

Owing to the intracellular function of HMGB1 as a transcriptional activator for gene regulation [Aizawa *et al.* 1994], we believe that when HMGB1 is co-translocated with the gene delivery complex and enters into the nucleus, it may attract transcriptional factors to the promoter region of the plasmid DNA, and may initiate the formation of transcriptional initiation complex. As a result, the luciferase gene is transcribed actively and expressed in high level.

4.3.3 Ligand binding to cell surface

Another possible function of HMGB1 in the gene delivery complex is that it may facilitate the gene internalization process during endocytosis. Before the gene delivery complex can be internalized into the cell, the complex must first bind to the cell surface. On the surface of cell membrane, there are many ligand binding receptors including those that have been reported to interact with the

HMGB1 protein, e.g. Toll-like receptors (TLR 2 and TLR 4) [Yu *et al.* 2006], the RAGE (the receptor for advanced glycation end products) [Hori *et al.* 1995] and syndecan -1 [Salmivirta *et al.* 1992]. Therefore, it is possible that once the HMGB1 protein in the NDH system binds with these receptors, the NDH complex is already on the cell surface, making it ready for internalization. This may lead to an increase in the number of complexes being internalized and thus a higher transfection efficiency of the NDH system.

4.4 Perspectives

In this study, we have demonstrated an effective gene delivery system with the inclusion of HMGB1 in our existing PMMA-PEI nanoparticle system. Although we propose that HMGB1 may have the nuclear targeting ability, it has yet to be proven. In order to prove the presence of NLS in the HMGB1 molecule or its nuclear targeting ability, studies on the interaction of the HMGB1-DNA- nanoparticle and the importin proteins should be carried out. During the cyto-nucleoplasmic transport, the NLS sequence of the molecule will bind to the importin-alpha and then to the importin beta receptors. Together with the whole cargo, the importin beta receptor then mediates the nucleus translocation process and transports the transgene into the nucleus. Therefore,

by the importin protein binding assay, we can examine whether HMGB1 indeed mediates the cyto-nucleoplasmic transport or enhances expression of the transgene by other mechanisms.

Furthermore, before our new system can be used in *in vivo* studies, further optimization of the system is required, for example, the amount of HMGB1 to be included in the gene delivery complex. In this project, HMGB1 was included as a nuclear targeting agent and the weight ratio of HMGB1 to DNA was 1:3. Recently, gene delivery studies with different amounts and types of NLS peptides have been carried out. However, up to now, the optimal number of NLS peptides required to improve the gene delivery process awaits to be identified. Some groups suggested that the nuclear accumulation rate of DNA is proportional to the amount of NLS used [Sebestyen *et al.* 1998] while others proposed that a single NLS is sufficient for improvement [Zanta *et al.* 1999]. Therefore, we should further optimize the amount of the three components (i.e. the HMGB1 protein, the PMMA-PEI nanoparticle and the DNA) used in our system. For an effective gene delivery system, we should have an optimal amount of NLS to interact with the transport receptors but without hindering the binding with the NPC or blocking the DNA template from transcription [Nakanishi *et al.* 2001 and Bremner *et al.* 2004].

Apart from optimization of our gene delivery system, we also need to elucidate the detailed mechanism of gene delivery process for the PMMA-PEI nanoparticle and the NDH complex. This can be achieved by tracking the intracellular pathway of the nanoparticle or the NDH complex at various time points under the confocal laser scanning microscope. The results obtained may help us to have a better understanding of our existing system and provide more fundamental information for improvement. We are confident that our system has the potential to be developed into an *in vivo* gene delivery tool and that our system could be used in clinical applications in the near future.

4.5 Conclusion

Our study has demonstrated the effectiveness of the addition of a new single component in a combinatorial gene delivery system. With the incorporation of the nuclear HMGB1 protein in our existing PMMA-PEI core-shell nanoparticle system, the resultant HMGB1-DNA-nanoparticle complexes still maintain their DNA condensing capacity, DNA release ability and DNA protection ability. Furthermore, from the *in vitro* transfection study, we found that the complexing order is critical. Complexes formed by first condensing the plasmid DNA with nanoparticles (N/P ratio of 5) and then bound with the HMGB1 protein have a transfection efficiency 3 to 4 folds higher than that of the commercially available LipofectaminTM 2000 system. In addition, from the confocal images, we found that our core-shell nanoparticle system has the similar intracellular path as that of the PEI polymer.

In conclusion, our results have shown that this new multipcomponent combinatorial delivery system is a very good DNA carrier system for *in vitro* transfection. It definitely has the potential to be developed into a viable and efficient non-viral gene carrier for use in gene therapy *in vivo*.

Chapter 5: Appendix

5.1 Raw data for HMGB1 protein extraction and purification from pig

thymus

Table 5.1: Raw data for CM Sephadex C25 chromatography

Fraction	Abs=280	Abs=230	Fraction	Abs=280	Abs=230	Fraction	Abs=280	Abs=230
1	0.016	0.025	31	0.381	1.709	61	0.171	0.983
2	0.010	0.011	32	0.418	1.851	62	0.209	1.173
3	-0.002	0.010	33	0.401	1.796	63	0.200	1.170
4	0.009	0.007	34	0.359	1.662	64	0.207	1.159
5	0.006	0.009	35	0.319	1.489	65	0.207	1.146
6	0.011	0.012	36	0.280	1.338	66	0.195	1.089
7	0.009	0.009	37	0.226	1.144	67	0.184	1.026
8	0.008	0.009	38	0.187	0.937	68	0.164	0.942
9	0.011	0.013	39	0.161	0.823	69	0.146	0.855
10	0.014	0.015	40	0.150	0.751	70	0.138	0.776
11	0.015	0.020	41	0.122	0.658	71	0.127	0.713
12	0.008	0.008	42	0.111	0.593	72	0.111	0.651
13	0.007	0.011	43	0.101	0.530	73	0.103	0.602
14	0.010	0.014	44	0.091	0.476	74	0.094	0.562
15	0.012	0.018	45	0.076	0.426	75	0.094	0.533
16	0.056	0.099	46	0.046	0.362	76	0.089	0.519
17	0.333	0.589	47	0.060	0.347	77	0.080	0.475
18	0.513	0.916	48	0.061	0.330	78	0.064	0.458
19	0.448	0.804	49	0.053	0.306	79	0.074	0.432
20	0.398	0.709	50	0.053	0.297	80	0.067	0.409
21	0.352	0.624	51	0.052	0.282	81	0.067	0.394
22	0.297	0.538	52	0.054	0.283	82	0.066	0.377
23	0.254	0.465	53	0.055	0.279	83	0.059	0.364
24	0.222	0.417	54	0.047	0.267	84	0.062	0.350
25	0.155	0.305	55	0.060	0.313	85	0.063	0.341
26	0.128	0.271	56	0.059	0.343	86	0.059	0.324
27	0.135	0.334	57	0.070	0.405	87	0.051	0.304
28	0.158	0.543	58	0.081	0.489	88	0.051	0.294
29	0.216	0.886	59	0.102	0.606	89	0.051	0.286
30	0.302	1.339	60	0.137	0.779	90	0.048	0.280

Cont'd Table 5.1

Fraction	Abs=280	Abs=230	Fraction	Abs=280	Abs=230	Fraction	Abs=280	Abs=230
91	0.049	0.269	124	0.032	0.163	157	0.003	0.009
92	0.044	0.259	125	0.030	0.150	158	0.009	0.016
93	0.044	0.245	126	0.028	0.144	159	0.007	0.011
94	0.044	0.251	127	0.028	0.123	160	0.007	0.012
95	0.044	0.242	128	0.027	0.123	161	0.011	0.017
96	0.032	0.234	129	0.023	0.116	162	0.007	0.012
97	0.040	0.224	130	0.024	0.113	163	0.010	0.013
98	0.038	0.219	131	0.020	0.106	164	0.008	0.013
99	0.039	0.214	132	0.021	0.103	165	0.008	0.013
100	0.042	0.213	133	0.019	0.096	166	0.012	0.014
101	0.035	0.196	134	0.018	0.087	167	0.007	0.013
102	0.034	0.189	135	0.016	0.081	168	0.006	0.011
103	0.054	0.266	136	0.014	0.079	169	0.004	0.010
104	0.054	0.256	137	0.014	0.068	170	0.007	0.012
105	0.050	0.269	138	0.012	0.064	171	0.006	0.009
106	0.055	0.274	139	0.014	0.062	172	0.006	0.018
107	0.044	0.261	140	0.018	0.060	173	0.008	0.013
108	0.040	0.245	141	0.010	0.048	174	0.004	0.008
109	0.038	0.220	142	0.007	0.033	175	0.005	0.009
110	0.040	0.239	143	0.009	0.025	176	0.004	0.009
111	0.043	0.227	144	0.009	0.020	177	0.006	0.011
112	0.039	0.222	145	0.006	0.017	178	0.003	0.009
113	0.036	0.213	146	0.007	0.014	179	0.009	0.012
114	0.040	0.210	147	0.012	0.018	180	0.009	0.013
115	0.033	0.197	148	0.007	0.014	181	0.010	0.014
116	0.038	0.196	149	0.007	0.015	182	0.011	0.014
117	0.036	0.191	150	0.007	0.013	183	0.011	0.014
118	0.034	0.182	151	0.004	0.010	184	0.005	0.008
119	0.034	0.134	152	0.005	0.012	185	0.000	0.002
120	0.031	0.142	153	0.007	0.011	186	0.002	0.007
121	0.027	0.147	154	0.005	0.011	187	0.011	0.013
122	0.030	0.157	155	0.006	0.013	188	0.007	0.009
123	0.033	0.161	156	0.007	0.012	189	0.007	0.010

5.2 Raw Data and data analysis for *in vitro* transfection efficiency of PMMA-PEI nanoparticles at various weight ratios in MCF-7 cells.

Table 5.2: Raw data and data analysis for transfection study

		Nanoparticle : DNA (w/w) ratio													
Lipofectamine 2000		0.23	0.46	0.91	2.29	4.57	9.14	13.71	18.28	22.85	27.42	32.00	36.57	41.14	45.71
Abs 595nm	0.529	0.392	0.599	0.496	0.497	0.544	0.469	0.517	0.491	0.465	0.421	0.452	0.361	0.393	0.392
	0.458	0.682	0.601	0.610	0.590	0.550	0.486	0.515	0.402	0.453	0.401	0.446	0.376	0.392	0.330
	0.456	0.583	0.582	0.479	0.437	0.568	0.221	0.509	0.461	0.423	0.390	0.429	0.363	0.404	0.324
Protein (ug)	0.003	0.001	0.003	0.002	0.002	0.003	0.002	0.003	0.002	0.002	0.002	0.002	0.001	0.001	1.323
	0.002	0.004	0.004	0.004	0.003	0.003	0.002	0.003	0.001	0.002	0.001	0.002	0.001	0.001	0.677
	0.002	0.003	0.003	0.002	0.002	0.003	0.000	0.003	0.002	0.002	0.001	0.002	0.001	0.001	0.615
Total protien	0.03	0.01	0.03	0.02	0.02	0.03	0.02	0.03	0.02	0.02	0.02	0.02	0.01	0.01	13.23
	0.02	0.04	0.04	0.04	0.03	0.03	0.02	0.03	0.01	0.02	0.01	0.02	0.01	0.01	6.77
	0.02	0.03	0.03	0.02	0.02	0.03	0.00	0.03	0.02	0.02	0.01	0.02	0.01	0.01	6.15
RLU reading 1	163.1	0.173	2.298	28.97	198.7	133.5	4.865	52.91	32.86	31.55	15.41	16.07	3.243	7.512	0.426
RLU reading 2	108.3	0.017	0.277	24.04	173.8	172.6	45.03	59.32	33.42	30.52	16.55	17.55	12.61	3.936	0.962
RLU reading 3	137.6	0.194	0.033	24.26	174	169.5	9.741	44.02	21.74	17.26	10.62	8.986	2.528	9.145	0.372

		Nanoparticle : DNA (w/w) ratio													
Lipofectamine 2000		0.23	0.46	0.91	2.29	4.57	9.14	13.71	18.28	22.85	27.42	32.00	36.57	41.14	45.71
LUR/Total protein	5935	13	66	1202	8209	4588	229	2013	1394	1511	946	825	323	561	0
	5376	0	8	669	5138	5808	1957	2279	2343	1555	1164	929	1086	298	0
	6920	6	1	1089	9716	5374	0	1733	1063	1049	813	525	248	632	0
Average	6077	6	25	987	7688	5257	729	2008	1600	1372	974	760	552	497	0
S.D.	781.60	6.36	35.70	280.62	2333.43	618.04	1070.01	273.19	664.36	280.38	177.60	209.93	463.82	176.17	0.06

5.3 Raw Data and data analysis for *in vitro* transfection efficiency of different HMGB1-DNA-nanoparticle systems in MCF-7 cells.

Table 5.3: Raw data and data analysis for transfection study

	Lipofectamine 2000	HMGB1: DNA:Nanoparticle (w/w/w) ratio													
		Nanoparticle :DNA (w/w) ratio				HMGB1: DNA (w/w) ratio	Complexing HMGB1 with DNA first				Complexing Nanoparticle with DNA first				
		0.91	2.29	3.66	4.57	1:3	1:3:2.73	1:3:6.87	1:3:10.98	1:3:13.71	1:3:2.73	1:3:6.87	1:3:10.98	1:3:13.71	
Abs 595nm	0.508	0.583	0.509	0.611	0.528	0.447	0.456	0.640	0.528	0.545	0.562	0.629	0.532	0.695	
	0.487	0.631	0.594	0.596	0.553	0.471	0.492	0.576	0.551	0.517	0.483	0.682	0.528	0.577	
	0.467	0.663	0.569	0.568	0.458	0.481	0.528	0.546	0.579	0.525	0.515	0.634	0.548	0.622	
Protein (mg)	0.002	0.003	0.002	0.003	0.003	0.002	0.002	0.004	0.003	0.003	0.003	0.004	0.003	0.004	
	0.002	0.004	0.003	0.003	0.003	0.002	0.002	0.003	0.003	0.003	0.002	0.004	0.003	0.003	
	0.002	0.004	0.003	0.003	0.002	0.002	0.003	0.003	0.003	0.003	0.003	0.004	0.003	0.004	
Total Protein (mg)	0.025	0.032	0.025	0.035	0.027	0.019	0.020	0.038	0.027	0.028	0.030	0.037	0.027	0.043	
	0.023	0.037	0.033	0.033	0.029	0.021	0.023	0.031	0.029	0.026	0.022	0.042	0.027	0.031	
	0.021	0.040	0.031	0.031	0.020	0.022	0.027	0.028	0.032	0.026	0.025	0.037	0.029	0.036	
RLU reading 1	557.5	88.44	609	335.1	117.9	0.027	194.9	1069	416.1	384.1	275.5	1920	1339	1676	
RLU reading 2	375.8	7.867	294.3	583.2	133.9	0.02	227.5	653.3	485.1	254.9	148.8	2188	1084	1284	
RLU reading 3	405.1	87.84	171.9	671.3	71.75	0	88.87	113	309.7	271.3	254.4	3060	857.5	624.3	

Cont' Table 5.3

		HMGB1: DNA:Nanoparticle (w/w/w) ratio												
		Nanoparticle: DNA (w/w) ratio				HMGB1: DNA (w/w) ratio	Complexing HMGB1 with DNA first				Complexing Nanoparticle with DNA first			
RLU/ mg of protein	Lipofectamine 2000	0.91	2.29	3.66	4.57	1:3	1:3:2.73	1:3:6.87	1:3:10.98	1:3:13.71	1:3:2.73	1:3:6.87	1:3:10.98	1:3:13.71
1	22592	2752	24630	9595	4421	1	9994	28272	15633	13545	9168	52293	49565	38721
2	16638	213	8869	17444	4593	1	9855	20810	16782	9968	6721	52169	40650	40772
3	19716	2191	5591	21940	3651	0	3333	3971	9757	10289	10026	82227	29923	17332
Mean	19649	1718	13030	16326	4222	1	7727	17684	14057	11267	8639	62230	40046	32275
S.D.	2978	1334	10179	6248	502	1	3806	12449	3768	1979	1715	17318	9835	12981

5.4 Raw Data and data analysis for cell viability assay

Table 5.4: Raw data and data analysis for MTS study

	Positive Control	70% Ethanol	Lipofectamine 2000	DNA only	PEI amount (ug)				Nanoparticle amount (ug)			
					0.026	0.066	0.106	0.131	0.09	0.23	0.37	0.46
Abs 490 nm	1.436	0.318	0.966	1.240	1.256	1.254	0.960	1.044	1.433	1.042	1.12	1.164
	1.366	0.346	0.964	1.321	1.245	1.279	1.061	0.982	1.238	1.302	1.399	1.168
	1.342	0.370	1.071	1.391	1.277	1.383	1.263	0.946	1.451	1.629	1.304	1.061
Mean	1.371	0.345	1.010	1.317	1.259	1.305	1.095	0.991	1.374	96.6	1.274	1.131
S.D.	0.056	0.026	0.055	0.076	0.016	0.068	0.154	0.050	0.118	0.294	0.142	0.061
Relative cell viability (%)	100.0	25.1	73.7	96.1	91.8	95.2	79.8	72.2	100.2	96.6	92.9	82.5
S.D. (%)	4.09	1.90	4.00	5.51	1.19	4.99	11.25	3.61	8.61	21.45	10.34	4.42

	PEI: DNA (w/w) ratio				Nanoparticle :DNA (w/w) ratio			
	0.26	0.65	1.04	1.31	0.91	2.29	3.66	4.57
Abs 490 nm	1.239	1.482	1.410	1.114	1.557	1.745	1.364	1.156
	1.327	1.438	1.252	1.29	1.582	1.582	1.263	1.277
	1.185	1.355	1.203	1.372	1.519	1.411	1.340	1.160
Mean	1.250	1.425	1.288	1.259	1.553	1.579	1.322	1.198
S.D.	0.072	0.064	0.108	0.132	0.032	0.167	0.053	0.069
Relative cell viability (%)	91.2	103.9	93.9	91.8	113.2	115.2	96.4	87.3
S.D. (%)	5.23	4.70	7.89	9.61	2.31	12.18	3.85	5.01

Cont' Table 5.4

	HMGB1: DNA (w/w) ratio	Complexing HMGB1 with DNA first				Complexing Nanoparticle with DNA first			
	1:3	1:3:2.73	1:3:6.87	1:3:10.98	1:3:13.71	1:3:2.73	1:3:6.87	1:3:10.98	1:3:13.71
Abs 490 nm	1.14	0.942	1.193	1.435	1.365	1.302	1.356	1.435	1.179
	1.4	1.222	1.155	1.158	1.199	1.219	1.342	1.368	1.108
	1.47	1.131	0.976	1.218	1.202	1.107	1.304	1.17	1.067
Mean	1.336	1.098	1.108	1.270	1.255	1.209	1.334	1.324	1.118
S.D.	0.174	0.143	0.116	0.146	0.095	0.098	0.027	0.138	0.057
Relative cell viability (%)	97.5	80.1	80.8	92.6	91.5	88.2	97.3	96.6	81.5
S.D. (%)	12.68	10.42	8.45	10.63	6.93	7.14	1.96	10.05	4.13

Chapter 6: References

1. Abdallah B., Hassan A., Benoist C., Goula D., Behr J.P., Demeneix B.A. A powerful nonviral vector for in vivo gene transfer into the adult mammalian brain: polyethylenimine. *Human Gene Therapy*, 1996; 7(16):1947-54.
2. Agresti A., Bianchi M.E. HMGB proteins and gene expression. *Current Opinion in Genetics and Development*, 2003; 13(2):170-8.
3. Agarwal A., Unfer R., Mallapragada S.K. Novel cationic pentablock copolymers as non-viral vectors for gene therapy. *Journal of Controlled Release*, 2005; 103(1):245-58.
4. Ahn C.H., Chae S.Y., Bae Y.H., Kim S.W. Biodegradable poly(ethylenimine) for plasmid DNA delivery. *Journal of Control Release*, 2002; 80(1-3):273-82.
5. Andersson U., Erlandsson- Harris H. HMGB1 is a potent trigger of arthritis. *Journal of Internal Medicine*, 2004; 255:344-350.
6. Aizawa S., Nishino H., Saito K., Kimura K., Shirakawa H., Yoshida M. Stimulation of transcription in cultured cells by high mobility group protein 1: essential role of the acidic carboxyl-terminal region. *Biochemistry*, 1994; 33(49):14690-5.
7. Baxevanis A.D., Landsman D. The HMG-1 box protein family: classification and functional relationships. *Nucleic Acids Research*, 1995; 23(9):1604-13.
8. Bergeron S., Anderson D.K., Swanson P.C. RAG and HMGB1 proteins: purification and biochemical analysis of recombination signal complexes. *Methods in Enzymology*, 2006; 408:511-28.
9. Bremner K.H., Seymour L.W., Logan A. Read M.L. Factors influencing the ability of nuclear localization sequence peptides to enhance nonviral gene delivery. *Bioconjugate Chemistry*, 2004; 15(1):152-61.
10. Bianchi M.E., Beltrane M. Upwardly mobile proteins: The role of HMG protein in chromatin structure, gene expression and neoplasia, *EMBO Reports*, 2000; 1(2):109-14.

11. Bieber T., Meissner W., Kostin S., Niemann A., Elasser H.P. Intracellular route and transcriptional competence of polyethylenimine–DNA complexes. *Journal of Controlled Release*, 2002; 82(2-3):441-54.
12. Bivas-Benita M., Romeijn S., Junginger H.E., Borchard G. PLGA-PEI nanoparticles for gene delivery to pulmonary epithelium. *European Journal of Pharmaceutics and Biopharmaceutics*, 2004; 58(1):1-6.
13. Boletta A., Benigni A., Lutz J., Remuzzi G., Soria M.R., Monaco L. Nonviral gene delivery to the rat kidney with polyethylenimine. *Human Gene Therapy*, 1997; 8(10):1243-51.
14. Bottger M., Vogel F., Platzer M., Kiessling U., Grade K., Strauss M. Condensation of vector DNA by the chromosomal protein HMG1 results in efficient transfection. *Biochimica et Biophysica Acta*, 1988; 950(2):221-8.
15. Bottger M., Platzer M., Kiessling U., Strau M. Transfection by DNA –nuclear protein HMG1 complexes: raising of efficiency and role of DNA topology. *Archiv für Geschwulstforschung*, 1990; 60(4):265-70.
16. Bottger M., Zaitsev S.V., Otto A., Haberland A., Vorob'ev V.I. Acid nuclear extracts as mediators of gene transfer and expression. *Biochimica et Biophysica Acta*, 1998; 1395(1):78-87.
17. Boussif O., Lezoualc'h F., Zanta M.A., Mergny M.D., Scherman D., Demeneix B., Behr J.P. A versatile vector for gene and oligonucleotide transfer into cells in culture and in vivo: polyethylenimine. *Proceedings of the National Academy of Sciences of the United States of America*, 1995; 92(16):7297-301.
18. Bozkir A., Saka O.M. Chitosan-DNA Nanoparticles: Effect on DNA integrity, bacterial transformation and transfection efficiency. *Journal of Drug Targeting*, 2004; 12(5):281-8.
19. Breunig M., Lungwitz U., Klar J., Kurtz A., Blunk T., Goepferich A. Polyplexes of polyethylenimine and per-N-methylated polyethylenimine cytotoxicity and transfection efficiency. *Journal of Nanoscience and Nanotechnology*, 2004; 4(5):512-20.
20. Bustin M. Regulation of DNA-dependent activities by the functional motifs of the high-mobility-group chromosomal proteins. *Molecular and Cellular Biology*, 1999; 19(8):5237-46.

21. Bustin M. Revised nomenclature for high mobility group (HMG) chromosomal proteins. *Trends in Biochemical Sciences*, 2001; 26(3):152-3.
22. Catez F., Yang H., Tracey K.J., Reeves R., Misteli T., Bustin M. Network of dynamic interactions between histone H1 and high-mobility-group proteins in chromatin. *Molecular and Cellular Biology*, 2004; 24(10):4321-8.
23. Cavazzana-Calvo M., Thrasher A., Mavilio F. The future of gene therapy: Balancing the risks and benefits of clinical trials. *Nature*, 2004; 427:779-81.
24. Chau K.Y., Lam H.K., Lee K.L. Estrogen treatment induces elevated expression of HMG1 in MCF-7 cells. *Experimental Cell Research*, 1998; 24(1):269-72.
25. Cho K.C., Kim S.H., Jeong J.H., Park T.J. Folate receptor-mediated gene delivery using folate-poly(ethylene glycol)-poly(L-lysine) conjugate. *Macromolecular Bioscience*, 2005; 5(6):512-9.
26. Choi J.S., Nam K., Park J.Y., Kim J.B., Lee J.K., Park J.S. Enhanced transfection efficiency of PAMAM dendrimer by surface modification with L-arginine. *Journal of Controlled Release*, 2004; 99(3):445-56.
27. Coll J.L., Chollet P., Branbilla E., Desplanques D., Behr J.P., Favrot M. In vivo delivery to tumors of DNA complexed with linear polyethylenimine. *Human Gene Therapy*, 1999; 10(10):1659-66.
28. Cook S.E., Park I.K., Kim E.M., Jeong H.J., Park T.G., Choi Y.J., Akaike T., Cho C.S. Galactosylated polyethylenimine-graft-poly(vinyl pyrrolidone) as a hepatocyte-targeting gene carrier. *Journal of Controlled Release*, 2005; 105(1-2):151-63.
29. Cristiano R.J. Targeted non-viral gene delivery for cancer gene therapy. *Frontiers in Bioscience*, 1998; 3: D1161-70. Review.
30. Curiel D.T., Douglas J.T. eds. *Cancer gene therapy*. Totowa, New Jersey: Humana Press, c2005, Chapter 24.
31. De Smedt S.C., Demeester J., Hennink W.E. Cationic polymer based gene delivery systems. *Pharmaceutical Research*, 2000; 17(2):113-26. Review.
32. Degryse B., Bonaldi T., Scaffidi P. The high mobility group (HMG) boxes of the Nuclear Protein HMG1 induce chemotaxis and cytoskeleton reorganization in rat smooth muscle cells. *The Journal of Biological Chemistry* 2001; 152(6):1197-206.

33. Dufes C., Uchegbu I.F., Schatzlein A.G. Dendrimers in gene delivery. *Advanced drug delivery reviews*, 2005; 57(15):2177-202. Review.
34. El-Aneed A. An overview of current delivery systems in cancer gene therapy. *Journal of Control Release*, 2004; 94(1):1-14. Review.
35. Erlandsson- Harris H., Andersson U. Mini-review: The nuclear protein HMGB1 as a proinflammatory mediator. *European Journal of Immunology*, 2004; 34(6):1503-12.
36. Escriou V., Carriere M., Scherman D., Wils P. NLS bioconjugates for targeting therapeutic genes to the nucleus. *Advanced Drug Delivery Review*, 2003; 55(2):295-306.
37. Ferrari S., Moro E., Pettenazzo A., Behr J.P., Zacchello F., Scarpa M. ExGen 500 is an efficient vector for gene delivery to lung epithelial cells in vitro and in vivo. *Gene Therapy*, 1997; 4(10):1100-6.
38. Fischer D., Li Y., Ahlemeyer B., Krieglstein J., Kissel T. *In vitro* cytotoxicity testing of polycations: influence of polymer structure on cell viability and hemolysis. *Biomaterials*, 2003; 24(7):1131-31.
39. Garnett M.C. Gene-delivery systems using cationic polymers. *Critical Reviews in Therapeutic Drug Carrier Systems*, 1999; 16(2):147-207. Review.
40. Gautam A., Densmore C.L., Xu B., Waldrep J.C. Enhanced gene expression in mouse lung after PEI-DNA aerosol delivery. *Molecular Therapy: The Journal of the American Society of Gene Therapy*, 2000; 2(1):63-70.
41. Gresch O., Engel F.B., Nestic D., Tran T.T., England H.M., Hickman E.S., Korner I., Gan L., Chen S., Castro-Obregon S., Hammermann R., Wolf J., Muller-Hartmann H., Nix M., Siebenkotten G., Kraus G., Lun K. New non-viral method for gene transfer into primary cells. *Method*, 2004; 33(2):151-63.
42. Godbey W.T., Wu K.K., Mikos A.G. Tracking the intracellular path of poly(ethylenimine)/DNA complexes for gene delivery. *Proceedings of the National Academy of Sciences of the United States of America*, 1999a; 96(9):5177-81.

43. Godbey W.T., Wu K.K., Mikos A.G. Poly(ethylenimine) and its role in gene delivery. *Journal of Controlled Release*, 1999b; 60(2-3):149-60. Review.
44. Godbey W.T., Wu K.K., Hirasaki G.J., Mikos A.G. Improved packing of poly(ethylenimine)/DNA complexes increases transfection efficiency. *Gene Therapy*, 1999c; 6(8):1380-8.
45. Godbey W.T., Barry M.A., Saggau P., Wu K.K., Mikos A.G. Poly(ethylenimine)-mediated transfection: a new paradigm for gene delivery. *Journal of Biomedical Materials Research*, 2000; 51(3):321-8.
46. Goodwin G.H., Nicolas R.H., Johns E.W. An improved large scale fractionation of high mobility group non-histone chromatin proteins. *Biochimica et Biophysica Acta*, 1975; 405(2):280-91.
47. Harris H.E., Raucica A. Alarmin(g) news about danger: Workshop on Innate Danger Signals and HMGB1. *EMBO Report*, 2006; 7(8):774-8
48. Hangai M., Kaneda Y., Tanihara H., Honda Y. *In vivo* gene transfer into the retina mediated by a novel liposome system. *Investigative Ophthalmology Visual Science*, 1996; 37(13):2678-85.
49. Hebert E. Improvement of exogenous DNA nuclear importation by nuclear localization signal-bearing vectors: a promising way for non-viral gene therapy? *Biology of the Cell*, 2003; 95(2):59-68.
50. Heiser W.C. ed., *Gene delivery to mammalian cells, Volume 1: Non-viral gene transfer techniques*. Totowa, New Jersey: Humana Press, 2004, Chapter 1 and 11.
51. Hori O., Brett J., Slattery T., Cao R., Zhang J., Chen J.X., Nagashima M., Lundh E.R., Vijay S., Nitecki D., Morser J., Stern D., Schmidt A.M. The receptor for advanced glycation end products (RAGE) is a cellular binding site for amphoterin. Mediation of neurite outgrowth and co-expression of rage and amphoterin in the developing nervous system. *The Journal of Biological Chemistry*, 1995; 270(43):25752-61.
52. Imamura T., Izumi H., Nagatani G., Ise T., Nomoto M., Iwamoto Y., Kohno K. Interaction with p53 enhances binding of cisplatin-modified DNA by high mobility group 1 protein. *Journal of Biological Chemistry*, 2001; 276(10):7534-40.

53. Ina S., Sawamura D., Meng X., Tamai K., Hanada K., Hashimoto I. *In vivo* gene transfer method in keratinocyte gene therapy: Intradermal injection of DNA complexed with high mobility group protein in rats. *Acta Dermato-Venereologica*, 2000; 80:10-13.
54. Isaka Y., Akagi Y., Kaneda Y., Ima E. The HVJ liposome method. *Experimental Nephrology*, 1998; 6(2):144-7.
55. Jeon E., Kim D.H., Kim J.S. Pluronic-grafted poly-(L)-lysine as a new synthetic gene carrier. *Journal of Biomedical Materials Research Part A*, 2003; 66(4):854-9.
56. Kato K., Nakanishi H., Kaneda Y., Uchida T., Okada Y. Expression of hepatitis virus surface antigen in adult rat liver. Co-introduction of DNA and nuclear protein by a simplified liposome method. *The Journal of Biological Chemistry*, 1991; 266(6):3361-4.
57. Kean T., Roth S., Thanou M. Trimethylated chitosans as non-viral gene delivery vectors: cytotoxicity and transfection efficiency. *Journal of Controlled Release*, 2005; 103(3):643-53.
58. Kichler A., Leborgne C., Coeytaux E., Danos O. Polyethylenimine-mediated gene delivery: a mechanistic study. *The Journal of Gene Medicine*, 2001; 3(2):135-44.
59. Kim J.B., Choi J.S., Nam K., Lee M., Park J.S., Lee J.K. Enhanced transfection of primary cortical cultures using arginine-grafted PAMAM dendrimer, PAMAM-Arg. *Journal of Controlled Release*, 2006; 114(1):110-7.
60. Kircheis R., Kichler A., Wallner G., Kursa M., Ogris M., Felzmann T., Buchberger M., Wagner E. Coupling of cell-binding ligands to polyethylenimine for targeted gene delivery. *Gene Therapy*, 1997; 4(5):409-18.
61. Kircheis R., Wightman L., Wagner E. Design and gene delivery activity of modified polyethylenimines. *Advanced Drug Delivery Reviews*, 2001; 53(3):341-58. Review.
62. Kircheis R., Ostermann E., Wolschek M.F., Lichtenberger C., Magin-Lachmann C., Kursa M., Wanger E. Tumor-targeted gene delivery of tumor necrosis factor-alpha induces tumor necrosis and tumor regression without systemic toxicity. *Cancer gene therapy*, 2002; 9(8):673-80.

63. Kuo J.H. Effect of Pluronic-block copolymers on the reduction of serum-mediated inhibition of gene transfer of polyethyleneimine-DNA complexes. *Biotechnology and Applied Biochemistry*, 2003; 37 (Pt3):267-71.
64. LeCasse C.E., Lefebvre Y.A. Nuclear localization signals overlap DNA- or RNA-binding domains in nucleic acid-binding proteins. *Nucleic Acids Research*, 1995; 23(10):1647-56.
65. Lechardeur D., Lukacs G.L. Intracellular barriers to non-viral gene transfer. *Current gene therapy*, 2002; 2(2):183-94.
66. Lee H., Jeong J.H. A new gene delivery formulation of polyethylenimine/DNA complexes coated with PEG conjugated fusogenic peptide. *Journal of Controlled Release*, 2001; 76(1-2):183-92.
67. Lee K.B., Thomas J.O. The effect of the acidic tail on the DNA-binding properties of the HMG1,2 class of proteins: insights from tail switching and tail removal. *Journal of Molecular Biology*, 2000; 304(2):135-49.
68. Li J., Kokkola R., Tabibzadeh S., Yang R., Ochani M., Qiang X., Harris H.E., Czura C.J., Wang H., Ulloa L., Wang H., Warren H.S., Moldawer L.L., Fink M.P., Andersson U., Tracey K.J., Yang H. Structural basis for the proinflammatory cytokine activity of high mobility group box 1. *Biochemical and Molecular Medicine*, 2003; 9(1-2):37-45.
69. Li S., Ma Z. Nonviral gene therapy. *Current Gene Therapy*, 2001; 1(2):201-26. Review.
70. Li X. W., Lee D.K., Chan A.S., Alpar H.O. Sustained expression in mammalian cells with DNA complexed with chitosan nanoparticles. *Biochimica et Biophysica Acta*, 2003; 1630(1):7-18.
71. Ludtke J.J., Zhang G., Sebestyen M.G., Wolff J.A. A nuclear localization signal can enhance both the nuclear transport and expression of 1 kb DNA. *Journal of Cell Science*, 1999; 112:2033-41.
72. Liu F., Huang L. Development of non-viral vectors for systemic gene delivery. *Journal of Control Release*, 2002; 78(1-3):259-66. Review.
73. Lum H.K., Lee K.L. The human HMGB1 promoter is modulated by a silencer and an enhancer-containing intron. *Biochimica et Biophysica Acta*, 2001; 1520(1):79-84.

74. Lundstrom K., Boulikas T. Viral and non-viral vectors in gene therapy: technology development and clinical trials. *Technology in Cancer Research & Treatment*, 2003; 2(5):471-86.
75. Luo D., Saltzman W.M. Synthetic DNA delivery systems. *Nature Biotechnology*, 2000; 18(1):33-37.
76. Mahato R.I., Han S.O. Cationic lipopolymer as biocompatible gene delivery agent. United States Patent 6,696,038, February 24, 2004.
77. Mao H.Q., Roy K., Troung-Le V.L., Janes K.A., Lin K.Y., Wang Y., August J.T., Leong K.W. Chitosan-DNA nanoparticles as gene carriers: synthesis, characterization and transfection efficiency. *Journal of Controlled Release*, 2001; 70(3):399-421.
78. Mesika A., Kiss V., Brumfeld V., Ghosh G., Reich Z. Enhanced intracellular mobility and nuclear accumulation of DNA plasmids associated with a karyophilic protein. *Human Gene Therapy*, 2005; 16(2):200-8.
79. Mistry A.R., Falciola L., Monaco L., Tagliabue R., Acerbis G., Knight A., Harbottle R.P., Soria M., Bianchi M.E., Coutelle C., Hart S.L. Recombinant HMG1 protein produced in *Pichia pastoris*: a nonviral gene delivery agent. *Biotechniques*, 1997; 22(4):718-29.
80. Munkonge F.M., Dean D.A., Hillery E., Griesenbach U., Alton E.W. Emerging significance of plasmid DNA nuclear import in gene therapy. *Advanced Drug Delivery Reviews*, 2003; 55(6):749-60.
81. Nakanishi M., Akuta T., Nagoshi E., Eguchi A., Mizuguchi H. Nuclear targeting of DNA. *European Journal of Pharmaceutical Sciences*, 2001; 13(1):17-24.
82. Namiki Y., Takahashi T., Ohno T. Gene transduction for disseminated intraperitoneal tumor using cationic liposomes containing non-histone chromatin proteins: cationic liposomal gene therapy of carcinomatosa. *Gene Therapy*, 1998; 5(2):240-6.
83. Nguyen H.K., Lemieux P., Vinogradov S.V., Gebhart C.L., Guerin N., Paradis G., Bronich T.K., Alakhov V., Kabanov A.V. Evaluation of polyether-polyethyleneimine graft copolymers as gene transfer agents. *Gene Therapy*, 2000; 7(2):126-38.

84. Niidome T., Huang L. Gene therapy progress and prospects: Nonviral vectors. *Gene Therapy*, 2002; 9(24):1647-52. Review.
85. Nishikawa M., Takemura S., Takakura Y., Hashida M. Targeted delivery of plasmid DNA to hepatocytes in vivo: optimization of the pharmacokinetics of plasmid DNA/galactosylated poly(L-lysine) complexes by controlling their physicochemical properties. *The Journal of Pharmacology and Experimental Therapeutics*, 1998; 287(1):408-15.
86. Panyam J., Labhasetwar V. Biodegradable nanoparticles for drug and gene delivery to cells and tissue. *Advanced Drug Delivery Review*, 2003; 55(3):329-47.
87. Park T.G., Jeong J.H., Kim S.W. Current status of polymeric gene delivery systems. *Advanced drug delivery reviews*, 2006; 58(4):467-86.
88. Parker A.L., Newman C., Briggs S., Seymour L., Sheridan P.J. Nonviral gene delivery: techniques and implications for molecular medicine. *Expert Reviews in Molecular Medicine*, 2003; 5:1-15.
89. Pollard H., Remy J.S., Loussouarn G., Demolombe S., Behr J.P., Escande D. Polyethylenimine but not cationic lipids promotes transgene delivery to the nucleus in mammalian cells. *The Journal of Biological Chemistry*, 1998; 273(13):7507-11.
90. Poulat F., Girard F., Chevron M.P., Goze C., Rebillard X., Calas B., Lamb N., Berta P. Nuclear localization of the testis determining gene product SRY. *The Journal of Cell Biology*, 1995; 128(5):737-48.
91. Pullerits R., Jonsson I.M., Verdrengh M., Bokarewa M., Andersson U., Erlandsson-Harris H., Tarkowski A. High mobility group box chromosomal protein 1, a DNA binding cytokine, induces arthritis. *Arthritis and Rheumatism*, 2003; 48(6):1693-700.
92. Rechsteiner M., Kuehl L. Microinjection of the nonhistone chromosomal protein HMG1 into bovine fibroblasts and HeLa cells. *Cell*, 1979; 16(4):901-8.
93. Salata O. Applications of nanoparticles in biology and medicine. *Journal of Nanobiotechnology*, 2004; 2(1):3.

94. Salmivirta M., Rauvala H., Elenius K., Jalkanen M. Neurite growth-promoting protein (amphoterin, p30) binds syndecan. *Experimental Cell Research*, 1992; 200(2):444-51.
95. Schatzlein A.G. Targeting of Synthetic Gene Delivery Systems. *Journal of Biomedicine Biotechnology*, 2003; 2003(2):149-158. Review.
96. Sebestyen M.G., Ludtke J.J., Bassik M.G., Zhang G., Budker V., Lukhtanov E.A., Hagstrom J.E., Wolff J.A. DNA vector chemistry: the covalent attachment of signal peptides to plasmid DNA. *Nature Biotechnology*, 1998; 16(1):80-5.
97. Segura T., Shea L.D. Materials for non-viral gene delivery. *Annual Review of Materials Research*, 2001; 31:25-46.
98. Sheflin L.G., Fucile N.W., Spaulding S.W. The specific interactions of HMG 1 and 2 with negatively supercoiled DNA are modulated by their acidic C-terminal domains and involve cysteine residues in their HMG 1/2 boxes. *Biochemistry*, 1993; 32(13):3238-48.
99. Shoji Y., Nakashima H. Current status of delivery systems to improve target efficacy of oligonucleotides. *Current Pharmaceutical Design*, 2004; 10(7):785-96. Review.
100. Soper R., Taylor D.J., Green N.P.O., Stout G.W. eds. *Biological science 1: Organisms, energy and environment*. Cambridge University Press. 3rd edition, 1997, Chapter 5.
101. Stone D., David A., Bolognani F., Lowenstein P.R., Castro M.G. Viral vectors for gene delivery and gene therapy within the endocrine system. *Journal of Endocrinology*, 2000; 164(2):103-18. Review.
102. Stros M., Reich J., Kolibalova A. Calcium binding to HMG1 protein induces DNA looping by the HMG-Box domains. *FEBS letters*, 1994; 344(2-3):201-6.
103. Sutrias-Grau M., Bianchi M.E., Bernues J. High mobility group protein 1 interacts specifically with the core domain of human TATA box-binding protein and interferes with transcription factor IIB within the pre-initiation complex. *The Journal of Biological Chemistry*, 1999; 274(3):1628-34.

104. Swanson P.C. A RAG-1/RAG-2 tetramer supports 12/23-regulated synapsis, cleavage, and transposition of V(D)J recombination signals. *Molecular and Cellular Biology*, 2002; 22(22):7790-801.
105. Tang M.X., Redemann C.T., Szoka F.C. Jr. *In vivo* gene delivery by degraded polyamidoamine dendrimers. *Bioconjugate Chemistry*, 1996; 7(6):703-14.
106. Thomas J.O., Travers A.A. HMG1 and 2, and related 'architectural' DNA-binding proteins. *Trends in Biochemical Sciences*, 2003; 26(3):167-74.
107. Thomas M., Klivanov A.M. Non-viral gene therapy: polycation-mediated DNA delivery. *Applied Microbiology and Biotechnology*, 2003; 62(1):27-34. Review.
108. Tsuneoka M., Imamoto S., Uchida T. Monoclonal antibody against non-histone chromosomal protein high mobility group 1 Co-migrates with high mobility group 1 into the nucleus. *The Journal of Biological Chemistry*, 1986; 261(4):1829-34.
109. Uherek C., Wels W. DNA-carrier proteins for targeted gene delivery. *Advanced Drug Delivery Review*, 2000; 44(2-3):153-66. Review.
110. van der Aa M.A., Mastrobattista E., Oosting R.S., Hennink W.E., Koning G.A., Crommelin D.J. The nuclear pore complex: the gateway to successful nonviral gene delivery. *Pharmaceutical Research*, 2006; 23(3):447-59.
111. van Gent D.C., Hiom K., Paull T.T., Gellert M. Stimulation of V(D)J cleavage by high mobility group proteins. *The EMBO Journal*, 1997; 16(10):2665-70.
112. Varga-Weisz P., van Holde K., Zlatanova J. Competition between linker histones and HMG1 for binding to four-way junction DNA: implications for transcription. *Biochemical and Biophysical Research Communications*, 1994; 203(3):1904-11.
113. Verrier C.S., Roodi N., Yee C.J., Bailey L.R., Jensen R.A., Bustin M., Parl F.F. High-mobility group (HMG) protein HMG-1 and TATA-binding protein-associated factor TAF(II)30 affect estrogen receptor-mediated transcriptional activation. *Molecular Endocrinology*, 1997; 11(8):1009-19.

114. Wiethoff C.M., Middaugh C.R. Barriers to nonviral gene delivery. *Journal of Pharmaceutical Science*, 2003; 92(2):203-17. Review.
115. Wiewrodt R., Thomas A.P., Cipelletti L., Christofidou-Solomidou M., Weitz D.A., Feinstein S.I., Schaffer D., Albelda S.M., Koval M., Muzykantov V.R. Size-dependent intracellular immunotargeting of therapeutic cargoes into endothelial cells. *Blood*, 2002; 99(3):912-22.
116. Wu G.Y., Wu C.H. Receptor-mediated in vitro gene transformation by a soluble DNA carrier system. *Journal of Biological Chemistry* 1987 April 5; 262(10):4429-32. Erratum in *Journal of Biological Chemistry* 1988 January 5; 263(1):588.
117. Wunderlich V., Bottger M. High-mobility-group proteins and cancer - and emerging link. *Journal of Cancer Research and Clinical Oncology*, 1997; 123(3):133-40.
118. Yang H., Wang H., Czura C.J., Tracey K.J. The cytokine activity of HMGB1. *Journal of Leukocyte Biology*, 2005; 78(1):1-8.
119. Yang Y.Y., Wang Y., Powell R., Chan P. Polymeric core-shell nanoparticles for therapeutics. *Clinical Experimental Pharmacology Physiology*, 2006; 33(5-6):557-62.
120. Yu M., Wang H., Ding A., Golenbock D.T., Latz E., Czura C.J., Fenton M.J., Tracey K.J., Yang H. HMGB1 signals through toll-like receptor (TLR) 4 and TLR2. *Shock*, 2006; 26(2):174-9.
121. Zaitsev S.V., Haberland A., Otto A., Vorob'ev V.I., Haller H., Bottger M. H1 and HMG17 extracted from calf thymus nuclei are efficient DNA carriers in gene transfer. *Gene Therapy*, 1997; 4 (6): 586-92.
122. Zanta M.A., Belguise-Valladier P., Behr J.P. Gene delivery: A single nuclear localization signal peptide is sufficient to carry DNA to the cell nucleus. *Proceedings of the National Academy of Sciences of the United States of America*, 1999; 96(1):91-6.
123. Zhang X.Q., Wang X.L., Huang S.W., Zhuo R.X., Liu Z.L., Mao H.Q., Leong K.W. In vitro gene delivery using polyamidoamine dendrimers with a trimesyl core. *Biomacromolecules*, 2005; 6(1):341-50.

124. Zhu J.M., Tang A., Law L.P., Feng M., Ho K.M., Lee K.L., Harris F.W., Li P. Amphiphilic core-shell nanoparticles with poly(ethylenimine) shells as potential gene delivery carriers. *Bioconjugate Chemistry*, 2005; 16(1): 139-146.